# CHARACTERIZATION OF THE ROLE OF CSLD PROTEINS IN *ARABIDOPSIS* CELL WALL DEPOSITION

**by**

**Fangwei Gu**

**A dissertation submitted in partial fulfillment**
**of the requirement for the degree of**
**Doctor of Philosophy**
**(Molecular, Cellular and Developmental Biology)**
**in the University of Michigan**
**2015**

**Doctoral Committee:**

**Associate Professor Erik E. Nielsen, Chair**
**Professor Jianming Li**
**Professor John W. Schiefelbein**
**Professor Joel A. Swanson**

# ACKNOWLEDGEMENTS

This thesis covers the majority of my research projects since the start of my Ph. D. program in fall, 2009. The journey towards this time point is with joys and tears. I am so grateful for the company of my family, friends and colleagues during this adventure. Without your support, this thesis can never be done.

First and foremost, I would like to express my sincere gratitude to my advisor Dr. Erik Nielsen for his continuous support during my Ph. D. study. Your guidance, inspiration, patience, encouragement, and great knowledge helped me in the entire process. Through the training under your supervision, I learned to think more critically, became more detail-orientated, and mastered new technical skills. Thank you so much for providing a great environment for me to grow as a young scientist, both professionally and personally.

I would also like to thank my committee members, Dr. Jianming Li, Dr. John Schiefelbein and Dr. Joel Swanson for their valuable advice and suggestions throughout this process. As plant biologists, both Dr. Li and Dr. Schiefelbein provided many useful ideas to fulfill my projects. Dr. Swanson also used his expertise in cell biology to lead insightful discussions. I could not have imagined a better committee.

I would like to thank all my current and former colleagues in the lab for creating an amazing working atmosphere. I really appreciate the ideas and the tips for experiment you provided in discussions. In particular, I would like to thank Dr. Sungjin Park, Dr. Daewon Kim, and Dr. Vincenzo Antignani. Dr. Sungjin Park helped me a lot in almost

all of my research projects. He also helped me to learn the basic skills and techniques in *Arabidopsis* research. I worked with Dr. Daewon Kim in the FER project and we made significant progress during his visit. I was also stimulated by the positive attitude towards life from Dr. Vincenzo Antignani. I also appreciate the joys based on our common interests such as movies, soccer, and coffee.

I must express my gratitude to the Clark lab, Schiefelbein lab, and Li lab for the ideas exchanged and reagent sharing. I also received many useful comments during the joint lab meetings with the Clark lab. I would also like to thank Gregg Sobocinski for his patience and knowledge when answering my uncountable number of questions regarding of the confocal microscopy.

I would like to thank my classmates and friends for making my past six years full of memories. In particular I would like to thank Tao Jiang, Zhuobin (Ben) Liang, Yidan Liu, Jing Lu, Shuai Niu, Gang Su, He Wang, Xiaolin Wang, Jingchen Wu, Chen Zhang, Qi Zhang, Yizi Zhang, Mantong Zhao, Xiaolei Zhao, and Zhichen Zhao. The journey pursuing my Ph. D. would have been much harder without your support.

I would like to offer my special thanks to my family. I would like to thank my parents for their support and encouragements from my application till now. I also would like to thank my two cats, Zura and Naicha, for the happiness they brought to me.

Lastly, I would like to thank my wife for her company in my life. We had a two-year long distance relationship before she quit her job and applied to MCDB. This was not an easy decision for her and I really appreciate what she has done for the family. During the past several years, we have traveled to many places as far north as Alaska and as far south as Puerto Rico. Wish we would experience more adventures in the rest of our lives.

# TABLE OF CONTENTS

# LIST OF FIGURES

# LIST OF TABLES

# ABSTRACT

Plant cells are surrounded by a rigid layer of polysaccharides, the plant cell wall, which defines the shape of plant cells as well as provides structural integrity to plant tissues and organs. Among the various classes of polysaccharides found in the plant cell wall, the major load-bearing component is cellulose. Cellulose is synthesized by CESA (Cellulose Synthase) proteins, which belong to the cellulose synthase like superfamily. Disruption of these *CESA* genes results in either lethality or in growth defects in various developmental processes. However, defects in root hair tip-growth were primarily observed in *csld2* (*Cellulose Synthase Like D2*) or *csld3* mutants rather than in *cesa* mutants. To better understand the role of CSLD proteins in *Arabidopsis* development, we examined the phenotypes of *csld2*, *csld3,* and *csld5* mutants. We found that *csld5* single mutants had shorter roots and smaller overall sizes, and these phenotypes were enhanced in *csld2/csld5* and *csld3/csld5* double mutants. Further phenotypic examination showed the existence of incomplete cell walls in *csld5* single and *csld2/csld5* and *csld3/csld5* double mutants. Using fluorescent fusions, we found that these three CSLD proteins localized on forming cell plates. A more precise temporal spatial analysis showed that CSLD5 was enriched on growing cell plates during cytokinesis. Shortly after cytokinesis

was completed, CSLD5 was rapidly depleted from these newly-deposited cell walls. We further confirmed that CSLD5 was an unstable protein that might be degraded via $APC^{CCS52A2}$ – 26S proteasome mediated pathways. We also investigated the functional redundancy of members of the CSLD family in root hair growth. We found that, when driven by the corresponding native promoters, only CSLD2 and CSLD3 proteins were detected in root hairs and both these proteins localized to apical membrane regions of growing root hairs. However, fluorescently tagged CSLD5 proteins could only be observed in the apical membrane regions in tip-growing root hairs when driven by a strong constitutive promoter. A promoter swap experiment showed that when expressed under control of the *CSLD3* promoter, *CSLD2* could fully restore root hair growth in *csld3* mutant background. By contrast, *CSLD5*, when driven by the *CSLD3* promoter, only partially rescued *csld3* root hair phenotypes. Combined, the results presented in this thesis have revealed a unique cell-cycle mediated regulation of CSLD5, and described novel roles for all three vegetatively-expressed CSLD proteins in cell wall synthesis during cytokinesis. In addition, the functional redundancy between *CSLD2*, *CSLD3*, and *CSLD5* during root hair growth was described.

# CHAPTER 1

# INTRODUCTION – REGULATION OF CELL WALL SYNTHESIS IN *ARABIDOPSIS THALIANA*

The plant cell wall is a load-bearing matrix which surrounds plant cells, and serves many essential functions in plants, including resisting high cellular turgor pressures, determining the cell shape, providing structural integrity for plants to grow upright, and protecting plants against environmental impacts (Cosgrove, 2005; Liepman et al., 2010). As the primary source of renewable biopolymer, plant cell walls also provide raw materials for industrial applications and they are used to manufacture paper, textiles, and biofuels (Cosgrove, 2005; Endler and Persson, 2011). Due to the importance of the plant cell wall, this essential plant structure has been the focus of significant research interest, and in the past two decades the molecular machinery involved in its synthesis and construction has been gradually elucidated using *Arabidopsis thaliana* as a model plant system.

**Major polysaccharide classes in *Arabidopsis thaliana* cell wall**

In general, the *Arabidopsis* cell wall is a complex network in which different classes of polysaccharides are heavily cross-linked (Figure 1.1). The primary cell wall, which is generally deposited only during initial cell expansion, consists of three classes of polysaccharides: cellulose, hemicelluloses, and pectins (Cosgrove, 2005). Cellulose is thought to be made of 18 – 36 parallel β-1,4-linked glucan chains which are assembled into microfibrils by hydrogen bonds and Val der Waals forces (Figure 1.2) (Somerville, 2006). During cell expansion and differentiation, multiple layers of crystalline cellulose microfibrils are deposited sequentially at the innermost side of existing cell wall (Emons, 1994; Emons and Mulder, 2000; Cosgrove, 2005; Somerville, 2006). Such cellulose microfibril scaffolds provide mechanical strength and load-bearing properties to the cell wall (Cosgrove, 2005). Initial observations made using electron microscopic techniques in the 1970s and 1980s, that cellulose microfibrils often terminated at the plasma membrane in association with large, circular protein assemblies, had led to the speculative model that these plasma membrane localized "rosette complexes" were putative cellulose synthase complexes (CSC) (Kiermayer and Sleytr, 1979; Mueller and Brown, 1980; Herth, 1983; Emons, 1985). This hypothesis was not experimentally supported until the identification of higher plant cellulose synthase (*CESA*) genes in late 1990s (Arioli et al., 1998). Immunogold labeling experiments using antibodies against the catalytic domain of a cotton CESA protein confirmed that this CESA protein was

localized to rosette complexes on plasma membranes in the vascular plant *Vigna angulari*s (Kimura et al., 1999). A typical rosette complex contains six globules, each of which might be composed of several CESA proteins (Figure 1.2) (Somerville, 2006).

There are ten *CESA* genes in the *Arabidopsis* genome (Richmond and Somerville, 2000). In the past two decades, *CESA1*, *CESA2*, *CESA3*, *CESA5*, *CESA6*, and *CESA9* have all been shown to be associated with primary cell wall biosynthesis, while *CESA4*, *CESA7*, *CESA8* are related to the production of secondary cell wall (Kumar and Turner, 2014). The precise role of *CESA10* remains unclear (Kumar and Turner, 2014). Genetic analysis showed that at least three unique CESA isoforms are required for the cellulose synthase complex involved in the synthesis of primary cell walls (Persson et al., 2007; Desprez et al., 2007). Two of these three CESA isoforms must be CESA1 and CESA3, while CESA2, CESA5, CESA6, and CESA9 have redundant functions and it is thought that these four proteins are interchangeable as the third required CESA isoform in the CSC (Persson et al., 2007; Desprez et al., 2007).

Other than the CESA proteins, additional accessory factors such as CSI and KORRIGAN proteins were found to be associated with the CSC (Gu et al., 2010; Lei et al., 2013, 2014; Vain et al., 2014). Cellulose synthase-interactive protein 1 (CSI1) was shown to interact with CESA1, CESA3, and CESA6 in yeast two-hybrid experiments, and in *csi1* mutants cellulose content was reduced and the plants showed defects in hypocotyl and root elongation (Gu et al., 2010). Further analysis also showed that the

CESA complexes displayed reduced motility in *csi1* mutants (Gu et al., 2010). In *Arabidopsis*, the movement of CESA complexes was thought to be guided by cortical microtubules (Paredez et al., 2006), and CSI1 has been proposed to mediate the association between CESA complexes and cortical microtubules (Lei et al., 2012; Li et al., 2012).

There are two additional *CSI1* homologs in the *Arabidopsis* genome (Gu et al., 2010). The expression of *CSI2* is restricted to male reproductive tissues, while *CSI3*, like *CSI1*, is widely expressed (Lei et al., 2013). Disruption of *CSI3* causes phenotypes similar to that in *csi1* mutants (Lei et al., 2013). Like CSI1, CSI3 also associates with primary CSCs (Lei et al., 2013). An enhanced cell expansion defect was observed in *csi1/csi3* double mutants (Lei et al., 2013). However, expression of *CSI3* under the control of the *CSI1* promoter failed to rescue *csi1* mutant phenotypes (Lei et al., 2013). Also, little co-localization between CSI1 and CSI3 was observed (Lei et al., 2013). These results have been interpreted to indicate that CSI1 and CSI3 might interact with distinct CSC populations, which if true, raises the potential for heterogeneity in CSC populations (Lei et al., 2013).

KORRIGAN (KOR) proteins are a unique class of integral membrane proteins containing endo-β-1,4-D-glucanase domains, which are required for cell wall assembly in *Arabidopsis* (Nicol et al., 1998). KOR1 has been shown to associate with CESA1, CESA3, or CESA6 in yeast two-hybrid studies and fluorescent fusions of KOR1 and

CESA proteins co-localize in CSCs *in planta* (Vain et al., 2014). Mutations of *KOR1* caused defects in cell elongation, cytokinesis, and the organization of cellulose microfibrils (Nicol et al., 1998; Zuo et al., 2000; Lei et al., 2014; Vain et al., 2014). Based on these observations it was proposed that KOR1 proteins might act like a regulatory component in the CSC by releasing the tensional stress generated during cellulose microfibrils assembly, regulating the length of individual glucan chains, or by releasing cellulose microfibrils from the CSC (Mølhøj et al., 2002; Somerville, 2006; Ueda, 2014). However, the detailed role of this cellulase during cellulose synthesis is still unknown (Ueda, 2014). Two additional *KOR1* homologs, *KOR2* and *KOR3,* are found in *Arabidopsis* (Mølhøj et al., 2001). Unlike *KOR1*, *KOR2* and *KOR3* are expressed in restricted cell types such as mature root hairs or trichome support cells (Mølhøj et al., 2001). Combined, these results indicate that KOR1 is an integral part of primary CSCs, while KOR2 and KOR3 might also be required for cellulose synthesis in some specific cell types.

*COBRA* encodes a glycosylphosphatidylinositol (GPI) anchored protein which when mutated resulted in defective cell expansion in root tissues and reduced levels of crystalline cellulose (Schindelman et al., 2001). A further link between *COBRA* activity and cellulose biosynthesis was subsequently identified when this gene was shown to display high degrees of coordinated expression with *CESA* genes (Persson et al., 2005). COBRA proteins were shown to interact with both individual β-1,4-linked glucan chains

and crystalline cellulose *in vitro*, but had higher affinity for individual glucan polymers (Sorek et al., 2014). Therefore, current models propose that COBRA proteins function to facilitate cellulose crystallization by acting as cellulose chaperones as individual glucan polymers emerge from the CSC (Sorek et al., 2014; Goodman, 2014).

Despite the essential role of CESA1, CESA3, and CESA6 in synthesizing cellulose, disruption of these three genes does not significantly affect root hair tip growth, a process requiring proper cellulose deposition at the growing tip (Gu and Nielsen, 2013). In *Arabidopsis*, CESA proteins belong to a large superfamily in which other six cellulose synthase like (CSL) protein families can be found (Figure 1.3) (Richmond and Somerville, 2000). It has been proposed that members from the CSLD family, a CSL family that shares highest amino acid sequence identity with the CESA family, might function as cellulose synthases during root hair tip growth (Park et al., 2011). This was supported by the discovery that only functional eYFP-CSLD3 proteins, not GFP-CESA3 or YFP-CESA6 proteins, were observed to be enriched in the apical plasma membranes of growing root hairs, a region where high levels of new cellulose synthesis were observed (Park et al., 2011; Galway et al., 2011). Additionally, a chimeric CSLD3 fusion protein in which the CSLD3 catalytic domain was replaced with the catalytic domain of CESA6 was able to rescue the phenotype of *csld3* mutants (Park et al., 2011). These results indicated that other than the CESA proteins, at least some members of the CSLD family, such as CSLD3, might also provide β-1,4- linked glucan synthase activity.

However, CSLD proteins have also been suggested to synthesize xylan, homogalacturonan, or mannan polysaccharides (Bernal et al., 2007; Yin et al., 2011). As a result, the true nature of CSLD biochemical activity remains an open question.

Hemicelluloses, whose backbones are made of various β-1,4-linked polysaccharides, include xyloglucans, xylans, and mannans (Cosgrove, 2005; Liepman et al., 2010; Scheller and Ulvskov, 2010). In the *Arabidopsis* primary cell wall, xyloglucan is the most abundant class of hemicelluloses (Liepman et al., 2010). Like cellulose, the backbone of xyloglucan is made of β-1,4-linked glucan polymer (Liepman et al., 2010). However, its backbone is extensively modified with side chains containing xylosyl, galactosyl, and fucosyl residues, and this elevated level of side chain branching is believed to increase xyloglucan solubility (Liepman et al., 2010; Scheller and Ulvskov, 2010). Due to the structural complexity of these xyloglucan side chains, xyloglucan biosynthesis requires at least four distinct enzyme classes for the synthesis of β-1,4-linked glucan backbone and the successive addition of xylosyl, galactosyl, and fucosyl residues (Liepman et al., 2010). Members of the CSLC protein family are thought to be responsible for the synthesis of the β-1,4-linked glucan backbone of xyloglucan. This is based on two lines of evidence. First, cDNAs of the nasturtium (*Tropaeolum majus*) *TmCSLC* gene were found to be highly enriched in tissues from developing seeds, which accumulate high levels of xyloglucan as a storage compound (Cocuron et al., 2007). Second, heterologous expression of the *Arabidopsis CSLC4* coding sequence, which contains the highest

sequence similarity to *TmCSLC,* in the yeast *Pichia pastoris* confirmed its β-1,4 glucan synthase activity (Cocuron et al., 2007). Therefore, at least some members of the *CSLC* family are responsible for xyloglucan backbone synthesis (Liepman et al., 2010; Liepman and Cavalier, 2012).

Enzymes from at least three glycosyltransferases families are involved in the modification of xyloglucan backbones. In *Arabidopsis,* XXT proteins are xylosyltransferases and they add xylosyl residues to β-1,4 glucan backbones (Faik et al., 2002; Cavalier and Keegstra, 2006; Zabotina et al., 2008). MUR3 protein was identified as a galactosyltransferase and it adds galactosyl residues to specific xylosyl residues during xyloglucan synthesis (Madson et al., 2003). Some of these galactosyl residues are further fucosylated via a fucosyltransferase called FUT1 (Perrin et al., 1999; Vanzin et al., 2002). Disruption of these genes altered the glycosyl residue composition of xyloglucan in the respective mutant lines (Vanzin et al., 2002; Madson et al., 2003; Cavalier et al., 2008). It has been recently shown that XXT1, XXT2, XXT, MUR3, FUT1, and CSLC4 are able to form multi-protein complexes in Golgi, further supporting their roles in xyloglucan synthesis (Chou et al., 2012, 2014).

A previously unidentified acidic xyloglucan was recently found to be present in *Arabidopsis* root hair cell walls (Peña et al., 2012). In these xyloglucan polymers, a β-D-galactosyluronic acid-1,2-α-D-xylosyl linkage was formed by a xyloglucan-specific galacturonosyltransferase (*XUT1*) (Peña et al., 2012). In some cases, the galactosyluronic

acid was further fucosylated by FUT1 (Peña et al., 2012). This acidic xyloglucan was shown to play important roles in root hair growth as mutation of *XUT1* resulted in a reduction of root hair length (Peña et al., 2012). The authors proposed that the acidic xyloglucan might function in maintaining the random orientation of the cellulose microfibrils at the growing root hair tips (Peña et al., 2012).

Hemicelluloses were previously thought to make the cell wall a strong and resilient network by non-covalently interacting and tethering cellulose microfibrils (Somerville et al., 2004; Cosgrove, 2005; Scheller and Ulvskov, 2010). However, no significant growth defects except shorter root hairs were observed in *xxt1/xxt2* double mutant, an *Arabidopsis* mutant with no detectable xyloglucan (Cavalier et al., 2008). Therefore it is now believed that xyloglucan hemicelluloses are not indispensable elements of the cell wall and a re-examination of the precise roles of this class of cell wall polysaccharides is needed (Scheller and Ulvskov, 2010).

Pectins are the most structurally complex polysaccharides in cell wall and they comprise approximately 35%-40% of the primary cell wall in *Arabidopsis* (Mohnen, 2008; Liepman et al., 2010). Pectins are believed to be covalently linked with each other (Mohnen, 2008). Recently evidence has been presented that pectins might also associate with cellulose and xyloglucan (Mohnen, 2008; Scheller and Ulvskov, 2010). In the primary cell wall, cross-linked pectic polysaccharides are thought to form hydrated gels

that help to separate individual microfibrils, and it is thought that this sequestration helps facilitate microfibril slippage during cell growth (Cosgrove, 2005).

Homogalacturonan (HG), rhamnogalacturonan I (RG-I), and rhamnogalacturonan II (RG-II) are three major pectin forms, whose biosynthesis requires at least 67 glycosyltransferases, methyltransferases, and acetyltransferases due to their structural complexity (Mohnen, 2008; Liepman et al., 2010). Homogalacturonan (HG) is the most abundant pectic polysaccharide and it comprises about 65% of total pectin (Mohnen, 2008). Unlike cellulose and xyloglucan, which contain backbones of β-1,4-linked glucan polymers, the backbone of HG is made of α-1,4-linked galacturonic acids (Mohnen, 2008). In *Arabidopsis*, the synthesis of HG requires GAUT1 (Galacturonosyltransferase 1) (Sterling et al., 2006). GAUT1 is a Golgi localized type II membrane protein (Sterling et al., 2006). However, later results called this localization into doubt, since the N-terminus of GAUT1, including the transmembrane domain, is post-translationally cleaved *in vivo* (Atmodjo et al., 2011). Further investigation showed that GAUT1 was still retained in Golgi by interacting with GAUT7 (Galacturonosyltransferase 7), another Golgi localized type II membrane protein (Atmodjo et al., 2011). Based on these results, the GAUT1 – GAUT7 complex was thought to serve as a catalytic core in the current model of HG biosynthesis (Atmodjo et al., 2011, 2013).

GAUT8 (Galacturonosyltransferase 8) and GAUT12 (Galacturonosyltransferase 12) proteins may also have HG synthesis function since galacturonic acid levels were

significantly reduced when either of these two genes were mutated (Bouton et al., 2002; Biswal et al., 2015). Interestingly, the level of xylan was also reduced in these mutants, perhaps revealing connections between the biosynthesis of HG and the biosynthesis of xylan (Orfila et al., 2005; Biswal et al., 2015).

Rhamnogalacturonan I is the second most abundant polysaccharide in pectin (Mohnen, 2008). RG I contains a backbone region consisting of a repeating rhamnose-galacturonic acid disaccharide subunit, and branching oligosaccharides that are attached to this backbone (Mohnen, 2008). Due to the structural complexity of RG1, multiple glycosyltransferases including galacturonosyltransferases, rhamnosyltransferases, galactosyltransferases, and arabinosyltransferases are required for its biosynthesis (Atmodjo et al., 2013). The synthesis of the RG I backbone might require GATL5 (Galacturonosyltransferase Like 5), based on the observation that *gatl5* mutants display significantly reduced levels of galacturonic acid and rhamnose contents extracted from digested seed mucilage (Kong et al., 2013). However, the exact role of *GATL5* still needs further investigation (Kong et al., 2013). In addition to the putative enzyme synthesizing the RG I backbone, some of the enzymes responsible for branching oligosaccharide synthesis have also been identified. It was recently shown that the activity of GALS1 (Galactan Synthase 1) was associated with the elongation of branching galactans (Liwanag et al., 2012). The β-1,4-linked galactan content was reduced in *gals1* mutants while the content was increased by 50% in the GALS1 overexpressing plants (Liwanag et

al., 2012). Biochemical assays confirmed that GALS1 is a galactosyltransferase (Liwanag et al., 2012). It was also proposed that GALS2 (Galactan Synthase 2) and GALS3 (Galactan Synthase 3), two proteins from the same glycosyltransferase family, may also have the same function (Liwanag et al., 2012). Additionally, *ARAD1* (*Arabinan Deficient 1*) and *ARAD2* (*Arabinan Deficient 2*) were shown to participate in synthesizing pectic arabinan (Harholt et al., 2006, 2012). In *arad1* mutants, the arabinose content was reduced significantly (Harholt et al., 2006). Also, an increase of unsubstituted arabinan epitope was observed in *arad2*, indicating ARAD2 was required for the proper elongation of arabinosyl polymers (Harholt et al., 2012). Furthermore, the interaction between ARAD1 and ARAD2 was confirmed by Bimolecular Fluorescence Complementation (BiFC) and Förster Resonance Energy Transfer (FRET) (Harholt et al., 2012). These results support assembly of a putative ARAD1-ARAD2 complex that might play important roles in arabinan side chain biosynthesis (Harholt et al., 2012). However, despite this progress, the molecular machinery responsible for RG I backbone and side chain synthesis still remain largely uncharacterized (Atmodjo et al., 2013).

While RG I contains a backbone region consisting of repeating rhamnose-galacturonic acid disaccharide subunits, rhamnogalacturonan II (RG II) instead has a HG-like homogalacturonan backbone domain, and domains where this HG-backbone contains branched side chains (Mohnen, 2008). Currently it remains unknown whether the GAUT proteins identified for the biosynthesis of homogalacturonan might also synthesize the

HG backbone of RG II (Funakawa and Miwa, 2015). RGXT1 (Rhamnogalacturonan xylosyltransferase 1) and RGXT2 (Rhamnogalacturonan xylosyltransferase 2) are among the few enzymes that have been characterized for RG II side chain synthesis (Egelund et al., 2006).

To summarize, cellulose, hemicelluloses, and pectins are three major classes of polysaccharides found in the *Arabidopsis* primary cell wall. They interact to form a complex network and thus provide required structural integrity and resilience for the plant cell wall. Cellulose, the major load-bearing component, is synthesized by plasma membrane localized cellulose synthase complexes. Based on current knowledge, CESA, CSI, and KORRIGAN proteins are integral parts of the CSC, while COBRA is also thought to participate in the assembly of the cellulose microfibrils. Meanwhile, hemicellulose and pectins are synthesized by Golgi localized proteins or multi-protein complexes. Although great numbers of cell wall synthases as well as CSC associated proteins have been identified in the past two decades, there are still many missing pieces in our understanding of how plant cell wall polysaccharide biosynthesis occurs in *Arabidopsis*.

**Major structural protein classes involved in cell wall deposition**

It has been estimated that about ten percent of the genes in *Arabidopsis* are related to cell wall biosynthesis (McCann and Carpita, 2008). In addition to the polysaccharide synthases, structural proteins involved in controlling cell expansion, regulating polysaccharide assembly, and sensing cell wall integrity also play major roles in the assembly and deposition of plant cell walls. It is likely that these cell wall proteins, along with their cell wall polysaccharide counterparts, also regulate the physical characteristics of the plant cell wall (Gu and Nielsen, 2013).

Expansins are proteins required for cell wall loosening and cell expansion (Sampedro and Cosgrove, 2005). It is believed that expansins perform wall loosening activities by physically separating cellulose and associated cell wall polysaccharides in a non-enzymatic mechanism (Sampedro and Cosgrove, 2005). The expansin gene family is divided into four distinct subgroups based on sequence similarity. These families are called α-expansins (EXPA), β-expansins (EXPB), expansin-like A (EXLA), and expansin-like B (EXLB) (Sampedro and Cosgrove, 2005). Studies in various species have confirmed cell wall loosening activities for both EXPA and EXPB proteins (Sampedro and Cosgrove, 2005). In *Arabidopsis*, upregulation of *EXPA10* increased cell length and the diameter of the rosette leaf cluster, while downregulation of *EXPA10* caused smaller cells and malformed leaves (Cho and Cosgrove, 2000). In rice, reducing the expression level of *EXPA4* by expressing antisense *EXPA4* RNA caused smaller cells and shorter plants (Choi et al., 2003) On the other hand, the length of coleoptile and

mesocotyl cells were increased in plants overexpressing *EXPA4* (Choi et al., 2003). When exogenously applied, purified *Zea mays* EXPB proteins induced extension of cell walls from maize, wheat, rice, and other grass species (Li et al., 2003). Proper levels of expansin expression are also required to maintain tip-growth for root hairs. Treatment of exogenously applied EXPA proteins caused cucumber root hair tips to burst in a dose-dependent manner (Cosgrove et al., 2002). On the other hand, downregulation of *EXPA7* using RNAi-based techniques shortened root hair length (Lin et al., 2011). The roles of *EXLA* and *EXLB* in cell wall deposition are not clearly understood (Sampedro and Cosgrove, 2005). Very recently it was shown that overexpression of *EXLA2* increased *Arabidopsis* root length and dark-grown hypocotyl length (Boron et al., 2015). Therefore a role of *EXLA* in inducing cell wall extension is also supported.

In addition to the expansins, *Arabidopsis* also contains a large family of plant cell wall structural proteins called hydroxyproline-rich glycoproteins (HRGPs) (Showalter, 1993). In HRGPs, specific proline residues are hydroxylated into hydroxyprolines (Hyp), which can be further modified by O-glycosylation (Kieliszewski and Lamport, 1994). Extensins, proline rich proteins (PRPs), and arabinogalactan rich proteins (AGPs) are three major classes of HRGPs (Showalter, 1993). There are twenty extensin genes in *Arabidopsis* (Cannon et al., 2008). Disruption of one extensin gene, *EXT3* (*Extensin 3*), resulted in defective cell walls in multiple tissues (Hall and Cannon, 2002; Cannon et al., 2008). Proline residues in the extensin-like HRGP proteins are first hydroxylated by

prolyl-4-OH hydroxylases and the newly formed Hyps can then be further modified by arabinosyltransferases (Velasquez et al., 2011; Ogawa-Ohnishi et al., 2013). The first arabinose is incorporated onto Hyp residues by HPATs, a group of hydroxyproline O-arabinosyltransferases (Ogawa-Ohnishi et al., 2013). The second and third arabinoses are then added by RRA3 (Reduced Residual Arabinose 3) and XEG113 (Xyloglucanse 113), respectively (Velasquez et al., 2011). Recently it has been shown that extensin proteins are able to self-assemble through tyrosine residues using reactive oxygen species to form covalent cross-links. In this manner, it is thought that these extensin proteins generate covalently-linked protein network within the plant cell wall (Cannon et al., 2008; Lamport et al., 2011). This positively charged, protein network may then recruit pectins and provide scaffold for the organization of cell wall polysaccharides (Cannon et al., 2008). Evidence has been presented that appropriate cell wall assembly requires O-glycosylation (mainly by arabinosylation) of these extensin proteins (Velasquez et al., 2011; Ogawa-Ohnishi et al., 2013), and a model was proposed to explain how the arabinosyl residues are sequentially added onto the hydroxyl residue of Hyp (Velasquez et al., 2011; Ogawa-Ohnishi et al., 2013).

Proline rich proteins (PRPs), a family of proteins characterized by repeating PPVYK or PPVEK motifs, also contribute to cell wall structure (Showalter, 1993). Four *PRP* genes and one *PRP*-like gene were identified in *Arabidopsis* (Fowler et al., 1999). One of these *PRP*s, *PRP3*, is specifically expressed in root hair cells and its expression level is

tightly connected to root hair development (Bernhardt and Tierney, 2000). The expression of *PRP3* was induced when GL2 (Glabra 2) protein, a transcriptional factor inhibiting root hair formation, was mutated, while the expression of *PRP3* was reduced in *rhd6* mutants, whose root hair growth was abolished (Bernhardt and Tierney, 2000). Similarly, expression levels of *PRP3* were increased or decreased when the seedlings were respectively treated by root hair promoting or inhibiting chemicals (Bernhardt and Tierney, 2000). These results indicated that *PRP3* might have a role during *Arabidopsis* root hair formation (Bernhardt and Tierney, 2000). However, a recent study showed that the root hairs in *prp3* mutants had similar morphology and cell wall polymer epitopes to wild type root hairs (Larson et al., 2014). The lack of phenotype might be due to the functional redundancy among *PRP*s and the *PRP*-like gene. In 2014, *PRP*-like gene 1 (*PRPL1*) was shown to regulate root hair elongation (Boron et al., 2014). The root hair length was increased or decreased when *PRPL1* was overexpressed or mutated, respectively (Boron et al., 2014). However, similar to what was observed in *prp3* mutants, the cell wall composition of root hairs was not changed in *prpl1* compared to that in wild type (Boron et al., 2014). Therefore the exact roles of PRPs and PRP-like proteins in cell wall formation remain an open question.

Arabinogalactan rich proteins (AGPs) are a specific class of highly glycosylated HRGPs (Showalter, 1993). Eighty-five *AGP* genes have been identified in the *Arabidopsis* genome, including twenty two classical *AGP*s, three *AGPs* containing Lys-

rich domains, sixteen genes encoding arabinogalactan peptides (proteins of 50 to 90 amino acids in length consisting of 35% or greater Pro, Ala, Ser, and Thr residues), twenty one chimeric fasciclin-like *AGP*s, seventeen chimeric plastocyanin *AGP*s, and six other chimeric *AGP*s (Showalter et al., 2010). These AGPs were identified based on their amino acids compositions, predicted molecular sizes, and other structural domains (Showalter et al., 2010). For example, classical AGPs contain more than 50% of Pro, Ala, Ser, and Thr residues, while a fasciclin-like domain could be found in fasciclin-like AGPs (Showalter et al., 2010). The Pro residues in the AGP backbone are mostly hydroxylated (Gaspar et al., 2001). It was proposed that GALT2 (AGP Galactosyltransferase 2) initiated the AGP galactosylation since it added a galactosyl residue to Hyp residues of synthetic AGP-like peptides *in vitro* (Basu et al., 2013). A group of β-1,3-galactosyltransferases might be involved in elongating the β-1,3-galactan backbone of AGP side chains (Qu et al., 2008; Liang et al., 2010). Other β-1,6-galactosyltransferases, α-1,3-arabinosyltransferases, α-1,5-arabinosyltransferases, and α-1,2-fucosyltransferases are also required for the synthesis of AGP side chains (Nguema-Ona et al., 2014). With these extensive post-translational modifications, individual arabinogalactan (AG) chains may consist of up to 120-150 sugar residues (Gaspar et al., 2001; Tan et al., 2013).

Proper glycosylation is essential for the functions of AGPs (Nguema-Ona et al., 2014). Disruption of fucosyltransferases required for AGP modification caused reduction

in root growth (Van Hengel and Roberts, 2002; Wu et al., 2010; Liang et al., 2013; Tryfona et al., 2014). In *Arabidopsis glcat14a* (*β-glucuronosyltransferase 14a*) mutants, the composition of arabinogalactan was altered and root elongation rates were shown to be significantly increased (Knoch et al., 2013). Intriguingly, one recent study has revealed that at least one form of AGP, APAP1 (Arabinoxylan Pectin Arabinogalactan Protein 1), can be found covalently attached to hemicellulose and pectin polysaccharides (Tan et al., 2013). A potential cross-linking role, in which AGPs are integrated into a covalent peptidoglycan network along with other plant cell wall polysaccharides, provides yet another mechanism by which distinct elements of the plant cell wall interact.

In conclusion, structural cell wall proteins play essential roles in cell wall deposition. Expansins have putative functions in loosening non-covalent cell wall polysaccharide interactions and they facilitate cell wall remodeling during cell expansion. Extensins, PRPs, and AGPs, three major classes of HRGPs, potentially function in assembling cell walls by forming covalently-linked scaffolds onto which cell wall polysaccharides can associate.

**Receptor like kinases involved in sensing cell wall integrity**

It has been proposed that a family of receptor like kinases (RLK), the *Catharanthus roseus* RLK1-like (CrRLK1L) family, may have important functions in sensing cell wall

integrity and regulating cell wall formation (Hématy and Höfte, 2008; Cheung and Wu, 2011; Boisson-Dernier et al., 2011). FERONIA (FER) was the first member characterized in this family (Huck, 2003). Originally FER was shown to function in the synergid cells of the female gametophyte, through which FER protein regulates the male-female interaction during pollen tube perception (Huck, 2003; Escobar-Restrepo et al., 2007). In *fer* mutants, the release of sperm nuclei for fertilization is affected because growing pollen tube tips fail to rupture after reaching the synergids (Huck, 2003; Escobar-Restrepo et al., 2007). In the current model, FER recognizes an as of yet undefined signal, but possibly specific polysaccharides of these pollen tubes and triggers the initiation of a signaling cascade that results in the rupture of the pollen tube (Boisson-Dernier et al., 2011). FER was later demonstrated to play an essential role in root hair growth and severe root hair growth defects were observed in *fer* T-DNA insertional mutants (Duan et al., 2010). In a pull down assay, FER was shown to interact with a ROP2 in a guanine nucleotide-regulated manner, indicating that the function of FER in root hair growth requires RAC/ROP signaling pathway which regulates reactive oxygen species (ROS) mediated root hair initiation and development (Duan et al., 2010). Interestingly, it was also shown that FER played roles in pathogen defense recognition, as *fer* mutants were resistant to powdery mildew infection (Kessler et al., 2010). Based on the potential ability to recognize cell wall signals during development or pathogen invasion, FER was proposed to serve as a part of a self-sensory system in regulating cell growth (Cheung and Wu, 2011).

Additional members from the CrRLK1L family have also been identified as potential cell wall sensors (Hématy and Höfte, 2008; Cheung and Wu, 2011; Boisson-Dernier et al., 2011). ANXUR1 and ANXUR2, which share the highest sequence similarity to FER in the CrRLK1L family, were shown to function redundantly in inhibiting pollen tube rupture (Miyazaki et al., 2009; Boisson-Dernier et al., 2009). It was proposed that ANXUR1 and ANXUR2 were deactivated by the FER mediated signaling cascade upon the arrival of pollen tubes, causing the rupture of pollen tubes and the release of sperm nuclei (Boisson-Dernier et al., 2009). THESEUS1 was initially identified as a partial suppressor for *cesa6* mutants (Hématy et al., 2007). In *the1/cesa6* double mutants, dark-grown hypocotyl growth defects were partially rescued (Hématy et al., 2007). Interestingly, *theseus1* single mutants did not display noticeable hypocotyl elongation phenotypes (Hématy et al., 2007). These results indicated that the activation of THESEUS1 required the presence of defects in cellulose synthesis, and therefore the THESEUS1 protein was proposed to function in sensing cell wall integrity (Hématy et al., 2007; Hématy and Höfte, 2008). Another CrRLK1L protein, HERCULES1, was shown to stimulate cell elongation when overexpressed (Guo et al., 2009). Although both *theseus1* and *hercules1* single mutants have no obvious phenotypes, the *theseus1/hercules1* double mutants showed a severe dwarf phenotype, indicating THESEUS1 and HERCULES1 may function redundantly in controlling cell elongation (Guo et al., 2009).

Despite the roles proposed for CrRLK1L in cell wall integrity sensing, the ligands for these RLKs as well as their downstream genes has remained largely unknown. Surprisingly, a peptide hormone, RALF, was recently shown to be recognized by FER and the phosphorylation level of FER was increased upon interaction of this ligand with FER (Haruta et al., 2014). Also, two glycosylphosphatidylinositol-anchored proteins (GPI-AP), LORELEI (LRE) and LRE-like GPI-AP1 (LLG1), were recently demonstrated to act as co-receptors for FER signaling (Li et al., 2015). Gene expression profiling also showed that the expression of many cell wall related genes were affected when these RLKs were mutated (Duan et al., 2010; Guo et al., 2009). Future work based on these recent discoveries could help us to better understand the classes of upstream signals, the structure of signaling complexes, and downstream targets of CrRLK1L receptor kinases.

To conclude, the CrRLK1L receptor like kinase family may provide mechanisms by which cell wall integrity can be detected and subsequently regulate cell wall deposition by triggering downstream signaling cascades. However, the detailed molecular mechanisms by which these distinct classes of polysaccharides and proteins participate in cell wall deposition remains largely undetermined.

**Cell wall synthesis during cell division**

In multicellular organisms development and differentiation is associated with successive rounds of cell division in self-renewing populations of embryonic and post-embryonic stem cells (Heidstra and Sabatini, 2014). Unlike most other eukaryotes, which undergo contractile cytokinesis to separate daughter cells upon completion of mitosis (Guertin et al., 2002), plants instead deposit a new dividing cell wall which is formed across the plane of division and separates the two daughter cells (Jürgens, 2005; Inagaki and Umeda, 2011) (Figure 1.4).

During plant cell division, the phragmoplast, a cytokinesis-specific microtubule-based array, is formed at the dividing plane during late anaphase (Jürgens, 2005). Golgi-derived vesicles are transported to the center of phragmoplast array, where these vesicles fuse to generate a transient membrane compartment, the cell plate (Seguí-Simarro et al., 2004; Jürgens, 2005). As additional Golgi-derived vesicles fuse with this newly-formed membrane compartment, the cell plate grows in a centripetal fashion towards the plasma membranes at the edges of the dividing cell. During this process the associated phragmoplast microtubules in the middle of the cell plate depolymerize, and new ones are formed at the cell plate margins (Seguí-Simarro et al., 2004; Jürgens, 2005). Golgi-derived vesicles are therefore continuously directed to and fuse with the leading edge of the growing cell plate, until eventually membranes surrounding the cell plate fuse with parental plasma membranes and physically separate the two newly-formed daughter cells (Jürgens, 2005).

During cell plate elongation, a new cell wall is synthesized in the cell plate lumen (Jürgens, 2005). The existence of xyloglucan in the cell plate was confirmed by immunogold labeling technique (Moore and Staehelin, 1988). Therefore it was suggested that cell wall polysaccharides such as hemicellulose and pectin, which are synthesized in Golgi, are delivered to the cell plate as vesicle cargo (Jürgens, 2005). Callose, which is a β-1,3-linked glucan polymer, was also found in these cell plates (Kakimoto and Shibaoka, 1992; Samuels et al., 1995), and CalS1 (Callose Synthase 1) may function as a cell plate-specific callose synthase (Hong et al., 2001). GSL8 (Glucan Synthase Like 8), another callose synthase, is also required for the new cell wall synthesis during cell division since incomplete cell walls were found in *gsl8* mutants (Chen et al., 2009; Thiele et al., 2009). Cell plate callose is thought to be replaced by cellulose and other cell wall polysaccharides during maturation of this newly-formed cell plate (Samuels et al., 1995). While this occurs the previously deposited callose in the cell plate is degraded by β-1,3-glucanase (Jürgens, 2005; Chen and Kim, 2009). Consistent with this model, cellulose was found in the developing cell plate when the seedlings were stained by a cellulose dye Pontamine Fast Scarlet 4B (Miart et al., 2014). Three distinct primary cellulose synthase isoforms, CESA1, CESA3, and CESA6, were also found to be localized in the cell plate (Miart et al., 2014).

**What roles do *CSLD* genes perform in tissues other than tip-growing cells?**

Cellulose synthase (CESA) and cellulose synthase like (CSL) proteins are thought to be processive β glycosyltransferases (Saxena et al., 1995). Among these protein families, CSLD family has higher structural similarity to CESA family than either of these two groups show to other CSL family (Richmond and Somerville, 2000). There are six *CSLD* genes in the *Arabidopsis* genome. Before I began my thesis research, the activities of *CSLD* were shown to be largely correlated with tip growth of *Arabidopsis* root hairs and pollen tubes (Favery et al., 2001; Wang et al., 2001; Bernal et al., 2008). However, three of these *CSLD* genes, *CSLD2*, *CSLD3*, and *CSLD5*, were shown to be broadly expressed in various tissues (Bernal et al., 2008), indicating that the function of these *CSLD* genes might not be restricted to tip growing cells. Consistent with this, disruption of *CSLD5* reduced the mutant size (Bernal et al., 2007). Given these results, there seemed to be a reasonable chance that these *CSLD* genes might also have roles in vegetative tissue development.

**Statement of problem and attribution**

There are six *CSLD* genes in the *Arabidopsis* genome and they displayed distinct expression patterns. *CSLD1* and *CSLD4* were shown to be highly expressed in pollen, while *CSLD6* was thought to be a pseudogene due to its extreme low expression level in all tissues examined (Bernal et al., 2008). The remaining three genes, *CSLD2*, *CSLD3*,

and *CSLD5* were shown to be broadly expressed in various tissues (Bernal et al., 2008). Consistent with their distinct expression patterns, these *CSLD* genes played roles in different tissues. *CSLD1* and *CSLD4* were required for pollen tube tip-growth (Bernal et al., 2008; Wang et al., 2011), while *CSLD2* and *CSLD3* played essential roles for root hair tip-growth (Favery et al., 2001; Wang et al., 2001; Bernal et al., 2008; Park et al., 2011; Galway et al., 2011). However, although *CSLD5* displayed a similar broad expression pattern as that for *CSLD2* or *CSLD3*, whether *CSLD5* also participates in root hair tip-growth was not investigated. Additionally, although the expression of *CSLD2*, *CSLD3*, and *CSLD5* was not restricted to root hair cells, potential roles in other tissues had not been demonstrated. As a result, the initial goal of my thesis research was to determine whether *CSLD5* also played a role in root hair tip-growth. An additional goal was to examine whether *CSLD2*, *CSLD3*, and *CSLD5* were involved in *Arabidopsis* vegetative tissue growth.

Determining the roles these *CSLD* genes play in various tissues will aid in understanding the cell wall synthesis during different developmental processes. This will further facilitate the understanding of the biochemical activities of these CSLD proteins in the future when more complete knowledge of distinct polysaccharides compositions in cell walls from different tissues becomes available.

Chapter Two describes the role and the unique protein dynamics of CSLD5 during cytokinesis. I performed all the experiments presented in this chapter and those

experiments were the main body of a submitted manuscript which is the result of a collaboration with the laboratory of Dominique Bergmann at Stanford University. I wrote the initial draft of the manuscript, which was later revised by Erik Nielsen and Dominique Bergmann. In addition to the experiments I performed, for this manuscript, Dominique Bergmann provided transcriptome data showing *CSLD5* was regulated directly by SPCH, and Martin Bringmann provided data showing CSLD5 was localized on cell plates in stomata lineage cells and disruption of *CSLD5* caused stomatal patterning and division defects.

Chapter Three describes the examination of functional redundancy of *CSLD2*, *CSLD3*, and *CSLD5* activities. I performed all the experiments in this chapter. The data in this chapter may form the basis of a future published manuscript, in which case I will be listed as either as an author or a co-author.

The appendix chapter describes the role of *LTL2*, a new temperature-sensitive allele of *FERONIA* (*FER*) receptor like kinase gene, in root hair growth. This part is based on a manuscript we have submitted, in which I am a co-author. In the manuscript, I identified that a mutation in the *FER* gene is responsible for the temperature-sensitive phenotype of *ltl2* mutants. I also examined the sub-cellular localization of FER(WT) and fer(G41S) proteins in permissive and non-permissive temperatures. The rest of the experiments described in this chapter were performed by a visiting graduate student, Daewon Kim.

In addition to the results presented in this thesis dissertation, I have been listed as an author or co-author on other publications:

I am an author of a review [Gu, F. and Nielsen, E. (2013) Journal of Integrative Plant Biology., 55(9):835-846]. I wrote this manuscript, which was later revised by Erik Nielsen.

Based on collaboration with Sungjin Park, I was listed as a co-author on a published manuscript [Park, S., Szumlanski, A., Gu, F., Guo, F. and Nielsen, E. (2011) Nature Cell Biology., 13(8):973-980]. I provided evidence that cellulose was present at the tip of growing root hairs using immunostaining based techniques. I also showed two mutated CSLD3 proteins, kjk-3 and kjk-4, failed to accumulate at the apical plasma membrane of growing root hairs.

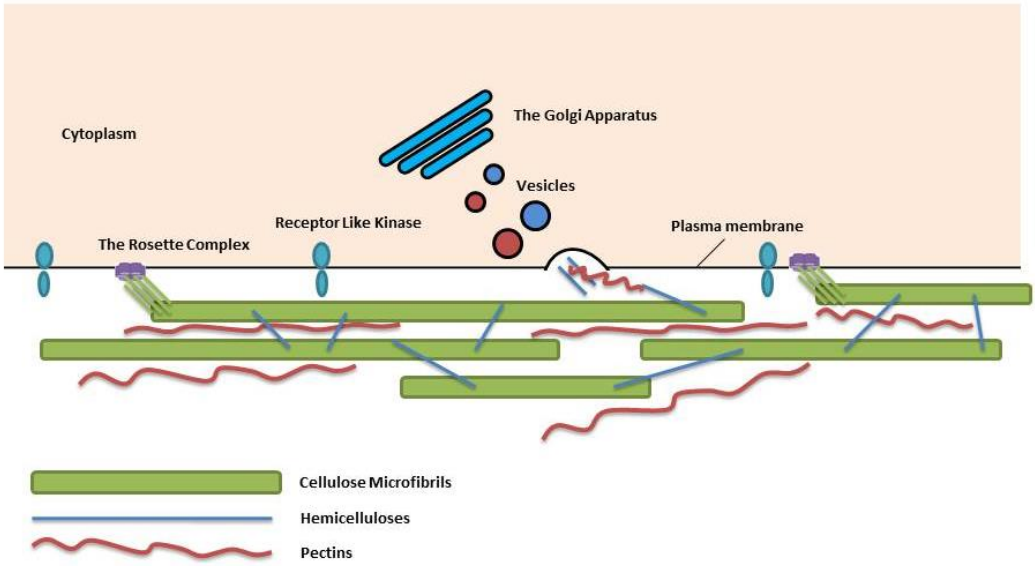


**Figure 1.1. Model of the *Arabidopsis* primary cell wall**

Schematic diagram of the *Arabidopsis* primary cell wall. The *Arabidopsis* primary cell wall contains three major classes of polysaccharides. Individual cellulose polymers (thin green lines) are synthesized at plasma membrane localized rosette complexes (purple). These polymers are further assembled into cellulose microfibrils (thick green bars) which function as the major load-bearing component of the cell wall. Hemicelluloses (blue lines) and pectins (auburn curved lines) are synthesized in Golgi apparatus. They are subsequently transported as cargo to the plasma membrane via vesicle trafficking from Golgi and incorporated into cell wall after the vesicles fuse with the plasma membrane. There they interact with cellulose microfibrils and via covalent and non-covalent crosslinking help assemble a gel like matrix. Plasma membrane localized receptor like kinases (cyan ovals) function as cell wall integrity sensors and they also participate in regulation cell wall deposition via their downstream signaling cascades.

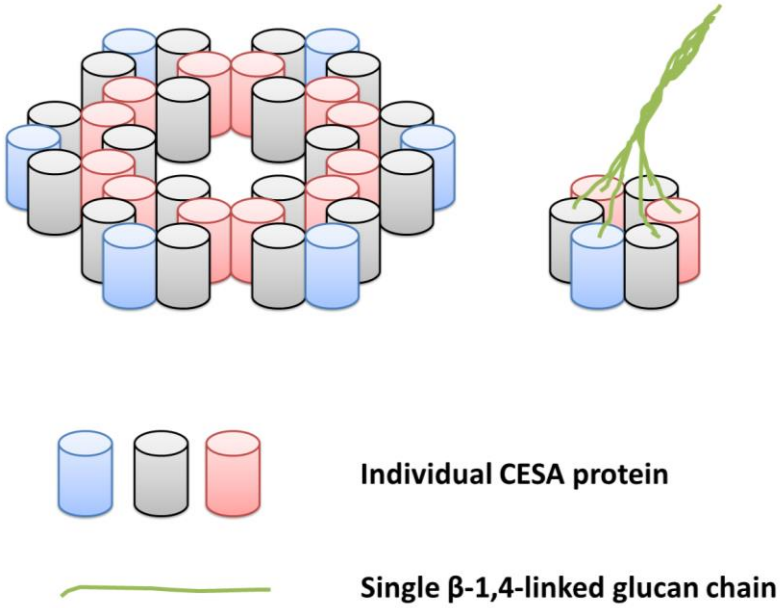


**Figure 1.2. A simplified model of the cellulose synthesis complex**

A simplified model of the cellulose synthesis complex. In this theoretical model, 36 CESA proteins containing three unique components form a rosette terminal complex with six subunits (left). One subunit consists of six individual CESA proteins (right). Each CESA protein synthesizes one β-1,4-linked glucan chain (green lines at right). These β-1,4-linked glucan chains are aligned and assembled into cellulose microfibrils.

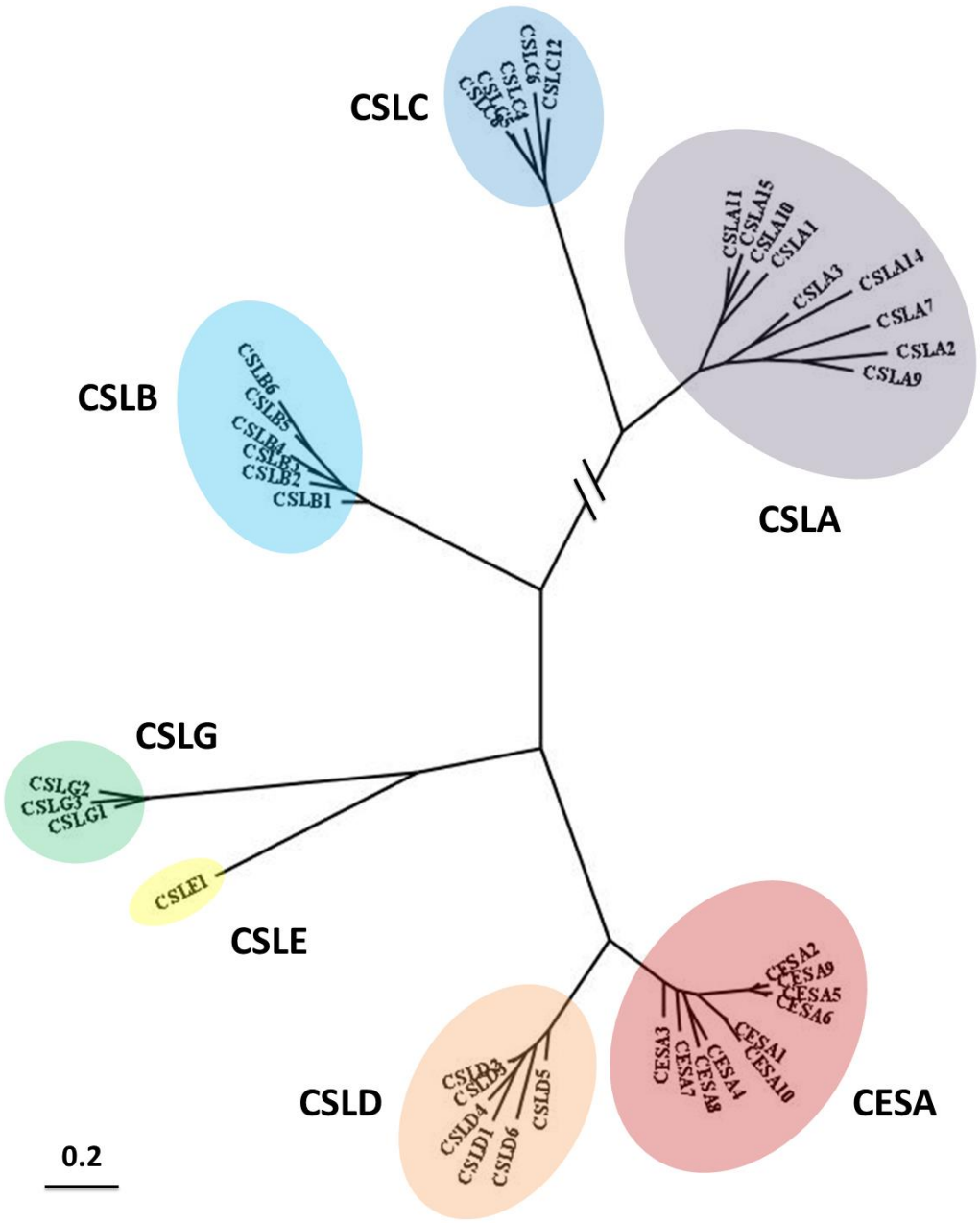


**Figure 1.3. Phylogenetic tree of the *Arabidopsis* CSL superfamily**

A phylogenetic tree of the *Arabidopsis* CSL superfamily. The unrooted tree was generated using MEGA5 (Koichiro Tamura, Glen Stecher, Daniel Peterson, and Sudhir Kumar) using the maximum likelihood method and tested by bootstrap method for 1000 times. Each clade represents a protein family. In the CSL superfamily, the CSLD family is closest to the CESA family. The tree was drawn to scale, with branch lengths represent the evolutionary distances. The broken line represents 10% of the exact length. Scale bar represents 0.2 substitutions per sequence position.

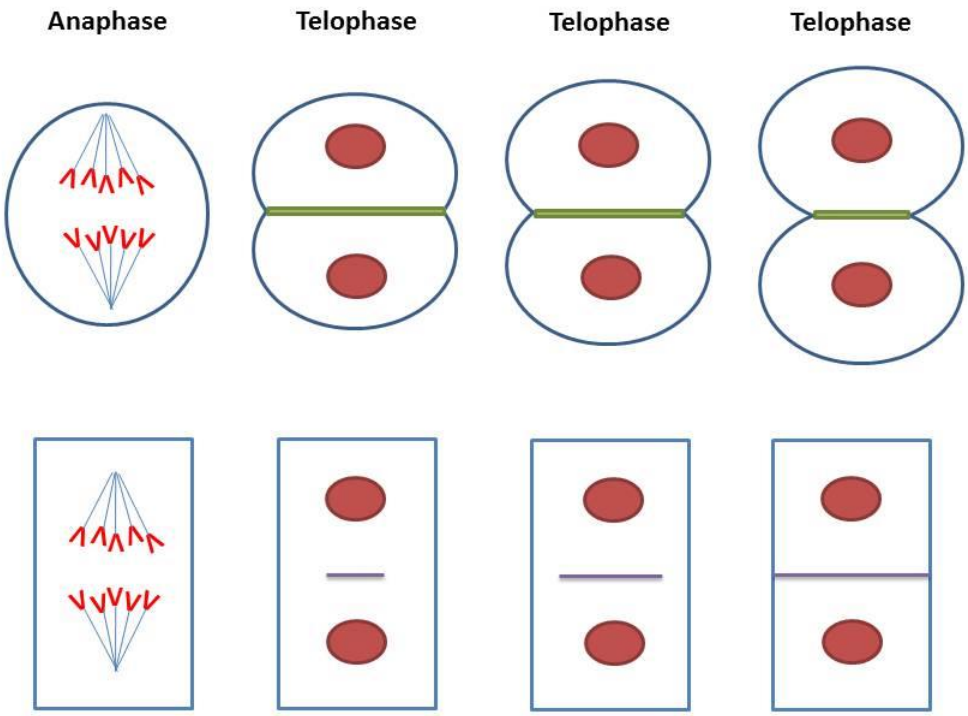


**Figure 1.4. Mechanisms of eukaryotic mitosis**

Schematic diagram of the animal mitosis (up) and plant mitosis (bottom). In animal cells (up), an actin-myosin contractile ring (green bar) cleaves the dividing cell in two. In plant cells (bottom), a new cell wall (purple line) is formed across the division plane and separates the two daughter cells.

# CHAPTER 2

# A ROLE FOR CSLD5 IN CELL WALL FORMATION DURING CELL DIVISION


## Abstract

During plant cell cytokinesis, the dividing mother cell is separated by a newly-formed cell wall across the dividing plane. The formation of this cell wall requires rapid synthesis and delivery of cell wall polysaccharides. Despite its fundamental role in plant development, plant cytokinesis is still poorly understood. In this chapter, a new role for *Arabidopsis* CSLD5 in cell wall formation during cytokinesis is reported. Disruption of *CSLD5* gene resulted in relatively mild growth and developmental phenotypes. Mutant *csld5* plants displayed shortened root length, and adult plants are about 70% the size of wild type plants. These phenotypes were strengthened in *csld2/csld5* and *csld3/csld5* double mutants. Incomplete cell walls were found in root and leaf tissues of *csld5* single or double mutants. Further examination showed that the incomplete cell walls were not caused by reduced cell plate elongation rates, supporting a role of CSLD5 in reinforcement of cell plate integrity during cytokinesis. Consistent with this, functional

Cerulean-CSLD5 proteins localized to cell plates in dividing cells. Additionally, Cerulean-CSLD5 specifically accumulated in cells undergoing cytokinesis. Comparing with the dynamics of a cell cycle marker, we found that Cerulean-CSLD5 displayed a specific and strong cell plate accumulation during cytokinesis. Upon completion of cell division, the level of Cerulean-CSLD5 was reduced rapidly. Cerulean-CSLD5 proteins were shown to be unstable compared to other CSLD and CESA proteins. We also showed that the turnover of Cerulean-CSLD5 might require the activity of $APC^{CCS52A2}$-26S proteasome. We propose that CSLD5 plays a unique and essential role in cell plate formation and that its accumulation and activity is regulated in cell cycle dependent manner.

## Introduction

In multicellular organisms, cell division is required for new organ differentiation and development (Heidstra and Sabatini, 2014). In animal and fungal cells, an acto-myosin based contractile ring drives the formation of a cleavage furrow which results in the separation of two daughter cells (Guertin et al., 2002; Jürgens, 2005). Plant cell division uses a different mechanism in which a phragmoplast, unique arrays of microtubules, actins, and vesicles formed in cytokinesis, is generated at the dividing plane (Guertin et al., 2002; Jürgens, 2005). Directed by the microtubules, vesicles containing cell wall materials are targeted and fused to the center of the phragmoplast, forming a transient

membrane compartment called cell plate (Guertin et al., 2002; Jürgens, 2005). The cell plate expands centripetally due to the continuous arrival of secretory vesicles that fuse to its periphery. This process continues until the expanding cell plate reaches the plasma membrane of the mother cell, at which point it fuses with the plasma membrane separating the two daughter cells (Guertin et al., 2002; Jürgens, 2005). During this expansion, a nascent cell wall is formed by the deposition of cell wall materials in the lumen of cell plates (Jürgens, 2005).

Evidence collected in the past two decades supported the idea that membrane trafficking to newly forming cell plates requires canonical regulatory proteins associated with vesicle trafficking, such as Rab GTPases and SNARE proteins (Jürgens, 2005). In *Arabidopsis*, members from RAB A family, which are most closely related to yeast and mammalian YPT3/RAB11 Rab GTPases, localize to newly forming cell plates (Chow et al., 2008; Qi and Zheng, 2013). Dominant negative mutants of *rab A2a* showed cytokinesis defects (Chow et al., 2008). Therefore RAB A regulated membrane trafficking pathways might be responsible for the membrane trafficking to the division plane. The docking of the incoming vesicles requires *KNOLLE*, a cytokinesis specific syntaxin (Lauber et al., 1997). KNOLLE localizes on Golgi stacks and cell plates during the mitosis (Lauber et al., 1997), and the unfused vesicles were observed to accumulate at the division plane in *knolle* mutants (Lauber et al., 1997). Upon completion of cytokinesis,

KNOLLE is removed from the cell plate membranes and degraded in vacuolar compartments (Touihri et al., 2011).

Several specific classes of polysaccharides and their associated cell wall synthases have been identified on cell plates. Callose, β-1,3-linked glucan polymers, is a major polysaccharide class found in cell plates at early stages of cell division (Kakimoto and Shibaoka, 1992; Samuels et al., 1995). Inhibition of callose synthesis causes arrest at later stages of cytokinesis (Park et al., 2014). Callose deposition during cell plate formation might involve more than one callose synthase (Chen and Kim, 2009). CALS1 is a cell plate specific callose synthase and localizes to growing cell plates (Hong et al., 2001). Additionally, GSL8 also potentially contributes to callose deposition on cell plates since *gsl8* mutants displayed severe cytokinesis defects (Thiele et al., 2009; Chen et al., 2009). These results delineate an important role for callose synthesis and deposition during cell plate formation.

In *Arabidopsis*, the major load-bearing component in primary cell walls is cellulose (Cosgrove, 2005). Therefore it is no surprise to find that mutants of *cesa1*$^{rsw1\text{-}20}$ and *kor1*, two key members of primary cellulose synthase complex, showed severe cytokinesis defects (Zuo et al., 2000; Beeckman et al., 2002). Recently, the deposition of cellulose from cell plate initiation was confirmed with the help of Pontamine Fast Scarlet 4B (S4B), a cellulose-specific fluorescent dye (Miart et al., 2014). Consistent with this, CESA1, CESA3, and CESA6, three cellulose synthases, also were shown to accumulate on

developing cell plates (Miart et al., 2014). However, the exact roles of CSLD proteins, a second class of putative cellulose synthases (Park et al., 2011), during cytokinesis have not been investigated. In this chapter, we report the novel role of CSLD proteins in cell plate formation.

## Results

### Disruption of *CSLD* genes causes cytokinesis defects

In *Arabidopsis*, two of the three *CSLD* genes that are expressed in vegetative tissues, *CSLD2* and *CSLD3*, are required for normal root hair growth (Wang et al., 2001; Favery et al., 2001; Bernal et al., 2008). Consistent with this, *CSLD2* and *CSLD3* are highly expressed in root hair cells (Figure 2.1) (Brady et al., 2011). To investigate whether *CSLD5*, the third *CSLD* gene expressed in vegetative tissues, also regulates root hair growth, we firstly examined its expression pattern in root hairs. We found the expression level of *CSLD5* in root hairs was relatively low (Figure 2.1) (Brady et al., 2011). The root hair morphology of *csld5* mutants was also examined and root hairs from wild type Col-0, *csld2*, and *csld3* were used for comparison. Consistent with previously published results and the expression patterns, *csld2* and *csld3* displayed root hair growth defects (Wang et al., 2001; Favery et al., 2001; Bernal et al., 2008). In *csld2* mutants, bulges were formed at the base of growing root hairs (Figure 2.2). Root hair growth was completely abolished

in *csld3* mutants (Figure 2.2). However, no noticeable morphological changes were found for *csld5* root hairs (Figure 2.2) (Table 2.1). The lack of root hair phenotype of *csld5* might due to the functional redundancy among *CSLD2, CSLD3,* and *CSLD5*. To test this possibility, *csld2/csld5* and *csld3/csld5* double mutants were generated and their root hair morphologies were examined. In these double mutants, the defects in root hair growth were not strengthened compared to that in *csld2* or *csld3* single knock out lines (Figure 2.2), indicating that CSLD5 is not required for root hair growth.

Although *csld5* mutants form largely normal root hairs, the mutant root length was only 67.85% of the wild type root length (Figure 2.3) (Table 2.2). Dwarf stature phenotypes were also observed in *csld5* mutants and the diameter of rosette leaves of *csld5* mutants was reduced to 69.25% of that in wild type (Figure 2.3) (Table 2.3). Finally, the leaves of *csld5* mutants were also relatively smaller compared to the wild type leaves (Figure 2.3). Interestingly, these phenotypes were strengthened in *csld2/csld5* and *csld3/csld5* double mutants (Figure 2.3), indicating that CSLD2 and CSLD3 functions in plant developmental processes other than root hair growth and their functions in these processes are masked by CSLD5 activity.

The short root phenotype in *csld5* might be caused by reduced cell length and/or reduced cell number. To distinguish these two possibilities, the length of mature root cortical cells from Col-0 and *csld5* was measured and no difference was found (Figure 2.4) (Table 2.4). To examine whether the root cell number might be altered, we counted

the cell numbers in one column of the root cortical cells in the root meristematic zone, which is between the quiescent center (QC), the center of the root meristem containing the stem cells that give rise to the distinct classes of root cells, and the initiation site of the root elongation zone at which the cortical cell length becomes larger than its width (Figure 2.4). We found that the cell number of one column root cortical cells of this root region in *csld5* single mutants and *csld2/csld5*, *csld3/csld5* double mutants was about 78.69%, 44.81% and 42.22%, respectively, of the cell number in wild type (Figure 2.4) (Table 2.5). Additionally, we also measured the number of cells per unit area on leaf epidermis, and fewer cells were found in the same leaf area of *csld5*, *csld2/csld5*, and *csld3/csld5* mutants (Figure 2.5) (Table 2.6). These results would be consistent with a case in which the reduced organ sizes observed upon disruption of *CSLD5* are due to reduced cell numbers rather than reduced cell size, suggesting that *CSLD5* may play a role in cell division.

To determine if *CSLD5* does indeed play a role in cytokinesis, we examined whether *csld5*, *csld2/csld5*, or *csld3/csld5* double mutants displayed defective cell division. Incomplete cell walls were found in root and leaf tissues of *csld5* single and double mutants (Figure 2.6). On the other hand, the cell walls in the tissues examined in *csld2* and *csld3* mutants remained intact (Figure 2.6). These observations further support that *CSLD5* plays a more important role in cytokinesis than *CSLD2* and *CSLD3* does. To explain the formation of these incomplete cell walls, two hypotheses were made. First,

the elongation rate of cell plates might be affected in *csld5* mutants. As a result, the cell plates fail to expand fast enough to separate two daughter cells when the cytokinesis is finished. Second, the structural integrity of cell plates might be affected in *csld5* mutants. Therefore the cell plates are fragile and are prone to break either during cell plate expansion, or once cytokinesis is completed. To test these two ideas, we used a GFP tagged membrane localized receptor like kinase, BRI1-GFP, as a membrane marker to follow the progression of cell plate formation during cytokinesis. Plants expressing BRI1-GFP in Col-0 or *csld5* background were generated and the cell plate elongation rates were determined (Figure 2.7). Quantitative analysis showed that cell plates in *csld5* mutants elongated at a similar rate compared to that in Col-0 (Figure 2.7). Based on these results, we concluded that loss of *CSLD5* function did not significantly impair the rate of cell plate formation. Loss of this cell wall synthase likely results in a reduced structural integrity of the newly forming cell plate.

**Functional fluorescently tagged CSLD proteins localize on cell plates**

During cell plate formation, callose and cellulose are synthesized at the cell plate, while xyloglucans and pectic polysaccharides are synthesized in the Golgi apparatus and delivered to the cell plate via vesicle trafficking (Jürgens, 2005; Miart et al., 2014). To investigate the sub-cellular localization of CSLD2, CSLD3, and CSLD5 in dividing cells, we fluorescently tagged these CSLD proteins, which are expressed under the control of

their respective promoters. We previously confirmed that CSLD3p::eYFP-CSLD3 was functional (Park et al., 2011). To confirm whether CSLD2p::Citrine-CSLD2 and CSLD5p::Cerulean-CSLD5 were functional, they were transformed into *csld2* and *csld5* mutants and the mutant phenotypes were examined to determine the extent of rescue. We found that the bulge-forming phenotype in *csld2* root hairs were rescued by CSLD2p::Citrine-CSLD2 (Figure 2.8). Additionally, while the root hair length in *csld2* mutants was only 72.63% of that in wild type, the root hair length in CSLD2p::Citrine-CSLD2 rescued *csld2* plants was indistinguishable from that in wild type (Figure 2.8) (Table 2.1). We also found that the short root phenotype in *csld5* mutants was rescued by CSLD5p::Cerulean-CSLD5 (Figure 2.8) (Table 2.2). Therefore, we concluded that the CSLD2 and CSLD5 fusion proteins were also functional. Using confocal microscopy, we observed that Citrine-CSLD2, eYFP-CSLD3, and Cerulean-CSLD5 were all highly enriched on cell plates in dividing cells (Figure 2.9). An interesting distinction between Cerulean-CSLD5 and Citrine-CSLD2 and eYFP-CSLD3 was that while both Citrine-CSLD2 and eYFP-CSLD3 accumulated in punctate structures in all non-dividing cells in the root and aerial tissues we examined (Figure 2.9), Cerulean-CSLD5 fluorescence was tightly correlated with patches of cells that were forming the cell plate (dividing cell) or displayed relatively smaller sizes (potentially completed cell division recently) (Figure 2.9).

**CSLD5 proteins accumulate in cell plates in a cell cycle dependent manner**

The patchy expression pattern that we observed for Cerulean-CSLD5 in *Arabidopsis* roots resembled the distribution pattern of CYCB1:1, a cyclin protein regulating the G2/M transition (Colon-Carmona et al., 1999) (Figure 2.10). This might indicate that the expression and accumulation CSLD5 is also controlled in a cell cycle dependent fashion. To test whether CSLD5 and CYCB1:1 expression patterns were the same or not, we generated lines expressing both Cerulean-CSLD5 and CYCB1:1-GFP and examined the fluorescence distribution of these two proteins. Surprisingly, the distribution of Cerulean-CSLD5 and CYCB1:1-GFP was almost completely mutually exclusive (Figure 2.11). Cerulean-CSLD5 was absent from the cells with strong CYCB1:1-GFP labeling and *vice versa* (Figure 2.11). To further examine the accumulation of Cerulean-CSLD5 and CYCB1:1-GFP during cell division, we examined the dynamics of these two proteins in time-lapse movies of dividing cells. We found that significant levels of Cerulean-CSLD5 fluorescence were observed only after the separation of CYCB1:1-GFP labeled chromatin and initiation of cytokinesis in these mitotic cells (Figure 2.12). Cerulean-CSLD5 fluorescence was unstable in these cells, however, and was rapidly lost once the newly-formed cell plate had separated the two daughter cells (Figure 2.12, 50 minute time point), perhaps indicating that CSLD5 is rapidly down-regulated upon exit of mitosis.

To further examine whether expression and accumulation of Cerulean-CSLD5 and CYCB1:1-GFP were linked to the cell cycle, the accumulation of these proteins were

observed upon growth in media containing aphidicolin, a DNA polymerase inhibitor that locks cells in the S-phase of the cell cycle (Menges and Murray, 2002). After two days of growth in the presence of aphidicolin, increased numbers of root cells displayed CYCB1:1-GFP accumulation enriched within cell nuclei, consistent with a blockade in the S-phase of the cell cycle (Figure 2.13). On the other hand, the level of Cerulean-CSLD5 was undetectable (Figure 2.13), perhaps indicating that significant levels of Cerulean-CSLD5 did not accumulate until after loss of CYCB1:1-GFP signal during the metaphase-anaphase transition of mitosis.

To obtain a more precise temporal-spatial accumulation pattern of Cerulean-CSLD5 during and after cell plate formation, we further compared its dynamics with that of GFP-KNOLLE (a cell cycle specific syntaxin) and GFP-CESA3 (a cellulose synthase), two cell plate localized proteins that are involved in cell plate formation (Lauber et al., 1997; Miart et al., 2014). We found that both GFP-KNOLLE and GFP-CESA3 co-localized with Cerulean-CSLD5 on the cell plate from its initiation (Figure 2.14). All of these three proteins were uniformly distributed on the cell plate, but only the signal of GFP-KNOLLE and Cerulean-CSLD5 was predominantly enriched on cell plates (Figure 2.14). The fluorescence of GFP-CESA3, on the other hand, was significantly enriched in punctuate sub-cellular structures during cytokinesis (Figure 2.14). Quantitative analysis on relative fluorescence enrichment also confirmed our observation. We found that during cell plate formation, only less than 20% of the GFP-CESA3 signal was enriched in

the cell plate (Figure 2.15). However, around 30% of GFP-KNOLLE signal and 60% of Cerulean-CSLD5 signal were enriched on cell plates (Figure 2.15). The predominant cell plate accumulation for CSLD5 indicates that it might function before CESA3 in making required polysaccharides during early stages of cell plate formation.

Upon completion of cytokinesis, GFP-KNOLLE, GFP-CESA3, and Cerulean-CSLD5 showed distinct dynamics. We observed punctate structures, containing Cerulean-CSLD5 fluorescence, budding off the newly formed cell wall within 30 minutes after the completion of cytokinesis (Figure 2.14). This coincided with a rapid reduction of Cerulean-CSLD5 signal on the membrane associated with the newly formed cell wall (Figure 2.14). 30 minutes after the completion of cytokinesis, the level of Cerulean-CSLD5 observed at the newly formed cell wall was reduced by around 65% (Figure 2.15). In the same time period, however, the signal level of GFP-CESA3 remained largely unchanged (Figure 2.14 and 2.15). The fluorescence level of GFP-KNOLLE, surprisingly, increased by about 10% (Figure 2.14 and 2.15). The distinct dynamics of Cerulean-CSLD5 observed during these stages of cytokinesis highlight the specific targeting of this protein during plant cytokinesis, and support the possibility that CSLD5 is uniquely regulated during this stage of the plant cell cycle.

**CSLD5 proteins are degraded after cytokinesis is completed**

To test the idea that the rapid signal reduction of Cerulean-CSLD5 is due to its degradation after the completion of cytokinesis, we examined the distribution of Cerulean-CSLD5 in self renewing meristemoid cells. These cells undergo up to three successive rounds of cell divisions so that we can easily track back recent cell division events (Figure 2.16) (Dong et al., 2009). Consistent with our hypothesis, Cerulean-CSLD5 showed a signal reduction gradient in the cells examined (Figure 2.17). The fluorescence intensity was highest in the cell which had most recently completed cytokinesis (Figure 2.17). For the rest of the cells in the lineage, the earlier a cell finished cell division, the weaker the Cerulean-CSLD5 fluorescence intensity in that cell (Figure 2.17). This observation further supported the hypothesis that Cerulean-CSLD5 might be degraded after the cell division is completed.

To further confirm Cerulean-CSLD5 is an unstable protein, we blocked new protein synthesis with cycloheximide, a protein synthesis inhibitor, and compared the stability of different proteins. Steady state protein levels were detected by immunoblotting with anti-GFP antibodies. Overall accumulation of Cerulean-CSLD5 was reduced significantly during the timecourse (Figure 2.18). The Cerulean-CSLD5 level started to decrease about six hours after the treatment, and its level was reduced by around 50% after nine hours (Figure 2.18). The signal decreasing trend of Cerulean-CSLD5 upon the cycloheximide treatment was reminiscent to that of bri1-9:GFP, an ER-retained mutant variant of BRI1 that is known to be degraded by an ER-associated protein degradation pathway (Hong et

al., 2009) (Figure 2.18). However, proteins from the CSLD family or closely related CESA family remained stable even after twenty four hours of cycloheximide treatment (Figure 2.18).

Often rapid protein turnover is associated with post-translational ubiquitin modifications that assist in the targeting of unstable proteins for proteolysis (Marrocco et al., 2010). It was intriguing that the rapid turnover characteristics of Cerulean-CSLD5 resembled that of bri1-9:GFP (Figure 2.18). We were curious whether CSLD5 turnover might also be regulated by ubiquitin-dependent processes. To test this, we treated seedlings with the 26S proteasome inhibitor, MG132, and examined effects on protein turnover characteristics of these two proteins. As with bri1-9:GFP, treatment with MG132 stabilized Cerulean-CSLD5 proteins (Figure 2.19), indicating that the rapid loss of Cerulean-CSLD5 signal observed upon completion of cytokinesis likely involves ubiquitin-dependent steps that regulate its stability.

In eukaryotic cells, cell-cycle progression and ubiquitin-mediated protein turnover are linked by the anaphase promoting complex (APC), a multisubunit E3 ubiquitin ligase (Marrocco et al., 2010). APC regulates cell cycle by degrading downstream targets, such as CYCB1:1 (Zheng et al., 2011). There are eight APC activators, five *CDC20* (*Cell Division Cycle 20*) genes, and three plant *CDH1* (*Cadherin 1*) homologues, *CCSA52A1* (*Cell Cycle Switch Protein 52 A1*), *CCS52A2* (*Cell Cycle Switch Protein 52 A2*), and *CCS52B* (*Cell Cycle Switch Protein 52 B*), in *Arabidopsis* which assist in determining

APC complex substrate specificity (Fülöp et al., 2005). Transcription of *CDC20* genes was stimulated during early G2 to late M phase, and CDC20 proteins had been shown to be degraded during the exit of mitosis (Fülöp et al., 2005). Both *CCS52A1* and *CCS52A2* were expressed and appear to function during late M and G1 phases of the cell cycle (Fülöp et al., 2005). *CCS52B* was expressed during the G2/M transition and in early stages of mitosis (Fülöp et al., 2005). Since the proteolytic turnover of Cerulean-CSLD5 appeared to occur after completion of cytokinesis, we hypothesized that CCS52A1 or CCS52A2 proteins may impact the stability of Cerulean-CSLD5. We therefore transformed Cerulean-CSLD5 under the control of its own promoter into different *ccs52* knock out lines. Interestingly, the strict accumulation of Cerulean-CSLD5 in actively dividing cells (Figure 2.9) was not observed in *ccs52a2* mutants, and instead Cerulean-CSLD5 appeared to accumulate uniformly in root epidermal cells (Figure 2.20). This loss of cell-division specific accumulation of Cerulean-CSLD5 appeared to be specific to loss of *CCS52A2* gene function, as the cell division associated accumulation pattern of Cerulean-CSLD5 was unchanged in the *ccs52b* mutant background (Figure 2.20). Further supporting the role of *CCS52A2* in cell cycle dependent regulation of Cerulean-CSLD5 stability, we observed that the rapid Cerulean-CSLD5 protein turnover kinetics observed in wild-type Col-0 plants was lost in the *ccs52a2* mutant background (Figure 2.21). Based on these results we conclude that the turnover of CSLD5 might be directly or indirectly mediated via $APC^{CCS52A2}$ regulated processes.

## Discussion

In plants, rapid and precise regulatory machineries are required for the new cell wall synthesis during cell division. In this study, we report the new finding that CSLD2, CSLD3, and CSLD5 play important roles in the *de novo* synthesis of newly forming cell walls during cell division. Using functional fluorescent fusion proteins, we were able to observe that these CSLD proteins are localized on forming cell plates during cytokinesis. While CSLD2 and CSLD3 are present in all cells examined, CSLD5 accumulation appeared to be tightly correlated with cells undergoing cytokinesis. Furthermore, unlike either *csld2* or *csld3* single mutants, cell division defects were detected in *csld5* mutant plants. In addition, the accumulation of CSLD5 is regulated by the cell cycle. Finally, the level of CSLD5 is reduced rapidly after the cytokinesis is completed. We showed that the reduction of Cerulean-CSLD5 signal is related to the activity of $APC^{CCS52A2}$ – 26S proteasome mediated proteolysis. All these results showed the activity of CSLD5, which is essential to *Arabidopsis* cytokinesis, is tightly regulated by the cell cycle.

The expression of *CSLD5* might be transcriptionally regulated. Our results showed that the protein level of CSLD5 remains low from S phase to at least the entry into mitosis. While low levels of fluorescent CSLD5-fusion proteins can be observed during early stages of mitosis, significant levels of fluorescence are only observed at late stages of mitosis as the cell undergoes cytokinesis. These observations are consistent with the

preferential expression of the *CSLD5* gene at the G2/M stages of the cell cycle. Consistent with this idea, we found an MSA (Mitosis Specific Activator) element in the promoter region of *CSLD5* (Figure 2.22). It was shown that MSA mediated mechanism is necessary and sufficient for G2/M specific gene expression (Ito et al., 2001). In *Arabidopsis*, the MSA site is bound by MYB3R1 and MYB3R4, two transcriptional factors regulating G2/M stage specific gene expression (Haga et al., 2011). Therefore it's possible that these transcriptional factors might also regulate the G2/M specific expression of *CSLD5*. Interestingly, we did not find the MSA sequence in the promoters of either *CSLD2* or *CSLD3* genes (data not shown).

What is the nature of the polysaccharide that CSLD5 synthesizes in newly forming cell plates? We showed that at the earliest stages of cell plate, the level of CSLD5 in these membrane compartments is much more predominant compared to that of CESA3. This might indicate that CSLD5 makes a polysaccharide scaffold for later cellulose deposition. In the current models of cell plate formation, callose, a β-1,3-glucan polymer, is initially deposited in newly-forming cell plates, and then this is later replaced by cellulose and other polysaccharides (Chen and Kim, 2009). Therefore it is possible that CSLD5 makes callose, which is later replaced by cellulose made by CESA proteins. However, callose synthases have previously been identified which participate in cell division (Hong et al., 2001; Chen et al., 2009; Thiele et al., 2009), and it is unclear why CSLD proteins would also be required for callose deposition. In addition, while CSLD

proteins do not share significant sequence similarity to other known callose synthases, they do share significant similarities with CESA proteins, and other Cellulose Synthase Like (CSL) proteins. The common feature of members of the CSL family of proteins is that they are all thought to synthesize β-1,4-polysaccharides, with CESAs producing the β-1,4-glucan for cellulose, CSLCs producing the β-1,4-glucan backbone for xyloglucan, and CSLAs producing the β-1,4-mannan for mannans and glucomannans (Arioli et al., 1998; Liepman et al., 2005; Cocuron et al., 2007). It was recently shown that CSLD3 likely synthesizes cellulose-like β-1,4-glucan polysaccharides in the tips of growing root hairs (Park et al., 2011). The high degree of sequence similarity and partial functional redundancy observed between CSLD3 and CSLD5 would support the possibility that CSLD5 may also produce a cellulose-like β-1,4-glucan polysaccharide. If that is the case, then CSLD5 might make a transient cellulose framework for further cellulose deposition, which could be performed by CESA proteins. Finally, it has also been suggested that CSLD proteins might have mannose synthase activity (Yin et al., 2011). However, significant levels of mannan deposition have not been demonstrated at early stages during cell plate formation. Therefore, additional biochemical analyses are still needed to confirm the activity of CSLD5.

After cytokinesis is completed, CSLD5 appears to be actively degraded via an ubiquitin dependent proteolysis process. We showed that CSLD5 was rapidly turned over during cycloheximide treatment, but could be stabilized when the activity of 26S

proteasome was blocked by MG132. Additionally, the CSLD5 protein was more stable when *CCS52A2*, an APC activator, was disrupted. These results strongly indicated that CSLD5 is degraded via $APC^{CCS52A2}$ – 26S proteasome pathways. However, how CCS52A2 regulates CSLD5 remains unknown, and additional investigation will be required to provide a more precise picture of how the cell cycle dependent regulatory machinery regulates both CSLD5 accumulation and stability in *Arabidopsis*.

## Materials and Methods

### Plant material and growth conditions

*Arabidopsis* seeds were surface-sterilized for fifteen minutes in 30% sodium hypochlorite / 0.02% Triton X-100 solution. The seeds were washed with sterilized double distilled water and stored at 4°C overnight before being transferred to ¼ MS growth medium. Seedlings were germinated and grown in growth chambers. After seven to fourteen days the seedlings were transferred from plates to soil and grown in growth rooms. Unless specified, the seedlings/plants were grown at 21°C in long-day condition (sixteen hours of light/eight hours of dark).

### Root hair and root phenotypes analysis

The root hair morphology was examined using five-day old seedlings. To measure the root hair length, the regions with mature root hairs were recorded using 4X lens (Fluorescent, NA=0.13) from a Nikon Eclipse 6600 microscope. The length of mature root hairs in these images was measured using ImageJ (NIH). To record the root hair growth defects, the images of root hairs of interest were collected using 10X lens (Apochromatic, NA=0.45). Seven-day old seedlings were grown vertically and used for root length comparison. The plates were scanned and the length of the roots was measured using ImageJ (NIH).

**Mature root cortical cell length, cell number in root meristematic zone, and cell number in leaf epidermis measurement**

To measure the root cortical cell length, the seedlings were first stained by FM4-64 to visualize the edges of the cells. Mature root cortical cells were defined as the cortical cells above the first emerging root hair cell. The length of five continuous cortical cells counting from the first mature one was measured using ImageJ (NIH).

To estimate the cell number in the root meristematic zone, the distance from QC to the initiation site of elongation zone the start of which was defined when the length of a cortical cell became larger than its width. The distance was measured using ImageJ (NIH).

To measure the number of leaf epidermal cells, the leaf epidermis at the distal end of the leaf was examined. A region of 300μm x 300μm was randomly assigned and all the non-stomatal cells in this region, including the cells flanking the edge of the region, were counted.

**Confocal microscopy**

The fluorescent imaging was performed with an Olympus spinning disk confocal using a 20x dry lens (Apochromatic, NA=0.70) or a 60x oil lens (Apochromatic, NA=1.42). Metamorph Advanced software (Molecular Devices, Inc) was used for image capture. For multi-channel imaging, the channels were switched sequentially from long wavelength to short wavelength. The signal from FM4-64 was excited at 561nm and collected at 607nm. The signal from YFP/Citrine was excited at 515nm and collected at 562nm. The GFP signal was excited at 488nm and collected at 525nm. The Cerulean signal was excited at 445nm and collected at 483nm. For time lapse imaging, 30 seconds were used as the time interval unless specified.

**Cell cycle inhibition**

Five-day old seedlings were transferred to liquid ¼ MS medium containing 75 μM aphidicolin for 48 hours before the seedlings were used for GUS reporter gene analysis or for confocal microscopy.

**GUS staining**

Histochemical analysis was performed on seedlings expressing CYCB1:1-GUS. five-day old seedlings were transferred to GUS staining solution (0.1M $NaPO_4$ pH 7.0, 10 mM EDTA pH 7.0, 0.75mM potassium ferricyanide, 0.75mM potassium ferrocyanide, 1% Triton X-100, 0.4mM X-Glucoronide) and incubated in 37°C for one hour. The stained seedlings were directly used for accumulation pattern analysis.

**Relative fluorescence enrichment analysis**

The relative fluorescence enrichment was used to examine the dynamics of GFP-KNOLLE, GFP-CESA3, and Cerulean-CSLD5 during cytokinesis. It was defined as the total fluorescence on the cell plate divided by the total fluorescence in the dividing cell. Elongating cell plate regions were selected manually based on the presence of enriched fluorescence on the cell plate. The entire cell was selected manually using plasma membrane associated FM 4-64 labeling to define the edges of the cells. The total fluorescence in these regions was measured by ImageJ (NIH).

**Protein stability analysis**

Five-day old seedlings were transferred to liquid ¼ MS medium containing 200μM cycloheximide or 150μM MG132 to inhibit new protein synthesis or to inhibit the activity of 26S proteasome, respectively. The seedlings were moved from the medium at each time point of interest and placed on filter paper to remove extra surface liquid. Ten seedlings were transferred into a 1.5ml centrifuge tube containing 50 μl 1x Laemmli buffer and were ground with a plastic pestle. The mixture was boiled for five minutes and spun at maximum speed for ten minutes to remove cell debris. The supernatant was transferred to a new tube for further Western Blotting methods. Mouse anti-GFP monoclonal antibodies (1:2500, Roche) were used as the primary antibody. For controls, mouse anti-tubulin monoclonal antibodies (1:2000, Millipore) were used. Goat anti mouse IgG conjugated with HRP (1:2000, Millipore) was used as the secondary antibodies.

a

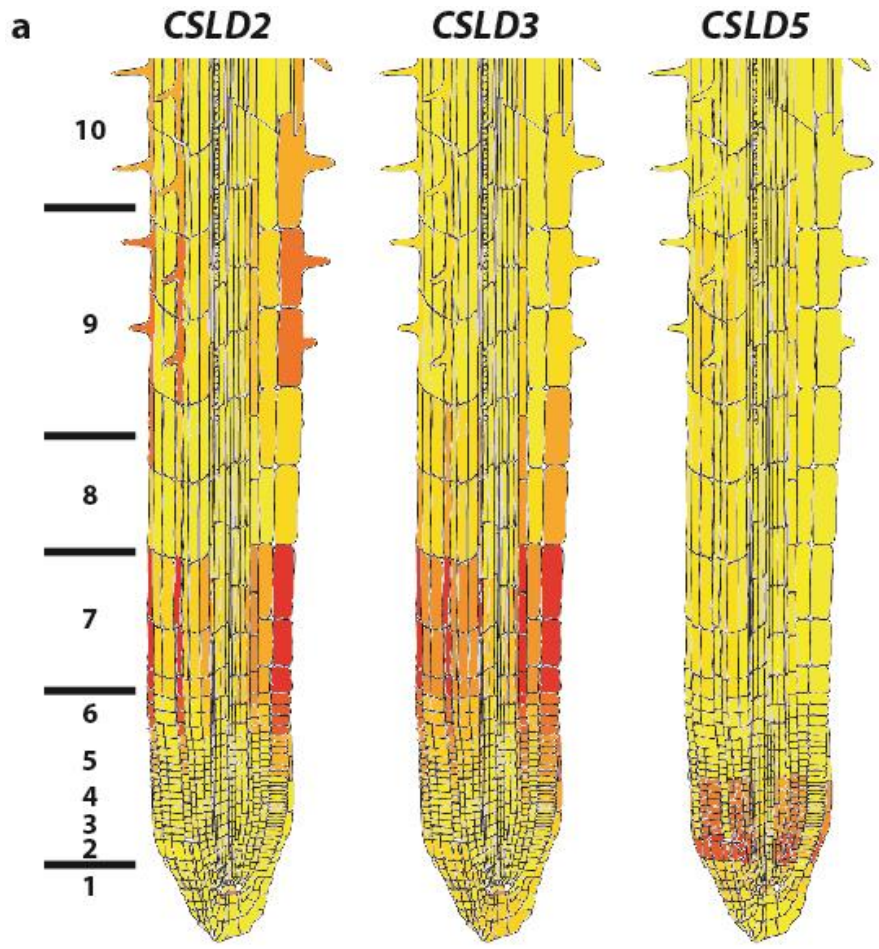


b

| Region | *CSLD2* | *CSLD3* | *CSLD5* |
|---|---|---|---|
| 2 (Cortex cells) | 143.41 | 144.55 | 333.98 |
| 8 (Root hair initiation) | 744.69 | 1091.58 | 14.79 |
| 9 (Root hair tip growth) | 2699.68 | 484.02 | 18.35 |
| 10 (Root hair tip growth) | 1527.0 | 442.38 | 8.92 |

**Figure 2.1. *CSLD2*, *CSLD3*, and *CSLD5* are differently expressed in root hair cells**

Root expression patterns of *CSLD2* (left), *CSLD3* (middle), and *CSLD5* (right) generated using the *Arabidopsis* eFP Browser (http://bar.utoronto.ca/efp/cgi-bin/efpWeb.cgi). (**a**) Both *CSLD2* and *CSLD3* displayed increased expression levels in root hair cells. However, *CSLD5* was lowly expressed in root hairs. . *CSLD3* was expressed in the cells initiating root hair growth (region 8), while *CSLD2* had high expression level after the root hairs were initiated (region 9 and 10). CSLD5 was highly expressed in root cortical cells in meristematic zone (region 2). (**b**) Absolute expression level of *CSLD2*, *CSLD3*, and *CSLD5* in various regions. The highest expression level was highlighted in red.

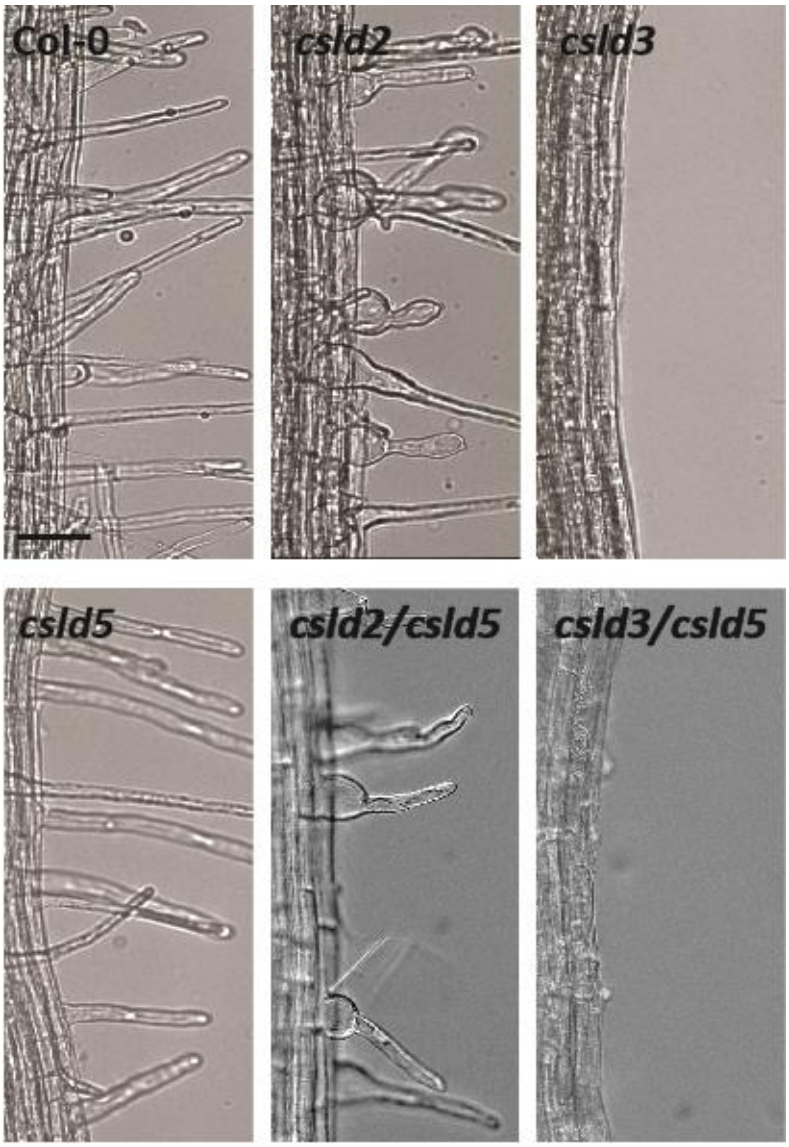


**Figure 2.2. Root hair phenotypes of five-day-old *csld* mutants**

Brightfield images of root hairs were collected from five-day old *Arabidopsis* seedlings using a Nikon E600 Eclipse microscope and 10X objective (Apochromatic, NA=0.45). Root hairs from wild type Col-0, *csld2*, *csld3*, *csld5*, and the double mutant *csld2/csld5 (csld2/5)*, *csld3/csld5 (csld3/5)* seedlings were compared. The *csld2* mutants often displayed bulges at the bases of the root hair, while root hair growth was completely abolished in *csld3* mutants. Root hair morphology of *csld5* mutants was unchanged when compared to wild type Col-0. No significant changes in root hair defects were detected in *csld2/csld5* and *csld3/csld5* when compared to *csld2* and *csld3* mutants, respectively. Scale bar represents 50 μm.

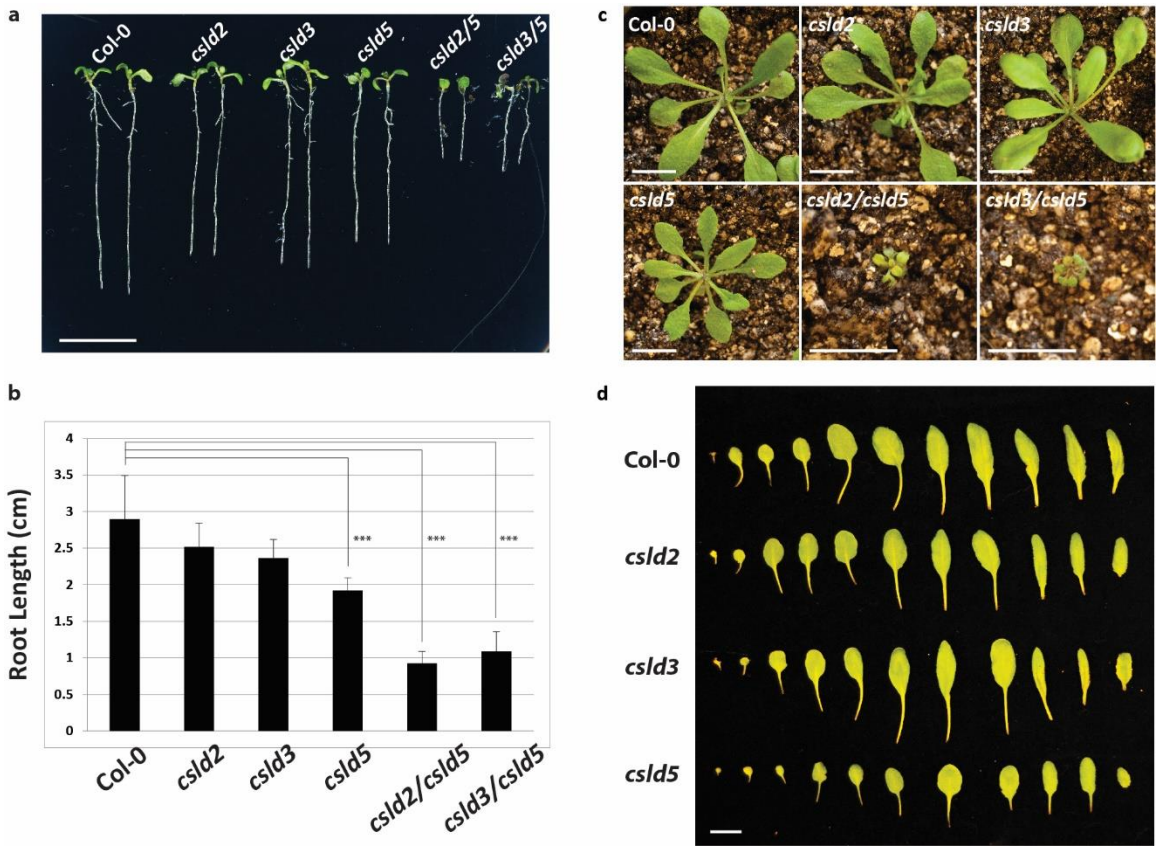


**Figure 2.3. Vegetative growth defects of *csld* mutants**

(**a**) Root length of seven-day old *csld* mutants. Compared to wild type Col-0, *csld* single and double mutants had shorter roots. (**b**) Quantitative analysis of root length of seven-day old *csld* mutants. The root length of *csld5*, and the *csld2/csld5* and *csld3/csld5* double mutants was significantly shorter compared to the root length of Col-0. (**c**) Rosette size of three-week-old plants. The rosette sizes of Col-0, *csld2*, and *csld3* plants were indistinguishable, but *csld5* plants had smaller rosettes. The rosette sizes of *csld2/csld5* and *csld3/csld5* are significantly smaller. Asterisks represent p-value (*** = less than 0.005) (**d**) Leaf sizes of three-week-old plants. The leaves of *csld5* mutants were smaller than the leaves of Col-0, *csld2*, and *csld3*. Scale bars represent 1cm.

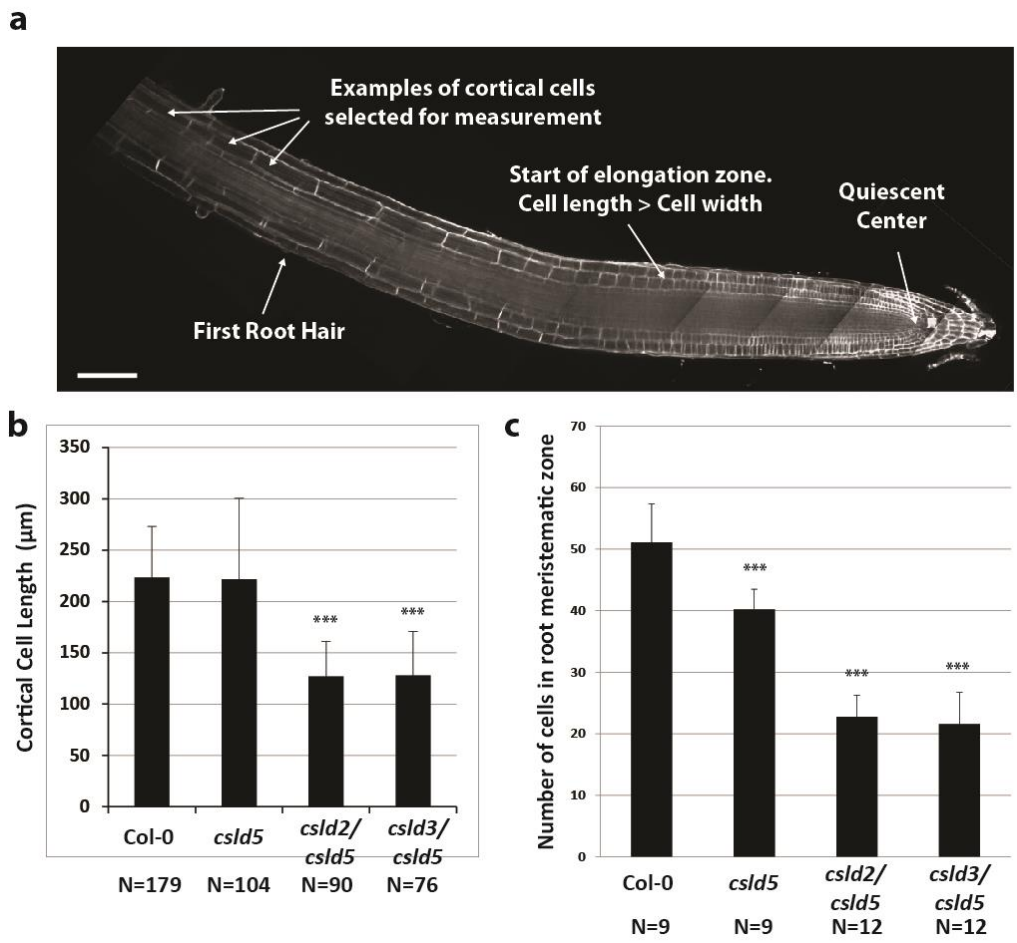


**Figure 2.4. Root phenotypes of *csld5* single and double mutants.**

(**a**) A representative root showing the region and the cells for the measurements described below. Fully expanded cortical cells were selected from the region above the first root hair initiation site. Start of elongation zone was defined where the cortical cell length was larger than its width. (**b**) Quantitative analysis of the cortical cell length from five-day old seedlings. The *csld5* mutants had similar cortical cell lengths when compared to wild type Col-0, while the cortical cell length in *csld2/csld5* and *csld3/csld5* was significantly shorter. (**c**) Quantitative analysis of the cell number in one column of root cortical cells in root meristematic zone. The cell number in *csld5* mutants was less compared to wild type Col-0. The reduction in cell number was more severe in *csld2/csld5* and *csld3/csld5* double mutants. Scale bar represents 50 µm. Asterisks represent p-value *** = less than 0.005). Error bars represent standard deviation.

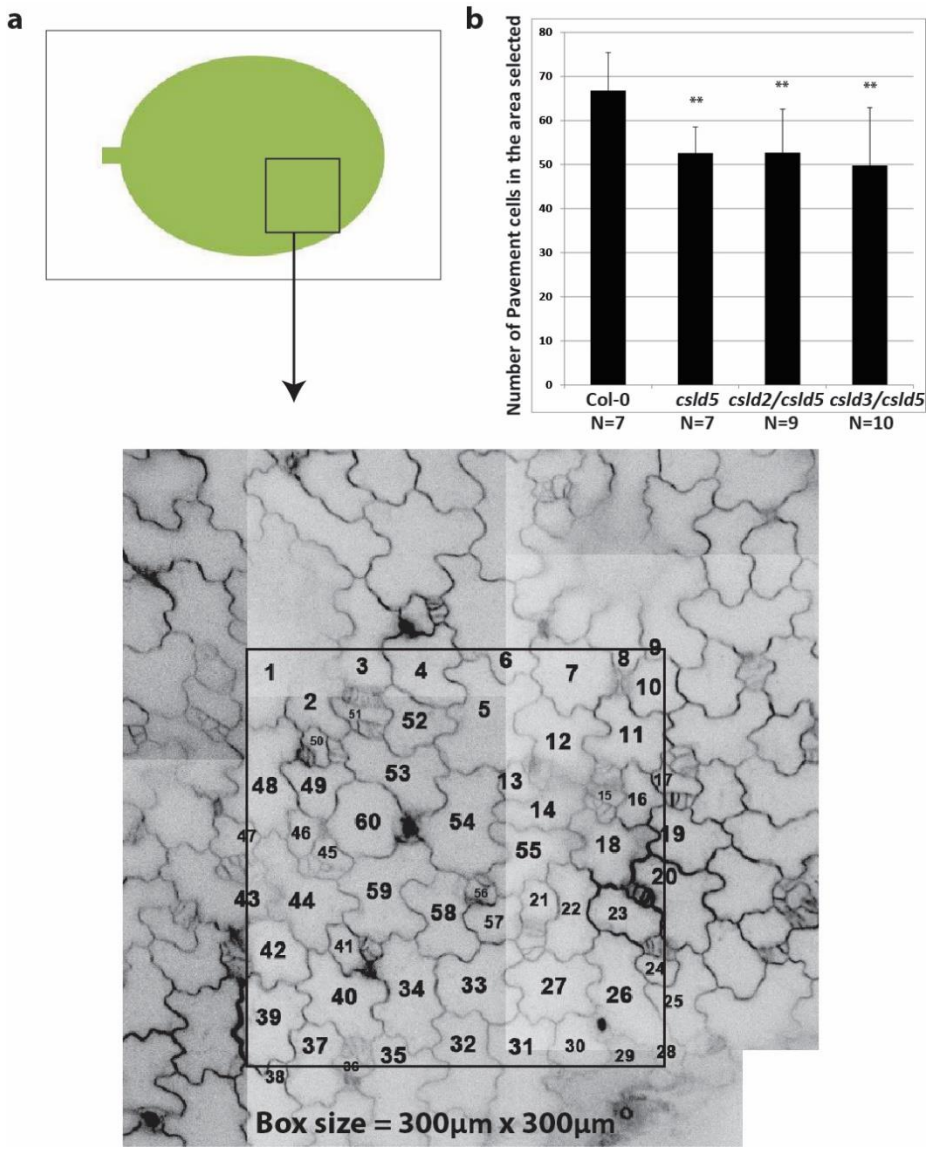


**Figure 2.5. Leaf cell size analysis of five-day-old seedlings.**

(**a**) An example showing the region and method used for the measurements described. An area of 300 µm x 300 µm in the distal end of the leaf was selected, and the number of pavement cells in/across the area was counted. (**b**) Quantitative analysis of the pavement cell numbers. Compared to wild type Col-0, *csld5*, and the *csld2/csld5* and *csld3/csld5* double mutants had fewer cells. Asterisks represent p-value (** = less than 0.05). Error bars represent standard deviation.

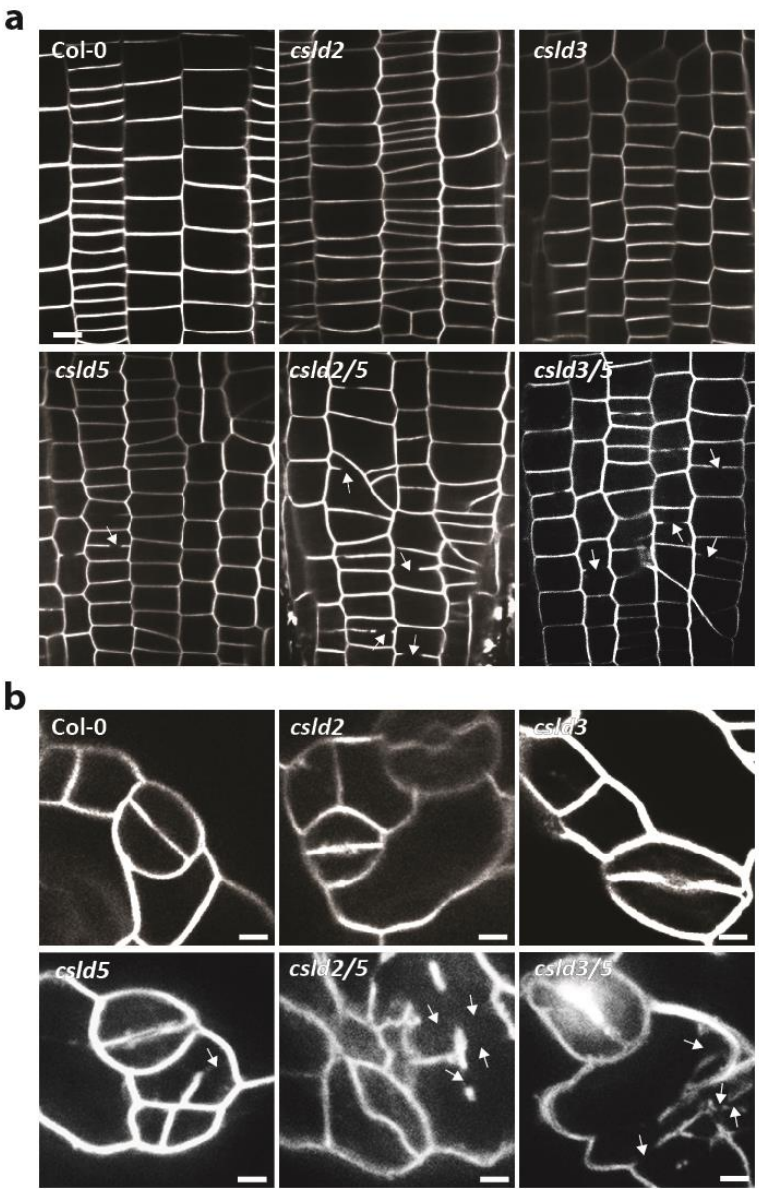


**Figure 2.6. Incomplete cell walls are found in *csld5* single and double mutants**

Examination of five-day old root cortex (**a**) and leaf epidermis (**b**) tissues showed incomplete cell walls (arrows) in *csld5* related mutants. The cell walls of *csld2* and *csld3* were unchanged when compared to wild type Col-0. However, incomplete cell walls were observed in both root and leaf tissues of *csld5* mutants, and these defects were more severe in *csld2/csld5* and *csld3/csld5* mutants. Scale bars represent 20μm.

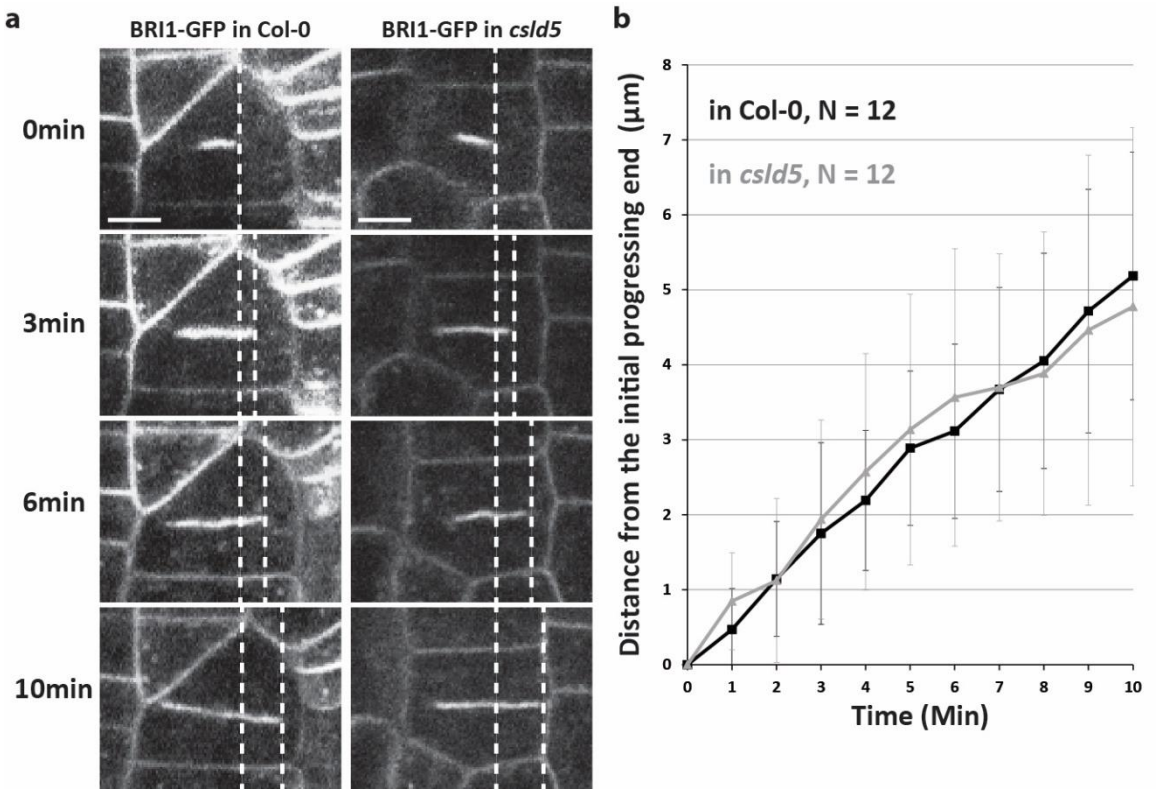


**Figure 2.7. Cell plate elongation rate is not affected in *csld5* mutants**

Analysis of cell plate elongation rate using BRI1-GFP to monitor the progression of the cell plate. (**a**) Representative snapshots from time-lapse movies showing the cell plate elongation in wild type Col-0 and *csld5*. At each time point, the elongated distance of the cell plate was measured to calculate the elongation rate. (**b**) Quantitative analysis of cell plate elongation rate in wild type Col-0 and *csld5* mutant cells. The cell plate elongation rate in *csld5* mutants was indistinguishable to that observed in wild type Col-0 plants. Scale bars represent 10µm. Error bars represent standard deviation.

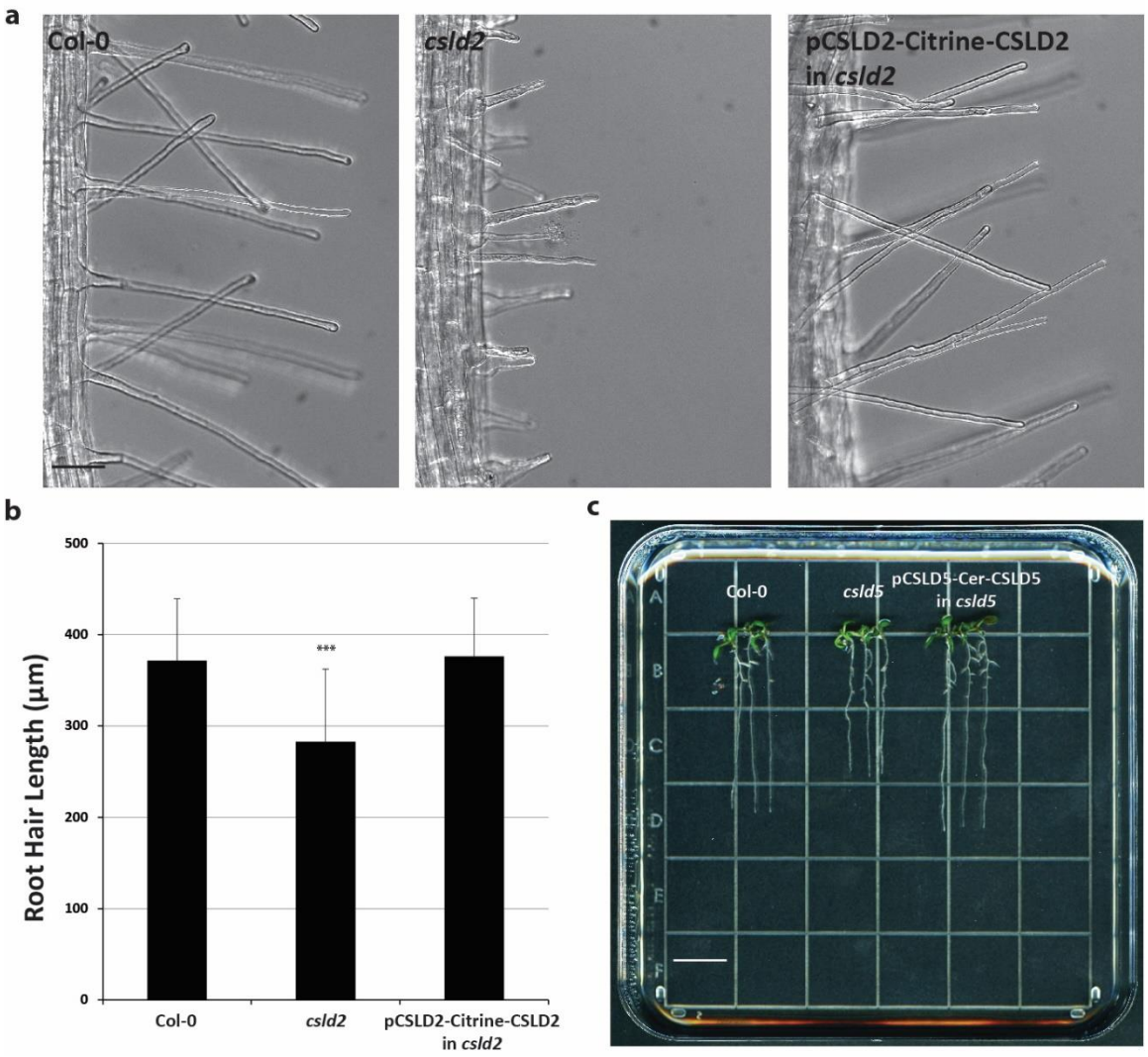


**Figure 2.8. Fluorescently tagged CSLD2 and CSLD5 are functional**

Citrine-CSLD2 and Cerulean-CSLD5 under the control of their respective promoters were transformed into *csld2* and *csld5* mutants, and functional rescue of mutant phenotypes was examined. (**a**) When transformed into *csld2* background, Citrine-CSLD2 was able to rescue root hair defects in the *csld2* mutant. **(b**) Quantitative analysis of root hair length rescue. The root hair length in *csld2* was significantly shorter compared to wild type Col-0. In the transformants expressing Citrine-CSLD2, the root hair length was indistinguishable from wild type Col-0. (**c**) The short root phenotype of *csld5* was rescued by Cerulean-CSLD5. Scale bars represent 10µm (**a**) and 1cm (**c**). Asterisks represent p-value (*** = less than 0.005). Error bars represent standard deviation. Scale bar represents 100µm.

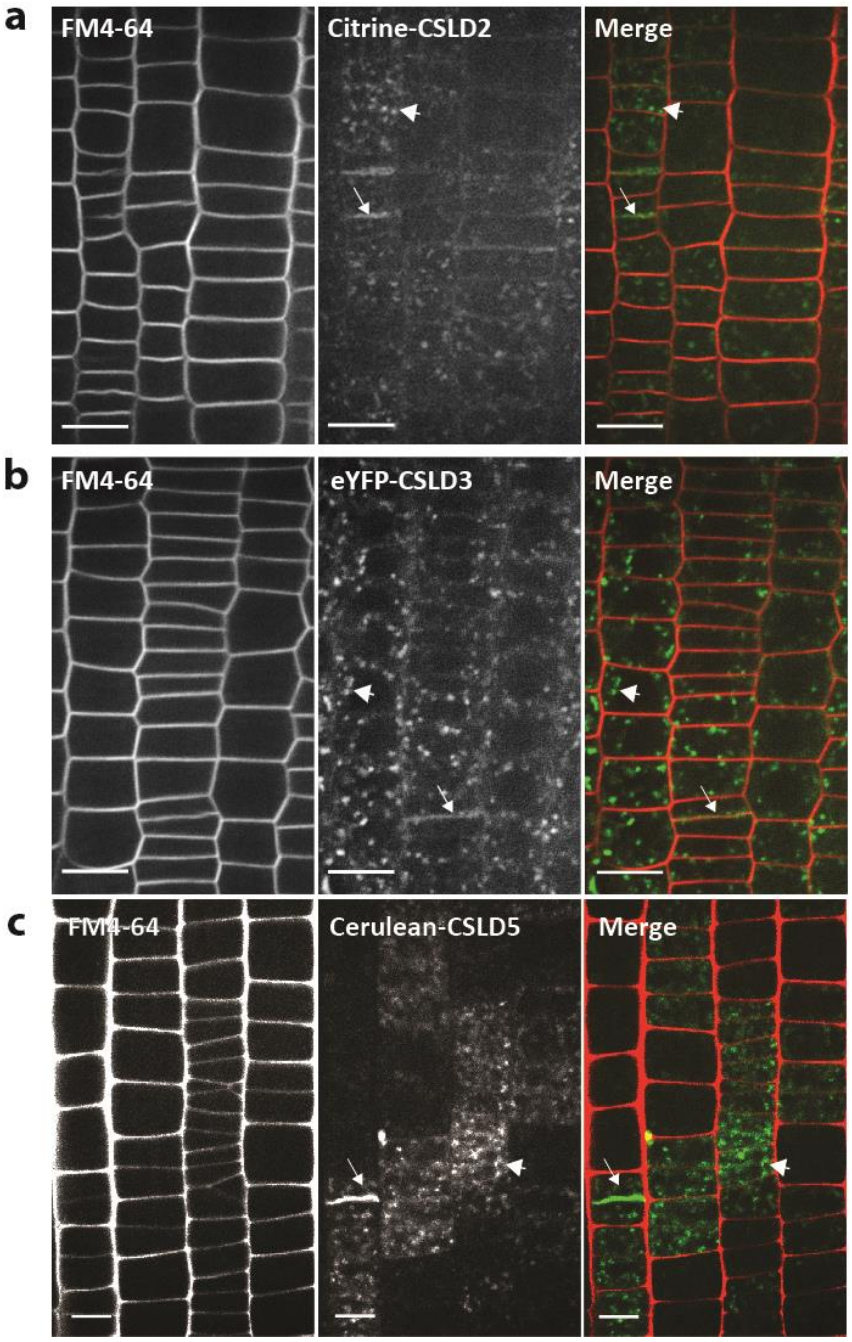


**Figure 2.9. Sub-cellular localization and distribution patterns of fluorescently tagged CSLD proteins in root tissues**

The sub-cellular localization and distribution patterns of Citrine-CSLD2 (**a**), eYFP-CSLD3 (**b**), and Cerulean-CSLD5 (**c**) were examined using confocal microscopy. All three fluorescent CSLD proteins were observed to be enriched in cell plates (arrows) and

cytoplasmic punctate structures (arrowheads). Citrine-CSLD2 and eYFP-CSLD3 were observed in all cells of the root tissue examined, Cerulean-CSLD5 fluorescence was mostly restricted to cells undergoing cell division or cells that had recently completed cell division. Scale bars represent 20µm.

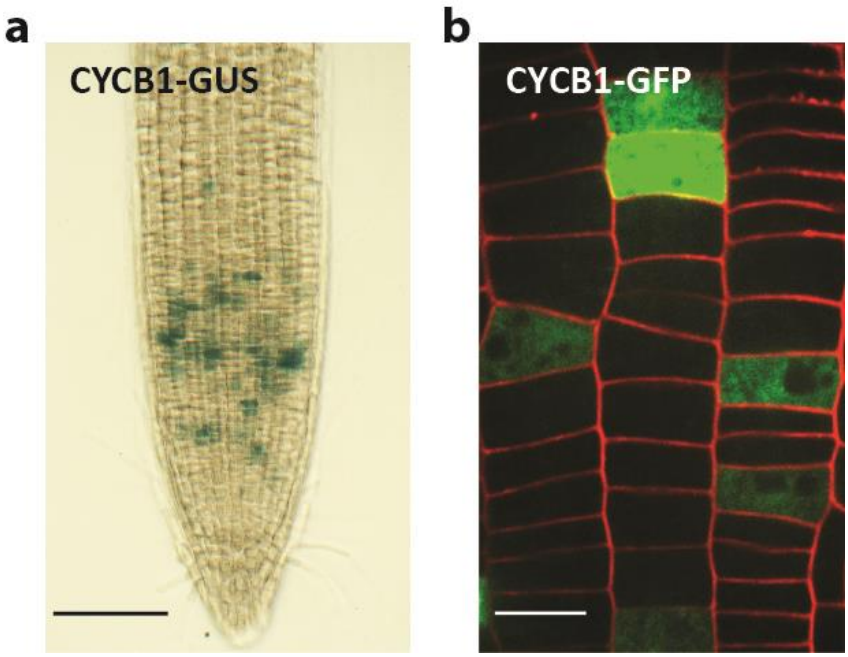


**Figure 2.10. Distribution patterns of CYCB1:1 in *Arabidopsis* root tissues**

The distribution pattern of CYCB1:1 was examined using both histochemical analysis and confocal microscopy. (**a**) Wild type plants expressing promoter-protein-reporter transgene CYCB1:1p::CYCB1:1-GUS were used to detect the distribution pattern of CYCB1:1 in the roots of five-day-old seedlings. CYCB1:1 selectively accumulated in small patches of root cells in these root tissues. (**b**) The distribution of CYCB1:1p::CYCB1:1-GFP was also examined. CYCB1:1-GFP fluorescence selectively accumulated only in actively dividing root cortical cells. Scale bars represent 0.1mm (**a**) and 20 µm **(b**).

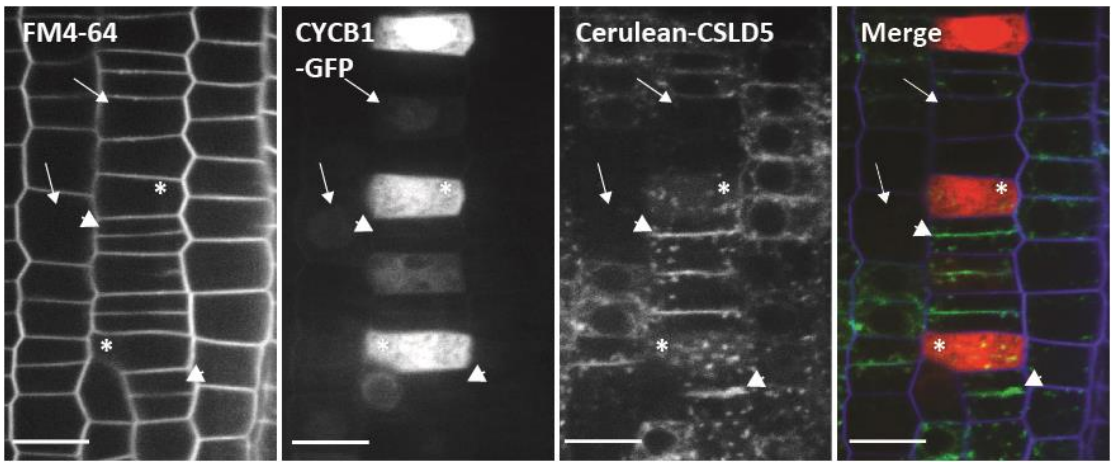


**Figure 2.11. The distribution patterns of CYCB1:1-GFP and Cerulean-CSLD5 are mutually exclusive**

The fluorescence in five-day old seedlings expressing both CYCB1:1-GFP and Cerulean-CSLD5 fluorescent fusion proteins was examined. In actively dividing cells (arrowheads), Cerulean-CSLD5 was highly enriched in the cell plates, while the signal level of CYCB1:1-GFP was undetectable. On the other hand, in cells with high CYCB1:1-GFP fluorescence (asterisks), the level of Cerulean-CSLD5 fluorescence detected was low. In some interphase cells (arrows), only weak CYCB1:1-GFP signal was observed. Scale bars represent 20 µm.

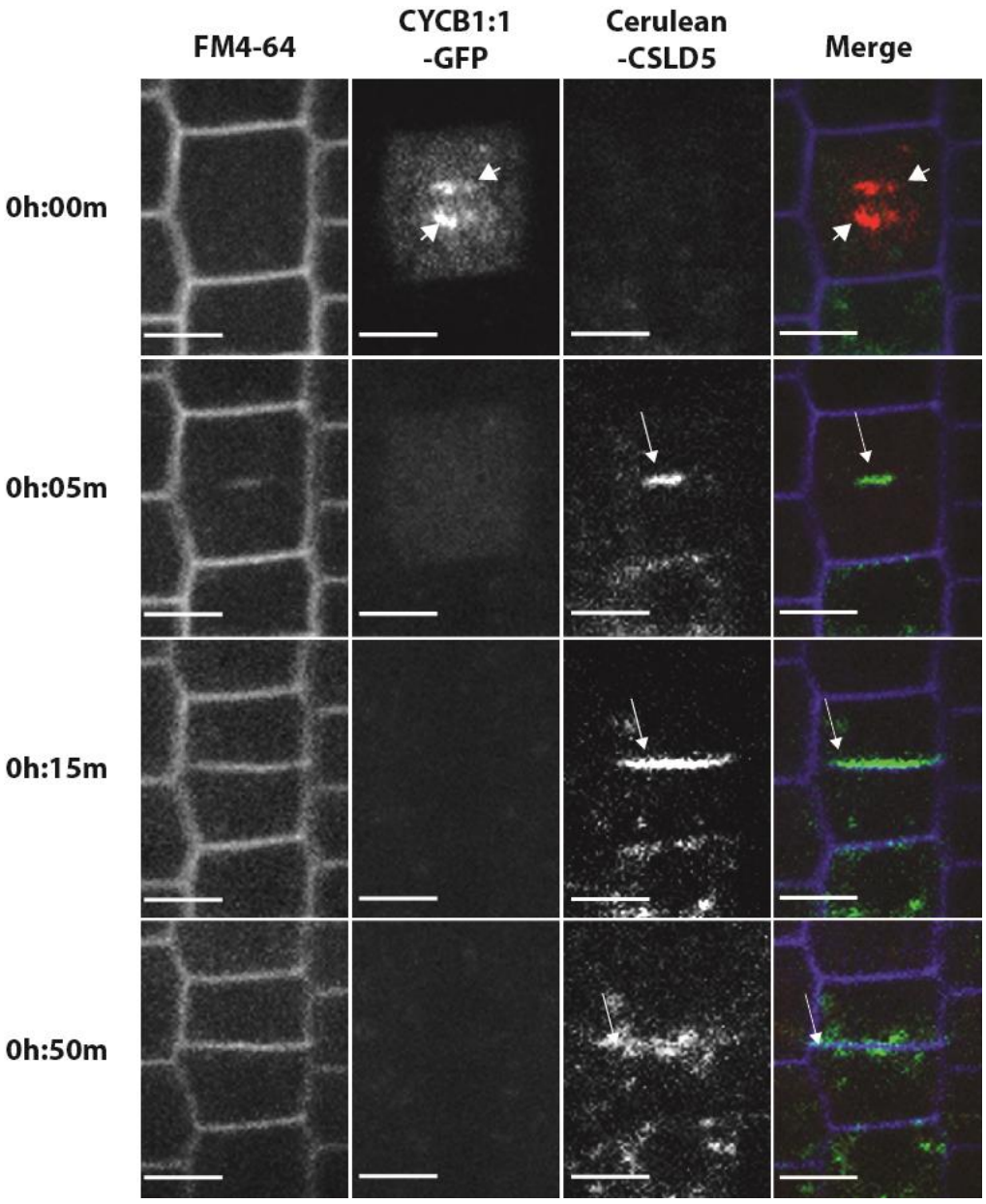


**Figure 2.12. Cerulean-CSLD5 is accumulated on cell plates after the degradation of CYCB1:1-GFP**

Snapshots from a time-lapse movie showing the dynamics of Cerulean-CSLD5 and CYCB1:1-GFP fusion proteins during cytokinesis. The time point when CYCB1:1-GFP labeled chromosomes (arrowheads) separated was set as 0h:00m. Cerulean-CSLD5 accumulated in the newly-forming cell plate (arrows) shortly after chromosomal separation. The level of Cerulean-CSLD5 was reduced significantly around 50 minutes after the chromatin separation. Scale bars represent 10 µm.

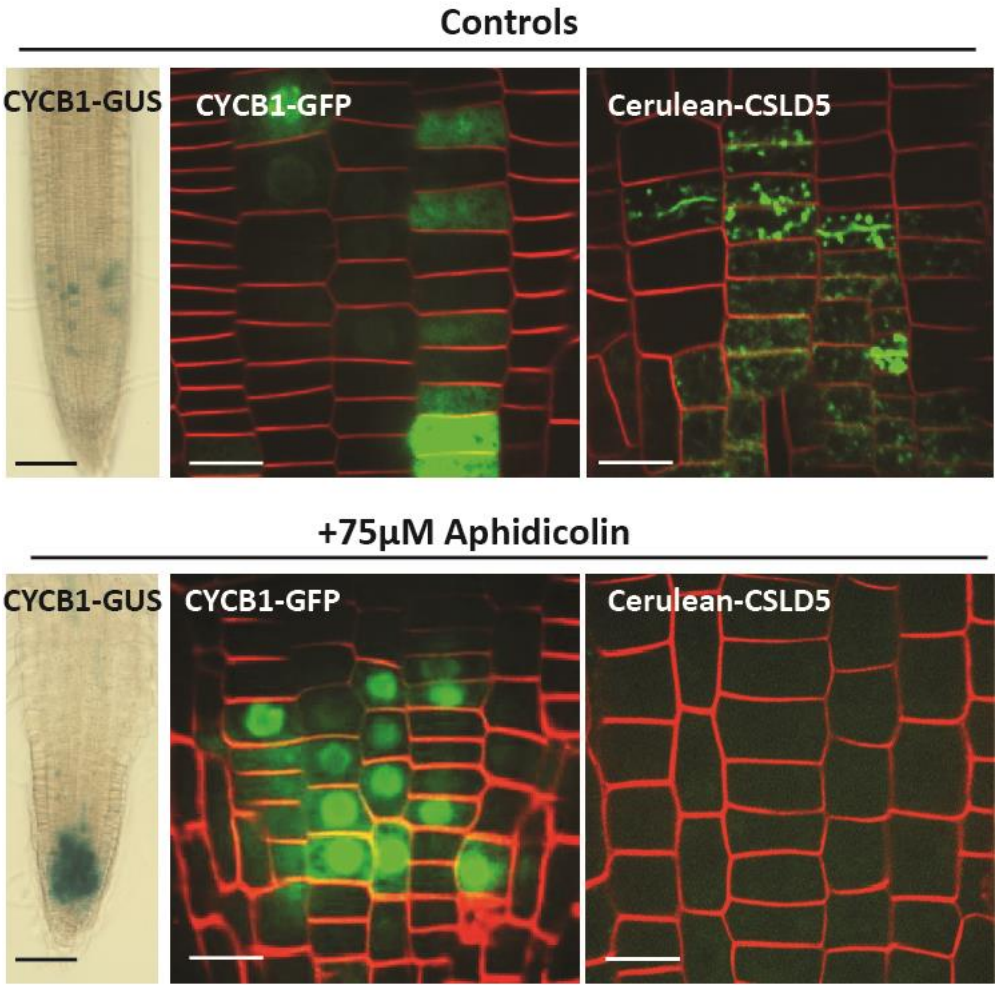


**Figure 2.13. Accumulation of Cerulean-CSLD5 is blocked by aphidicolin treatment**

The effect of 75µM aphidicolin on CYCB1:1-GUS, CYCB1:1-GFP, Cerulean-CSLD5 accumulation was examined. After 48 hours of aphidicolin treatment, the level of CYCB1:1-GUS and CYCB1:1-GFP was elevated dramatically (left and middle). Cerulean-CSLD5 signal was undetectable upon the same treatment (right). Scale bars represent 0.1mm (left) and 20 µm (middle and right).

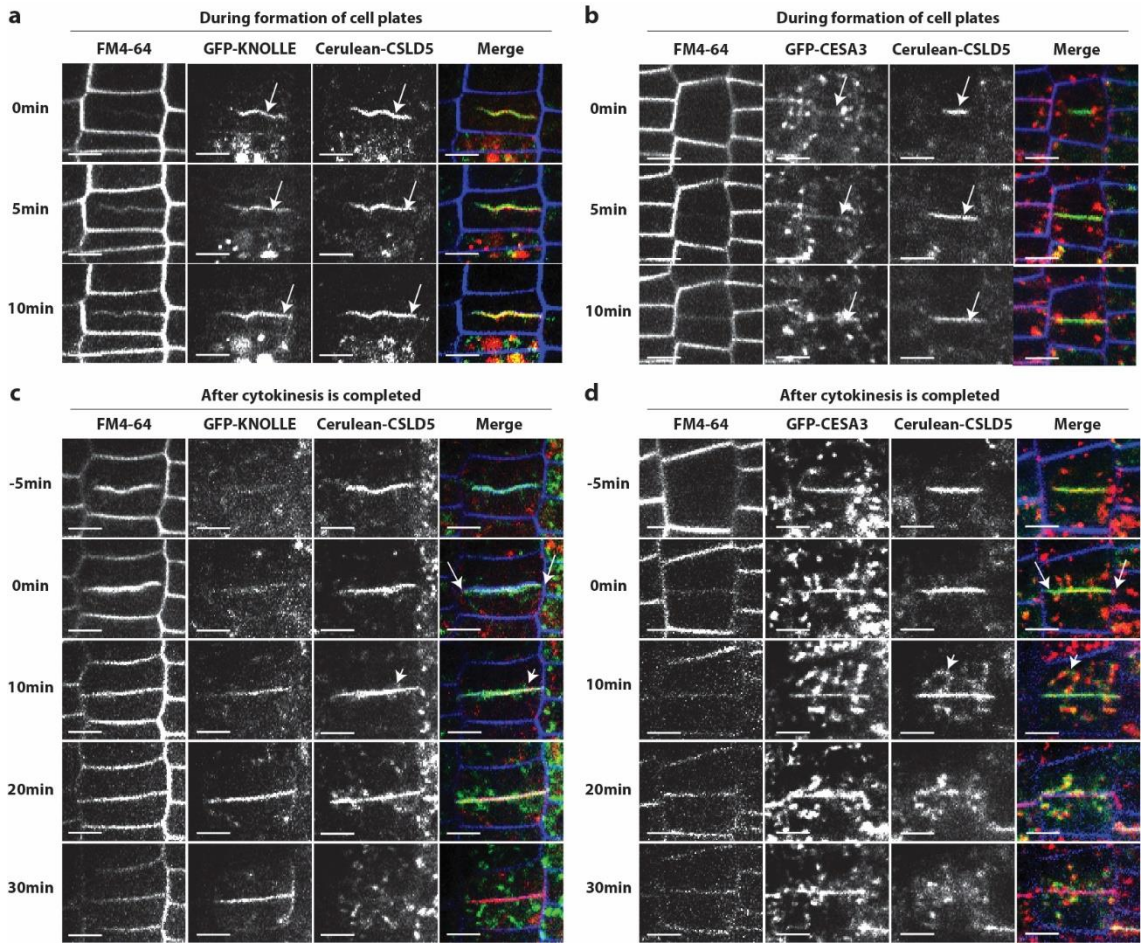


**Figure 2.14. The spatial-temporal dynamics of GFP-KNOLLE, GFP-CESA3, and Cerulean-CSLD5 are different during/after cytokinesis.**

The fluorescence from five-day old seedlings expressing both GFP-KNOLLE and Cerulean-CSLD5 (**a** and **c**) or seedlings expressing both GFP-CESA3 and Cerulean-CSLD5 (**b** and **d**) as examined using confocal microscopy. Cerulean-CSLD5 co-localized with GFP-KNOLLE (**a**) and GFP-CESA3 (**b**) on elongating cell plates. The signal of GFP-KNOLLE and Cerulean-CSLD5 were predominantly enriched in the cell plates (**a**). However, a significant amount of GFP-CESA3 fluorescence was enriched in cytoplasmic vesicles (**b**). Upon completion of cytokinesis, the elongating cell plates merged with existing plasma membranes (**c** and **d**, 0 min, arrows). Punctate structures containing Cerulean-CSLD signal were observed to bud from membranes adjacent to newly-formed cell walls around 10 minutes after the completion of cytokinesis (**c** and **d**). 30 minutes after the completion of cytokinesis, the fluorescence of Cerulean-CSLD5 was undetectable (**c** and **d**). However, unlike Cerulean-CSLD5, the fluorescence of GFP-KNOLLE still could be observed to be predominantly enriched in membranes adjacent to

newly synthesized cell walls (**c**). 30 minutes after the completion of cytokinesis, the fluorescence intensity of GFP-KNOLLE increased (**c**). The distribution and intensity of GFP-CESA3 fluorescence was unchanged during the initial 30 minutes after completion of cytokinesis (**d**). Scale bars represent 10 µm.

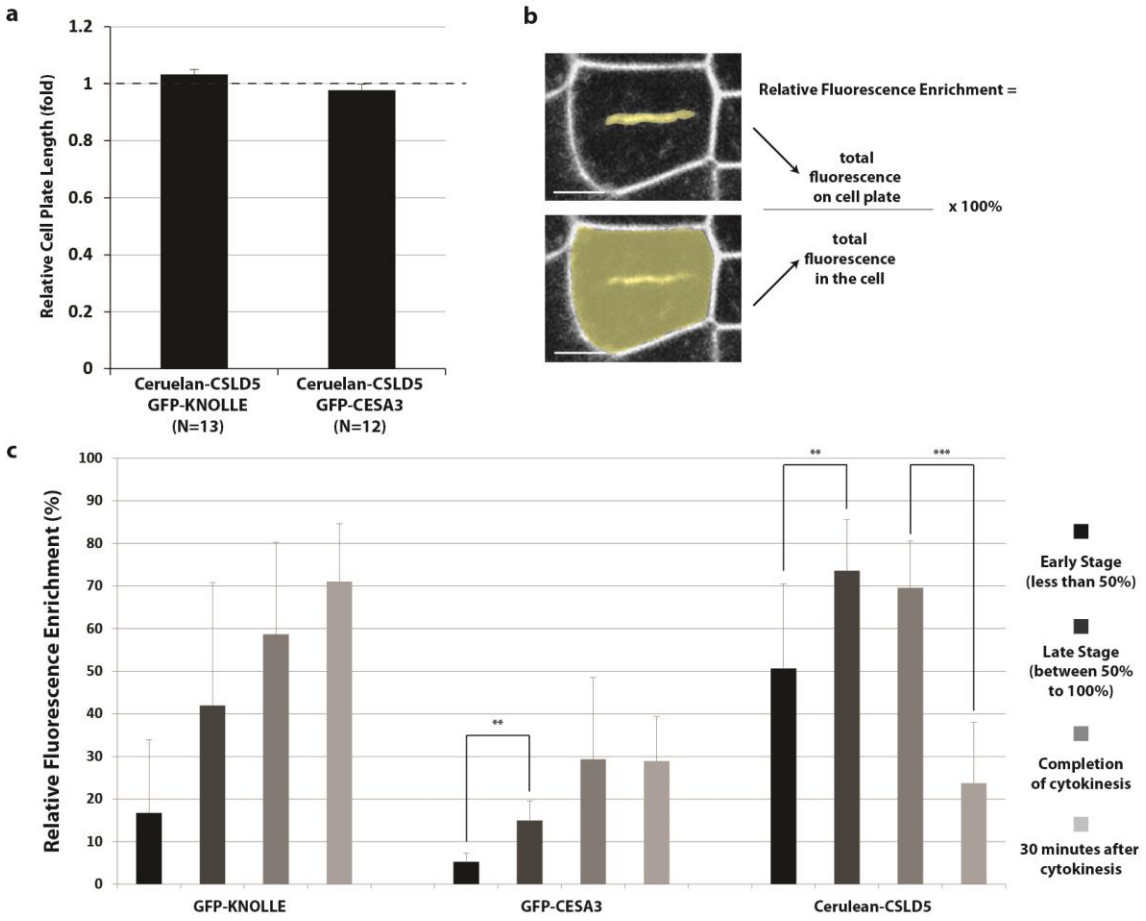


**Figure 2.15. Quantitative analysis of the dynamics of Cerulean-CSLD5, GFP-KNOLLE, and GFP-CESA3 during and after cytokinesis**

(**a**) Quantitative analysis of the cell plate length labeled by different fluorescent fusion proteins. The cell plate length labeled by Cerulean-CSLD5 was not significantly different compared to the cell plate length labeled by either GFP-KNOLLE or GFP-CESA3. (**b**) An example showing the measurement of relative fluorescence enrichment. Relative fluorescence enrichment was calculated as the quotient when the total fluorescence on the cell plate divided by the total fluorescence in the cell. The closer the number is to 100%, the more enriched the fluorescence is in the cell plate. (**c**) Quantitative analysis showing the dynamics of GFP-KNOLLE, GFP-CESA3, and Cerulean-CSLD5 during and after cytokinesis. The level of GFP-KNOLLE increased over time during cytokinesis. Compared to its level at the beginning of cytokinesis, the level of GFP-CESA3 on cell plates increased significantly only in late stages of cytokinesis. When cytokinesis completed, the level of GFP-CESA3 remained unchanged. The level of Cerulean-CSLD5 labeling on cell plates also significantly increased during cytokinesis. However, its level

dropped dramatically during the initial 30 minutes after completion of cytokinesis. Error bars represent standard error (**a**) and standard deviation (**c**). Asterisks represent p-value (** = less than 0.05; *** = less than 0.005).

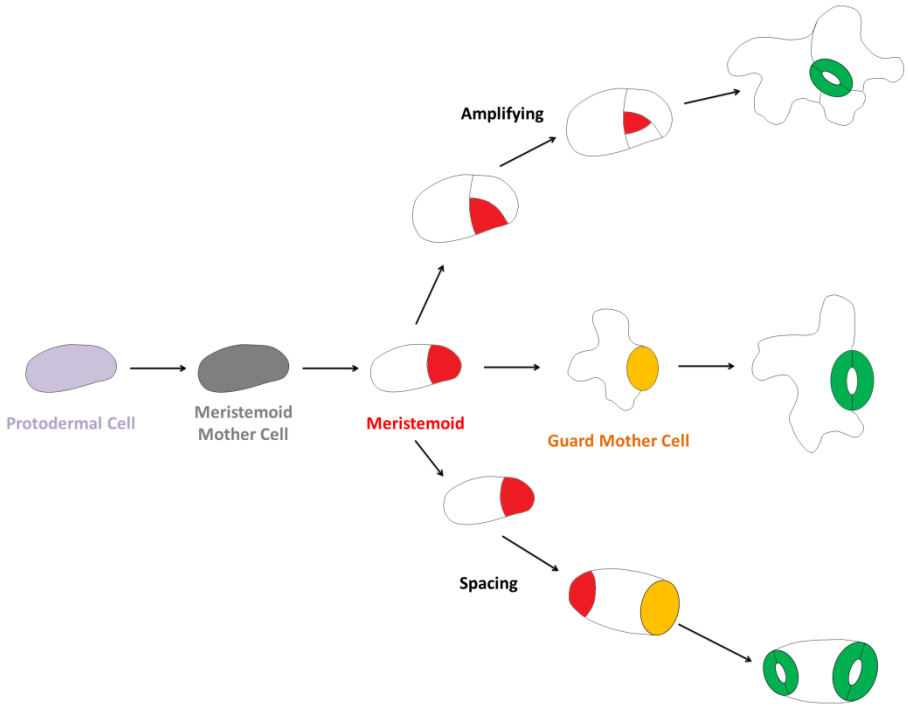


**Figure 2.16. Different pathways in stomatal development**

In current models of stomatal development, a meristemoid cell (red) is formed through an asymmetric division of the meristemoid mother cell (grey). In the default pathway the newly formed meristemoid cell can then differentiate into a guard mother cell (orange), which subsequently divides symmetrically, forming two guard cells (green) which form a stomatal guard cell complex (middle). In some cells, the meristemoid cell (red) undergoes several rounds of asymmetric cell division before differentiating into a guard mother cell (top), in a process called amplifying. Alternatively, sometimes the meristemoid mother cell undergoes an additional asymmetric division forming a second meristemoid cell (red) at the opposite end of the cell from the original meristemoid cell, causing the formation of two close stomata (bottom).

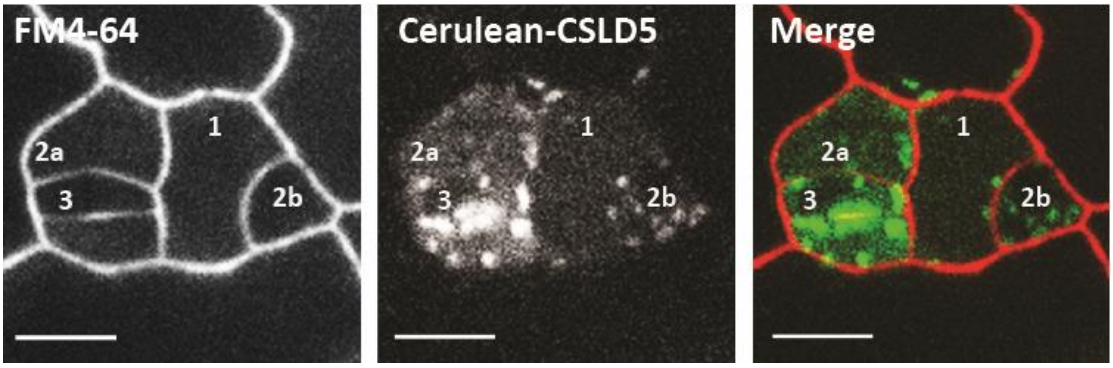


**Figure 2.17. Cerulean-CSLD5 shows a signal reduction gradient in leaf stomata lineage cells**

Cotyledons from four-day old seedlings expressing Cerulean-CSLD5 were used to examine Cerulean-CSLD5 fluorescence in stomatal lineage cells. The cells selected were generated from three rounds of asymmetric cell divisions, and the numbers represent the order in which successive cell divisions were thought to have occurred. Cerulean-CSLD5 fluorescence levels displayed a signal reduction gradient in these cells, with the highest signal in the cells most recently undergoing a cell division (#3). In the two cells generated earlier (#2a and #2b), the fluorescence level of Cerulean-CSLD5was lower, and Cerulean-CSLD5 fluorescence was lowest in the cell which likely completed cell division the earliest (#1). Scale bars represent 50 µm.

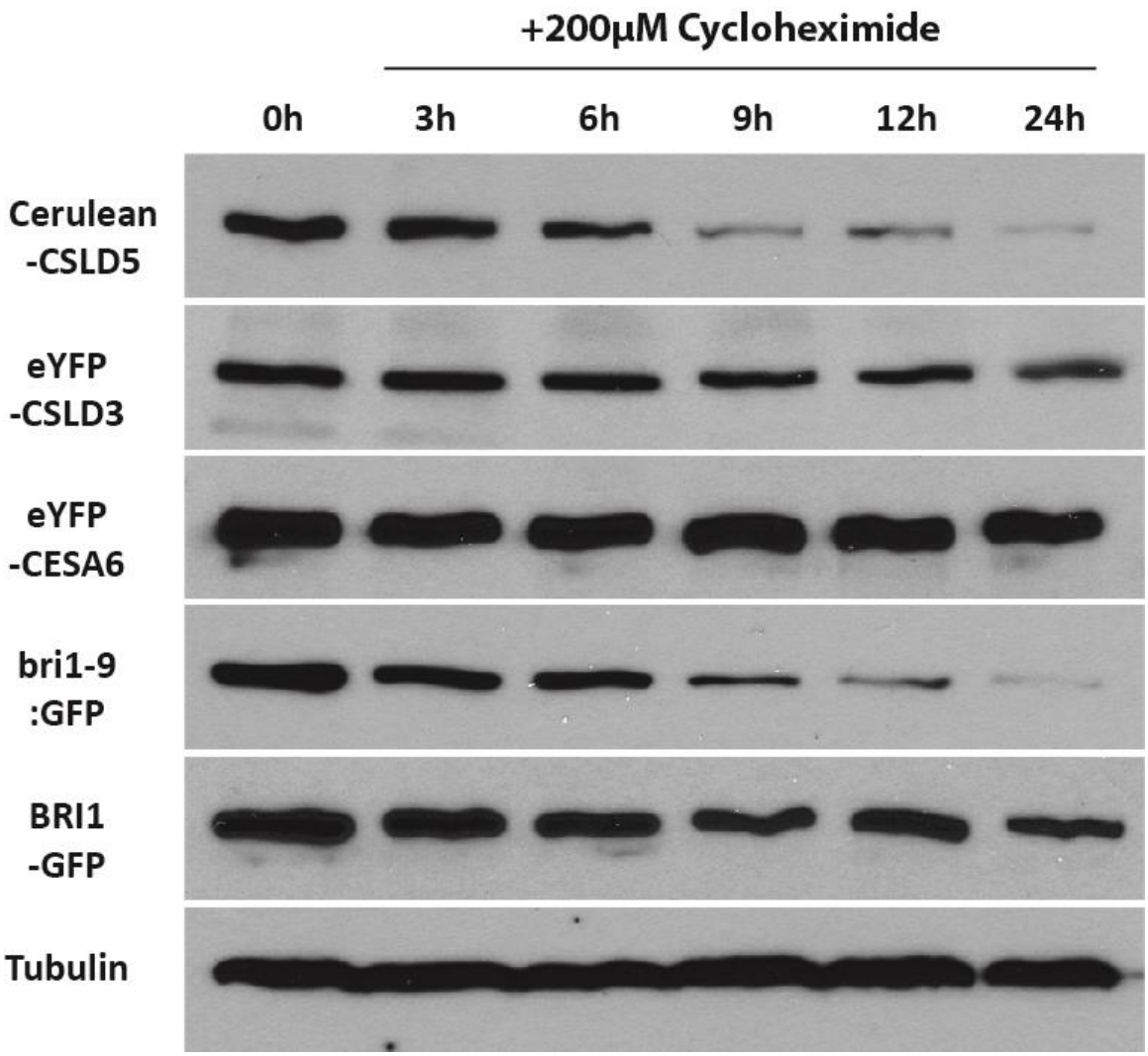


**Figure 2.18. Cerulean-CSLD5 is an unstable protein**

Analysis of protein stability for Cerulean-CSLD5, eYFP-CSLD3, and eYFP-CESA6. BRI1-9-GFP, BRI1-GFP, and Tubulin were included as positive, negative, and loading controls, respectively. New protein synthesis was blocked by addition of 200μM cycloheximide and the protein level at each time point was detected by immunoblotting methods. Cerulean-CSLD5 levels decreased significantly during the course of the cycloheximide treatment. This trend was similar to the BRI1-9-GFP, which was previously shown to undergo rapid protein turnover in the endoplasmic reticulum. The levels of eYFP-CSLD3 and eYFP-CESA3, proteins structurally similar to Cerulean-CSLD5, remained stable during the cycloheximide treatment.

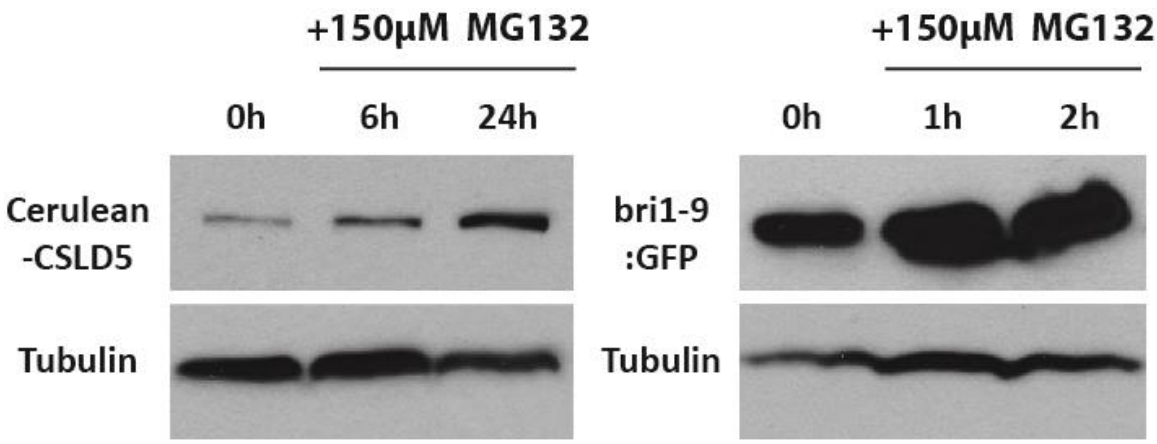


**Figure 2.19. Cerulean-CSLD5 is stabilized by 150µM MG132**

Analysis of protein stability for Cerulean-CSLD5 upon 150µM MG132 treatment. BRI1-9-GFP was used as a positive control for proteins undergoing ubiquitin-mediated proteolysis. Tubulin was used as a loading control. The activity of 26S proteasome was blocked by addition of 150µM MG132 and protein levels for both Cerulean-CSLD5 and BRI1-9-GFP increased as measured by immunoblotting.

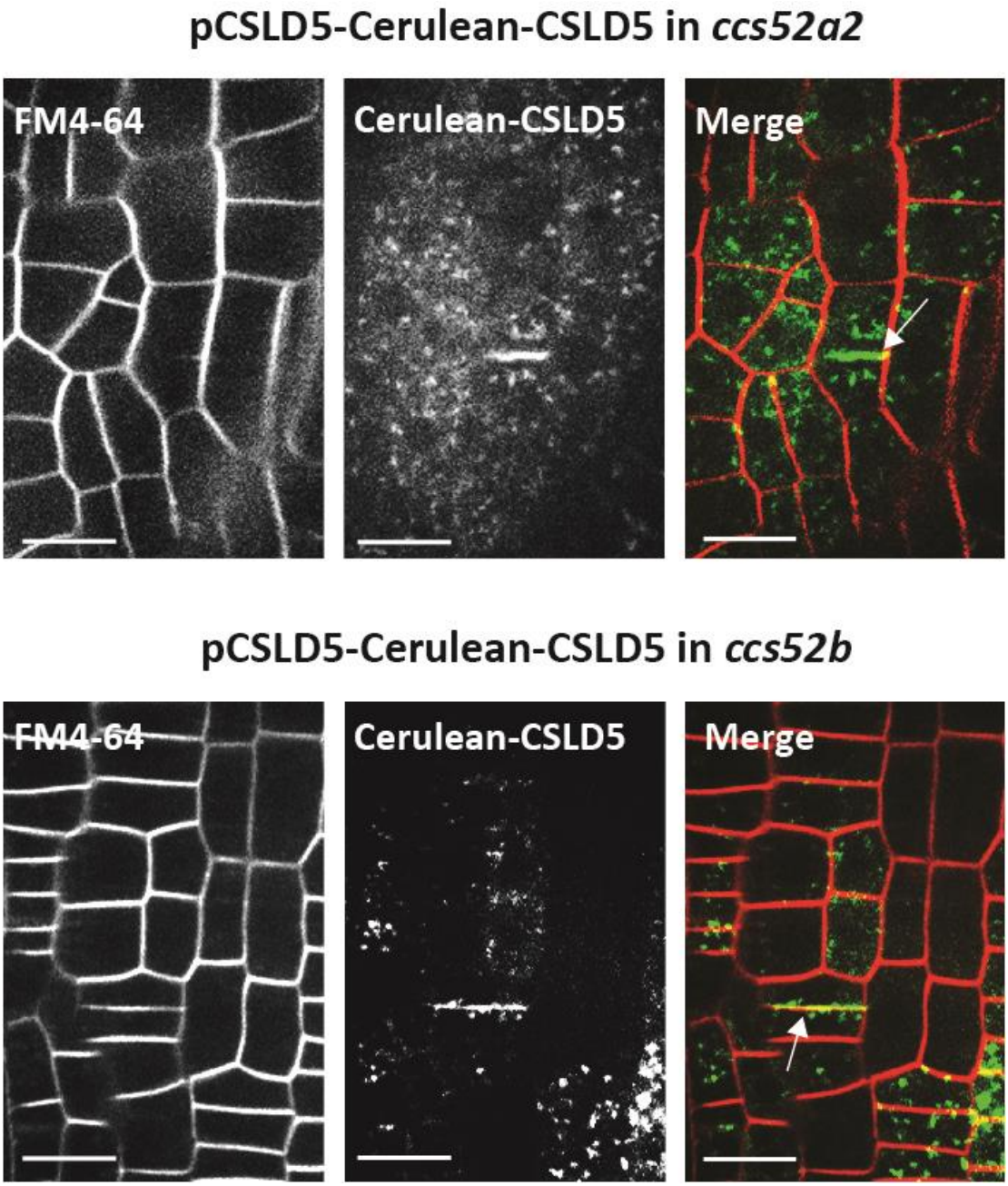


**Figure 2.20. Cerulean-CSLD5 accumulates in non-dividing cells in *ccs52a2* mutants**

Fluorescence of Cerulean-CSLD5 in five-day old *ccs52a2* and *ccs52b* mutant seedlings was examined by confocal microscopy. Cerulean-CSLD5 was detected at cell plates (arrows) in both backgrounds. However, Cerulean-CSLD5 fluorescence distribution was unchanged from wild type in *ccs52b* mutants, Cerulean-CSLD5 fluorescence could be observed even in non-dividing cells in the *ccs52a2* mutant background. Scale bars represent 20 µm.

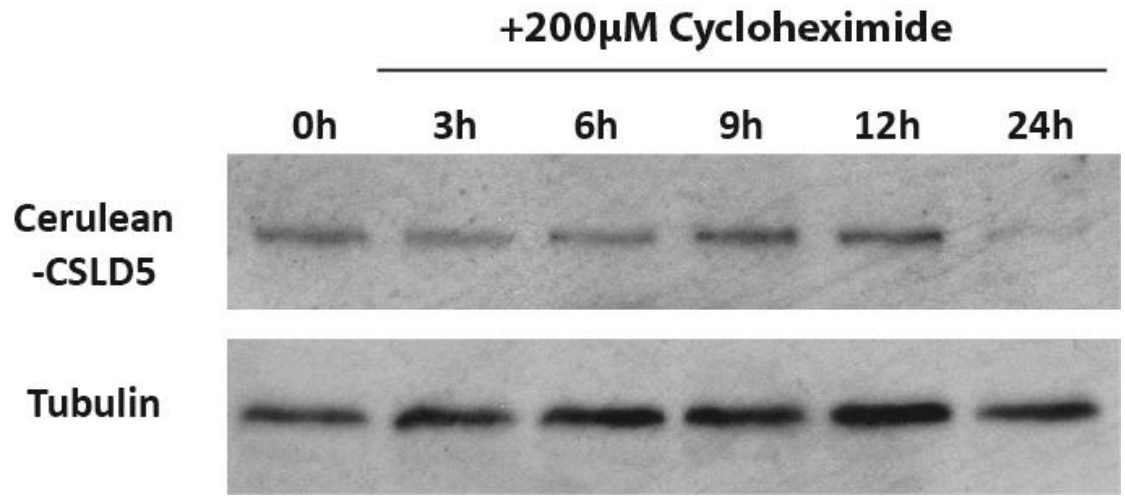


**Figure 2.21. Cerulean-CSLD5 protein instability is reduced in *ccs52a2* mutants**

Analysis of Cerulean-CSLD5 protein stability in the *ccs52a2* mutant background. Tubulin was used as a loading control. New protein synthesis was blocked by 200µM cycloheximide and the protein levels at each time point was detected by immunoblotting methods. The protein turnover rate of Cerulean-CSLD5 was significantly reduced. The protein level remains stable even after twelve hours of cycloheximide treatment.

GAAATTGTGCCTAATGACGTGTTCTTGTAAGTATGTGCAGCGAATCTTCTCTTTGTAGTATTTT
GTAACGAGACCTAAGACCATCCTGACCATCCTTATTGATGGTCTCTTAACATAACTCTTATGTT
AAGAGATATGTCTTATAATTAACAAAAGTGACTTAAAGTCTCTTATATAAGAAATTTTGTTAG
TTATAAAACATGTCTCTTAGCATAAGAATTGTTTTAAGAGATCATCAATAATGATGATCTAAG
AACTATTATACTATGTTCCGTCTCGATTTTGAAAGTACTTAAACGTCGTTATCGTGTTTGTCTCG
GCGTTTTAAATTCCACTGTATTAGTAAGAATTTATTTTTAAAATAACTTTAGTCATTTTTAATTA
TCTCTTCTCCCTTTTCAATTATTAATGATCATAGTAACTTCTCTTGATTTGTAAATATGCTACATA
GTTGATCTTTTGAATATACGAATGAAAACATATTATAATAGTATGTGTTCAAAATCTTTTGAGT
TTTATGAGTACAGAACTATATGTTTAATGGGCAGATTAGTATATAAAATTACCAGTGCATCAG
AAGGAATAATGATCTACTCGAGTAGTATATCAAAATAATACTATTCAAATGTATACCAACGAC
AATGAGTTCAAAATCATCAAACCCCATGGGATGATGAGCAAATAATATTTTTATCAGCTACTC
TATACATCATTTGATGATAATATGCAAAAATTGTATACCAATGAGTTCAAAATTATCAAACCAC
ATGGGATGAGAAAAAAGCATATTACTATTTTTAAACAGCTTCTCCAATATAAATTTATTTGACC
GTTACGGAAAGGGAGAGAGATACACACACTCTTTCTCTTTTATTATTTTCCGTTTATTTGACTTT
TCTTCTTTATAGATCGACCTGGTCCCACGTAATCTTTTCAAACTTACCGTTTGGATTCGATAATC
ACCGTCCGATCTCACATGAAGCAACGTGAATAAAATGAACGGTTTAGATCTATCGACCGTTTA
TAGCAATACCTTTCTCCTTTATAATCTCTATATCTCTCTCTCTCTGAATTTCGAAAATTATAATGC
TCTTCTGCTTCGTACTAGCTGCTTCAGCTTCTTCTTCTTCCTTAGATTCAAAATCTCTCTTCTT
CTGAGTTTCTGATTTTCAAGTTTGAGAACTACTCTTTTCCTTCTAAATCTTTGATTTTTTTCTCTC
GTGATTTTTGTGGTTCACTGCTAATTGTGAACCAAAGATGGTGAAATCAGCAGCTTCTCAGTC
ACCATCTCCGGTGACTATAACGGTGACACCATGTAAAGGATCCGGCGACAGAAGCTTAGGAT
TGACGAGTCCTATCCCACGCGCCTCCGTCATCACCAACCAAAACTCTCCTCTAAGCTCAAGAGC
CACGCGTCGCACTTCCATTAGCAGCGGGAATCGGAGATCTAACGGTGATGAAGGAAGATACT
GTTCTATGTCTGTGGAAGATCTAACGGCGGAGACGACTAATTCAGAGTGCGTTCTGAGCTATA
CTGTTCATATCCCACCTACGCCGGATCATCAGACGGTGTTCGCTTCACAGGAGAGTGAAGAAG
ACGAGATGCTAAAAGGGAATTCGAATCAAAAAAGTTTCCTCTCTGGGACGATTTTCACCGGTG
GGTTTAAATCGGTGACACGTGGTCATGTGATCGATTGTTCTATGGATAGAGCTGATCCGGAG

**Figure 2.22. An MSA transcriptional factor binding site is found in the promoter region of *CSLD5***

Part of the genomic DNA sequence as well as the promoter region (black), the 5' UTR (red) of *CSLD5* was obtained from TAIR. The region close to the start codon (orange, underlined) is shown. The location of a potential MSA site (green) is underlined. Orange color represents the predicted first exon.

| | Number of root hairs measured | Length of root hairs (µm) | Percentage of Col-0 |
|---|---|---|---|
| **Col-0** | 268 | 389.10 ± 63.08 | 100% |
| ***csld2*** | 95 | 282.60 ± 79.65 | 72.63% |
| ***csld3 (kjk-2)*** | 152 | 16.40 ± 9.43 | 4.21% |
| ***csld5*** | 117 | 362.86 ± 72.60 | 93.26% |
| **pCSLD2::Citrine-CSLD2 in *csld2*** | 98 | 376.15 ± 63.89 | 96.67% |
| **pCSLD3::Cerulean-CSLD2 in *kjk-2*** | 123 | 383.00 ± 77.86 | 98.43% |
| **pCSLD3::Cerulean-CSLD5 in *kjk-2*** | 231 | 184.52 ± 119.46 | 47.42% |

**Table 2.1. Root hair length in the lines examined in Chapter Two and Chapter Three**

| | Number of roots measured | Length of roots (cm) | Percentage of Col-0 |
|---|---|---|---|
| **Col-0** | 12 | 3.36 ± 0.44 | 100% |
| ***csld2*** | 19 | 2.80 ± 0.21 | 83.30% |
| ***csld3*** | 16 | 2.62 ± 0.23 | 77.87% |
| ***csld5*** | 11 | 2.28 ± 0.30 | 67.85% |
| ***csld2/csld5*** | 12 | 1.28 ± 0.20 | 38.12% |
| ***csld3/csld5*** | 8 | 1.29 ± 0.26 | 38.43% |
| **pCSLD5::Cerulean-CSLD5 in *csld5*** | 7 | 3.40 ± 0.26 | 101.07% |

**Table 2.2. The root length in Col-0, *csld* single mutants, and *csld* double mutants**

| | Number of plants measured | Diameter of rosette leaves (cm) | Percentage of Col-0 |
|---|---|---|---|
| **Col-0** | 19 | 5.56 ± 0.80 | 100% |
| ***csld5*** | 22 | 3.85 ± 0.37 | 69.25% |
| ***csld2/csld5*** | 17 | 0.61 ± 0.09 | 11.03% |
| ***csld3/csld5*** | 7 | 0.61 ± 0.14 | 10.94% |

**Table 2.3. Diameter or rosette leaves in Col-0, *csld5* single mutants, and *csld5* double mutants**

| | Number of cortical cells measured | Length of cortical cells (µm) | Percentage of Col-0 |
|---|---|---|---|
| **Col-0** | 179 | 223.35 ± 49.79 | 100% |
| ***csld5*** | 104 | 221.71 ± 78.74 | 99.26% |
| ***csld2/csld5*** | 90 | 126.98 ± 34.26 | 56.84% |
| ***csld3/csld5*** | 76 | 127.88 ± 42.94 | 57.26% |

**Table 2.4. Length of root cortical cells in Col-0, *csld5* single mutants, and *csld5* double mutants**

| | Number of roots measured | Number of cells | Percentage of Col-0 |
|---|---|---|---|
| **Col-0** | 9 | 51.11 ± 6.25 | 100% |
| ***csld5*** | 9 | 40.22 ± 3.27 | 78.69% |
| ***csld2/csld5*** | 12 | 22.75 ± 3.52 | 44.51% |
| ***csld3/csld5*** | 12 | 21.58 ± 5.12 | 42.22% |

**Table 2.5. Number of one column of root cortical cells in the root meristematic zone in Col-0, *csld5* single mutants, and *csld5* double mutants**

| | Number of plants examined | Number of cells | Percentage of Col-0 |
|---|---|---|---|
| **Col-0** | 7 | 66.71 ± 8.71 | 100% |
| ***csld5*** | 7 | 52.57 ± 5.94 | 78.80% |
| ***csld2/csld5*** | 9 | 52.67 ± 9.89 | 78.94% |
| ***csld3/csld5*** | 10 | 49.8 ± 13.10 | 74.65% |

**Table 2.6. Number of leave epidermal cells counted in selected regions in Col-0, *csld5* single mutants, and *csld5* double mutants**

| Primers | Primer Sequence (5’ -> 3’) |
|---|---|
| CSLD2 F | AAGGTACCATGGCATCTAATAAGCATTTTGATAAAAGT |
| CSLD2 R | AAGGATCCGAGACCTCATGGAAAACTGAAGTTTCC |
| CSLD2 Promoter F | GAATTCTTTGGTTCGGGAATGACTCC |
| CSLD2 Promoter R | CCATGGTCTAACTTGGCAGATCCCTGC |
| CSLD5 F | GGTACCATGGTGAAATCAGCAGCTTC |
| CSLD5 R | GGTACCTCAAGGGAATTGAAACTGCA |
| CSLD5 Promoter F | GAATTCCGGTGATGTTGCTTTACAA |
| CSLD5 Promoter R | TCATGATTGGTTCACAATTAGCAGTGA |
| CSLD3 Promoter F | GAATTCTGTTCTTTAATCGGCTTGAAAACCGTC |
| CSLD3 Promoter R | CCATGGCTGAAACAAAGCAAAACAGTAATATTGG |

**Table 2.7. A list of the primers used for PCR amplification and assembly of *CSLD2, CSLD3,* and *CSLD5* constructs in Chapter Two and Chapter Three**

# CHAPTER 3

# *CSLD* FUNCTIONAL REDUNDANCY DURING *ARABIDOPSIS* ROOT HAIR TIP GROWTH


## Abstract

In plant root hair cells undergoing a highly-polarized form of cell expansion called tip growth, newly synthesized cell wall polysaccharides are targeted and delivered to apical plasma membrane regions where they are then integrated into rapidly expanding cell walls in the tips of these cells. *CSLD3*, which is essential for root hair tip-growth, was previously determined to be enriched at the apical plasma membrane regions of growing root hairs. In *Arabidopsis*, two additional *CSLD* genes, *CSLD2* and *CSLD5*, are also expressed broadly in vegetative plant tissues. While *csld2* mutants also display root hair growth defects, the root hair morphology of *csld5* mutants has not been described. To examine to what extent three *CSLD* genes function during root hair growth, and whether they display any functional redundancy, the expression patterns and the sub-cellular localization of CSLD2, CSLD3, and CSLD5 were examined. Both *CSLD2* and *CSLD3* were highly expressed in root hair cells, but *CSLD5* was not. When expressed

under control of their cognate promoter sequences only fluorescent CSLD2 and CSLD3 proteins could be detected in root hair cells, where they both displayed enrichment in membranes at the tips of growing root hairs. However, when fluorescently-tagged CSLD2 and CSLD5 were placed under control of the *CSLD3* promoter, CSLD2 quantitatively restored root hair growth in *csld3* mutant backgrounds, while CSLD5 only partially rescued the root hair phenotype. Combined these observations, we proposed that CSLD2, CSLD3, and CSLD5 have similar functions in root hair growth.

## Introduction

Root hairs are tubular structures formed from root epidermal cells and they function in nutrient uptake and mycorrhizal interactions (Grierson et al., 2014). In *Arabidopsis*, epidermal cells located over the junction between two underlying cortical cells adopt root hair fate (Schiefelbein et al., 2009). These epidermal cells initially expand through a process called diffuse growth in which cellulose, the major load-bearing component in cell wall, is often transversely deposited to the axis of cell expansion (Nielsen, 2009; Grierson et al., 2014). Additionally, in diffuse growth, new cell wall components are uniformly deposited along one or more entire cell surfaces (Nielsen, 2009). Later in these cells, a swelling starts to form at the site where the root hair would initiate (Grierson et al., 2014). Once the swelling is formed, the root hair growth occurs from this limited region of the cell through a highly-polarized form of cellular expansion called tip growth

(Grierson et al., 2014). During root hair tip growth, new cell wall deposition is limited primarily to the tip of the cell where the cellular expansion occurs (Nielsen, 2009). However, continued cell wall deposition still occurs in the non-expanding flanking regions of the root hair (Nielsen, 2009). Since these cell walls are no longer expanding, they are considered to be secondary cell walls (Nielsen, 2009). These two distinct layers of cell wall in growing root hairs were observed in ultrastructural studies (Newcomb and Bonnett, 1965; Emons, 1994; Galway et al., 1997; Emons and Mulder, 2000). Electron microscope images showed that the initial cell wall layer arose at the extreme apical 20-30 µm of growing root hairs and the arrangement of the cellulose microfibrils found in this layer was random (Newcomb and Bonnett, 1965; Galway et al., 1997; Emons and Mulder, 2000). Beginning about 25 µm from the tip of root hair, an additional inner cell wall layer containing parallel arrays of cellulose microfibrils was deposited and these cellulose microfibrils were often organized in a helical orientation along the length of the root hair (Emons and Wolters-Arts, 1983; Emons, 1994; Emons and Mulder, 2000).

During tip growth, the cytoplasm containing all the cellular constituents required for tip growth is enriched in a sub-apical region which generally excludes the large central vacuole of the growing root hair (Grierson et al., 2014). During root hair tip growth, rapid, actin-dependent cytoplasmic streaming facilitates the continuous delivery of vesicles to the root hair apex (Grierson et al., 2014). Post-Golgi secretory vesicles, which contain cell wall materials such as polysaccharides and cell wall proteins, become enriched in the

extreme apical region of this cytoplasmic domain, called the “vesicle rich zone,” which localizes directly under apical plasma membranes at the tip of the cell (Grierson et al., 2014). The cell wall materials in these cargo vesicles selectively fuse with the apical plasma membrane and their contents are incorporated into the newly formed cell wall (Grierson et al., 2014).

Cellulose is enriched at the growing tips of root hairs and inhibiting cellulose synthesis causes root hair growth defects (Park et al., 2011; Galway et al., 2011). However, root hair tip growth does not appear to be significantly inhibited in *cesa* mutants (Gu and Nielsen, 2013). Additionally, CESA3 and CESA6, two known components of canonical cellulose synthase complexes, do not display levels of distribution in the apical plasma membranes in growing root hairs (Park et al., 2011). These results indicate that the root tip enriched cellulose may not be made by CESA proteins.

CESA proteins belong to a larger cellulose synthase-like superfamily, and members of several classes of this superfamily have been demonstrated to synthesize β-1,4-glycan backbones for various structural cell wall polysaccharides (Arioli et al., 1998; Richmond and Somerville, 2000; Liepman et al., 2005; Cocuron et al., 2007). In this superfamily, the CSLD protein family has higher structural similarity to the CESA protein family than either of these two groups show to any other CSL protein families (Richmond and Somerville, 2000). CSLD3 has been shown to play an essential role in root hair growth

(Favery et al., 2001; Wang et al., 2001; Galway et al., 2011). Therefore, it is possible that CSLD3 might be responsible for synthesis of tip enriched cellulose-like polysaccharides during root hair tip growth. It was recently shown that a functional eYFP-CSLD3 localized in the apical plasma membranes of growing root hairs (Park et al., 2011). Additionally, a chimeric CSLD3 protein containing the catalytic domain of CESA6 protein was able to restore root hair growth in *csld3* mutant background (Park et al., 2011). Taken together, these results would support the possibility that CSLD3, and possibly other CSLD proteins, might synthesize cellulose or cellulose like polysaccharides in apical cell wall domains during root hair tip growth.

Both CESA and CSLD families contain multiple members (Richmond and Somerville, 2000). In *Arabidopsis*, CESA2, CESA5, CESA6, and CESA9 segregate into a distinct subgroup of the CESA protein family, reflecting the maintenance of a high degree of sequence similarity between these CESA isoforms (Figure 1.3) (Persson et al., 2007). Consistent with this, CESA2, CESA5 and CESA9 were all shown to display some degree of functional redundancy with CESA6 (Persson et al., 2007; Desprez et al., 2007). *CESA6* encodes a cellulose synthase protein and mutations in *CESA6* resulted in inhibition of dark-grown hypocotyl elongation (Fagard et al., 2000). In *cesa2* mutants, the length of dark-grown hypocotyls was also significantly reduced (Persson et al., 2007), and in *cesa2/cesa6* double mutants these effects were additive, consistent with these two CESAs sharing functional redundancy (Persson et al., 2007). The *cesa9* single mutants

did not have apparent phenotypes, and *cesa2/cesa9* and *cesa6/cesa9* mutants were morphologically indistinguishable to single *cesa2* and *cesa6* mutants, respectively (Persson et al., 2007). However, the c*esa2/cesa6/cesa9* triple mutants were shown to be gametophytic lethal, which was taken as evidence that loss of *CESA2* and *CESA6* activities were being at least partially masked by *CESA9* (Persson et al., 2007). Additionally, CESA5 expressed under the control of the *CESA6* promoter partially restored the elongation defects of dark-grown hypocotyls in *cesa6* mutants, indicating CESA5 and CESA6 proteins have partially redundant functions (Desprez et al., 2007).

Examination of microarray based spatiotemporal gene expression maps showed that three of the six *Arabidopsis CSLD* genes, *CSLD2*, *CSLD3*, and *CSLD5*, are broadly expressed in various vegetative tissues (Brady et al., 2007), and loss either *CSLD2* or *CSLD3* function results in defective root hair development (Favery et al., 2001; Wang et al., 2001; Bernal et al., 2008; Yoo et al., 2012). The root hairs in *csld2* mutants are shorter than Col-0 and bulges are often formed at the base of these root hairs (Bernal et al., 2008), whereas root hair growth is completely abolished in *csld3* mutants (Wang et al., 2001; Favery et al., 2001). On the other hand, the root hair morphology of *csld5* mutants has not been reported in previous studies (Bernal et al., 2007; Zhu et al., 2010; Yin et al., 2011). Because both *CSLD2* and *CSLD3* genes are expressed in root hairs, it is intriguing that disruption of either of these two genes appears sufficient to interfere with appropriate root hair development. This might reflect one of several possibilities. Perhaps CSLD2

and CSLD3 proteins provide distinct biochemical activities. Alternatively, these two proteins may display distinct subcellular localizations within root hairs, or their gene expression patterns may limit when these protein activities are available during root hair development. Finally, why does *CSLD5* not appear to be required for root hair development at all? To distinguish between these possibilities, the individual roles of *CSLD2*, *CSLD3*, and *CSLD5* in root hair growth were investigated.

## Results

### Expression patterns of *CSLD* genes and sub-cellular localization of CSLD proteins in growing root hairs

Disruption of different *CSLD* genes causes distinct classes of root hair developmental defects (Figure 2.2). In *csld2* mutants, the root hairs often rupture during tip growth and the length of the root hairs was 72.63% to that in Col-0 (Figure 2.2) (Table 2.1). In these short root hairs of *csld2* mutants, bulges were formed at the bases of growing root hairs (Figure 2.2). In *csld3* mutants, the root hairs often rupture before tip growth, resulting in a bald root phenotype (Figure 2.2). However, root hair morphology in *csld5* mutants was largely similar to Col-0 controls (Figure 2.2). These results indicated that *CSLD2* and *CSLD3*, but not *CSLD5*, are necessary for root hair growth. To investigate the possibility that only *CSLD2* and *CSLD3* are expressed in root hair cells, we utilized an online root

gene expression pattern database (Brady et al., 2007) to examine the expression level of these three *CSLD* genes during the course of root hair development. As expected, both *CSLD2* and *CSLD3* are expressed in root hair cells (Figure 2.1). *CSLD2* transcript was detected in the mature region (region six, Figure 2.1) of the meristematic zone, and reached the peak in the young region (region seven, Figure 2.1) of the elongation zone. In the maturation zone where the root hairs underwent tip growth (region nine to ten, Figure 2.1), 50% to 60% of the peak *CSLD2* transcript level was still detected preferentially in the root hair cells. *CSLD3* was more broadly expressed in the meristematic and the elongation zones (region four to eight, Figure 2.1). Notably, unlike *CSLD2*, *CSLD3* showed a high transcript level in cells undergoing root hair initiation (region seven and eight, Figure 2.1). The transcript level of *CSLD3* was not significantly above background in the young and intermediate regions of the maturation zone (region nine to ten, Figure 2.1), and it was only later detected in mature root (region twelve, Figure 2.1). The spatial differences of the expression patterns of *CSLD2* and *CSLD3* might at least partially explain why losing *CSLD3* and *CSLD2* caused root hair rupture during the early and middle stages of root hair tip growth, respectively. Unlike *CSLD2* and *CSLD3*, the *CSLD5* transcript was high in the early meristematic zone (region two to four, Figure 2.1). However, the transcript of *CSLD5* was not detected at levels above background in root hair cells (region eight to ten, Figure 2.1). Therefore the lack of root hair phenotypes observed in *csld5* mutants might simply be due to the fact that *CSLD5* is not expressed at any significant level in root hair cells.

During root hair tip growth, cell wall synthases as well as cell wall materials are enriched in the extreme tip of growing root hairs (Gu and Nielsen, 2013; Grierson et al., 2014). Previously, eYFP-CSLD3 was shown to be enriched in apical plasma membranes in growing root hair tips (Park et al., 2011). Since *CSLD2*, like *CSLD3*, is expressed in root hair cells and is required for root hair development, we hypothesized that CSLD2 might also display a similar enrichment in apical plasma membranes as that observed for CSLD3. Therefore, we fused the optimized yellow fluorescence protein variant, Citrine, to the amino-terminal end of CSLD2 and expressed it under the control of endogenous *CSLD2* promoter sequences (*CSLD2p::Citrine-CSLD2*). Phenotypic analysis showed that the length of the short root hairs in *csld2* mutants, whose length is typically 72.63% of that observed in wild type, was fully restored to the wild type level by *CSLD2p::Citrine-CSLD2*, indicating that the fusion protein is functional (Figure 2.8) (Table 2.1 and 2.2). When expressed in plants, Citrine-CSLD2 proteins were localized to large cytoplasmic structures, which presumably to be the Golgi apparatus, and secretory vesicle-like structures which primarily accumulated in the apical vesicle-rich zone of growing root hairs (Figure 3.1). Additionally, similar to eYFP-CSLD3, fluorescence of Citrine-CSLD2 was also observed to be enriched on the apical plasma membrane (Figure 3.1). Because both eYFP-CSLD3 and Citrine-CSLD2 displayed similar sub-cellular localizations, and in particular both were enriched in apical plasma membranes, it is unlikely that the root hair defects observed in *csld2* and *csld3* mutants were caused by distinct protein sub-cellular localizations.

**CSLD2 can functionally replace CSLD3 activity during root hair development**

The fact that eYFP-CSLD3 and Citrine-CSLD2 localize to apical plasma membrane domains when expressed under the control of their endogenous promoters indicates that both these proteins are present where CSLD function is thought be required during root hair tip-growth. As a result, it is unlikely that the lack of redundancy observed upon loss of either of these two genes was due to differing subcellular localization. We therefore wondered whether root hair tip-growth defects might be the result of gene dosage effects, due to differing expression profiles, or whether these two CSLD proteins had distinct functions in root hairs.

To test these possibilities, we examined whether CSLD2 could rescue the root hair defects in *csld3* mutants. Therefore, we fused Cerulean, a cyan fluorescence protein variant, to the amino-terminal end of CSLD2 and expressed it under the control of endogenous *CSLD3* promoter sequences (*CSLD3p::Cerulean-CSLD2*). When expressed in *csld3* mutants, *CSLD3p::Cerulean-CSLD2* quantitatively rescued the root hair defects (Figure 3.2). Cerulean-CSLD2 also showed a similar sub-cellular distribution to what was observed for eYFP-CSLD3, and Citrine-CSLD2 when expressed under its own *CSLD2* promoter sequences (Figure 3.3). The fluorescence of both eYFP-CSLD3 and Cerulean-CSLD2 was found in vesicle like structures, which accumulated at the apically-localized vesicle rich zones, and in apical plasma membrane domains in growing root

hairs (Figure 3.3). These results demonstrated that if expressed at the appropriate times, CSLD2 can functionally replace CSLD3.

**CSLD5 partially substitutes CSLD3 activity during root hair development**

The *csld3/csld5* double mutants displayed more incomplete cell walls compared to single *csld5* mutants, indicating that *CSLD3* and *CSLD5* both can participate in cell plate formation during cytokinesis (Figure 2.6). We were therefore curious whether CSLD5 could also functionally replace CSLD3 in root hair tip growth. We examined whether *CSLD3p::Cerulean-CSLD5* constructs were able to quantitatively rescue the root hair defects in *csld3* mutants. We found that root hairs could be formed when *CSLD3p::Cerulean-CSLD5* was expressed in *csld3* mutants (Figure 3.2). However, this rescue was quantitatively different from that observed when using the *CSLD3p::Cerulean-CSLD2* constructs, as these root hairs were only 47.42% of the root hairs in wild type (Figure 3.2) (Table 2.1). These results showed that CSLD5, unlike CSLD2, cannot entirely substitute for CSLD3 function during root hair growth.

The failure of *CSLD5* to fully rescue *csld3* mutant root hair defects might be due to differing sub-cellular distributions, due to differing expression level, or due to differing functions between CSLD3 and CSLD5. To distinguish between these possibilities, we examined the sub-cellular distribution of CSLD5 in growing root hair cells. When

expressed under the control of the *CSLD5* promoter, the fluorescence of Cerulean-CSLD5 was undetectable in growing root hairs (Figure 3.4). The lack of Cerulean-CSLD5 fluorescence might be due to the low transcription level of *CSLD5* in this cell type (Figure 2.1). When Cerulean-CSLD5 was ectopically expressed under the control of the *CSLD3* promoter, the fluorescence of Cerulean-CSLD5 in root hairs remained significantly lower than either eYFP-CSLD3 or Cerulean-CSLD2 when these constructs were expressed under control of *CSLD3* promoter sequences (Figure 3.3 and 3.4). The weak Cerulean-CSLD5 fluorescence observed in partially rescued root hairs in the *csld3* mutant background was detected in cytoplasmic structures, and in plasma membranes in these cells, but no significant enrichment in the apical regions of these cells was detected (Figure 3.4). When expressed under the control of the *35S* promoter, a strong constitutive promoter, Cerulean-CSLD5 showed a similar sub-cellular distribution pattern in growing root hairs to that observed for Citrine-CSLD2 or eYFP-CSLD3 (Figure 3.5). The fluorescence of Citrine-CSLD5 was localized to both cytoplasmic punctate structures and the apical plasma membranes (Figure 3.5). While the fluorescence level of Citrine-CSLD5 remained significantly lower compared to those observed for Citrine-CSLD2 and eYFP-CSLD3 (Figure 3.5), the fluorescence was significantly higher than what have been observed for plants expressing *CSLD5p::Cerulean-CSLD5* and *CSLD3p::Cerulean-CSLD5* (Figure 3.4). Consistent to this, it was also shown that CSLD5 expressed under the control of *35S* promoter could fully rescue the root hair growth defects in *csld3* mutants (Yin et al., 2011). Based on these results, the failure of CSLD5 to fully rescue

the root hair growth defects in *csld3* mutants appears to be correlated with decreased levels of CSLD5 protein accumulation in root hairs, regardless of whether these constructs were expressed behind the *CSLD3* promoter, or the strong, constitutive *35S* promoter sequences.

## Discussion

Functional redundancy is a common phenomenon in higher eukaryotic systems, and particularly in plants (The Arabidopsis Genome Initiative, 2000; Bouché and Bouchez, 2001). For example, in *Arabidopsis*, several cellulose synthases, namely CESA2, CESA5, CESA6, and CESA9, have redundant functions (Persson et al., 2007; Desprez et al., 2007). Recently, the functional redundancy of *CSLD2* and *CSLD3* genes was investigated (Yoo et al., 2012). Although *CSLD2* and *CSLD3* were shown to function redundantly in *Arabidopsis* root hair and female gametophyte development, whether CSLD2 and CSLD3 were functionally interchangeable was not examined (Yoo et al., 2012). Additionally, whether CSLD5 displays redundant function to CSLD3 is unknown. In this chapter we investigated the functional redundancy in the CSLD protein family. We found that *csld2*, *csld3*, and *csld5* mutants each displayed different levels of root hair development defects. Loss of *CSLD2* reduced root hair length and these root hairs ruptured during root hair tip growth. Additionally, bulges were formed at the base of these root hairs. Loss of *CSLD3* resulted in root hair rupture during the transition to the

tip growth when the root hair initiation occurred, causing a root lacking any appreciable root hairs. Meanwhile, the root hair morphology in *csld5* mutants was indistinguishable to that of wild type plants.

Based on the results presented in this study, we propose that the different root hair defects of *csld2* and *csld3* mutants are likely to be a result of gene dosage effects. This is based on several lines of evidence. First, *CSLD2* and *CSLD3* displayed different expression patterns during root hair growth. Based on data obtained from a root gene expression pattern database, *CSLD3*, but not *CSLD2*, was expressed during the transition to tip-restricted expansion that is associated with root hair initiation. On the other hand, once root hair tip growth was established, the transcription level of *CSLD2* in root hairs remained 50% to 60% of its peak transcription level in root tissues. However, the level of *CSLD3* transcription was not significantly above background in these cells. Combined, it appeared that only one of these two *CSLD* genes was expressed at significant levels during root hair initiation (*CSLD3*), while the other provides the majority of CSLD expression once root hair tip growth is established (*CSLD2*). Second, when expressed under the control of the *CSLD2* endogenous promoter, the fluorescently tagged CSLD2 proteins showed similar sub-cellular localization to what observed for CSLD3. Both of these fluorescent fusion proteins localized in vesicle like structure accumulated in apically-localized vesicle rich zones. As was observed for eYFP-CSLD3, Citrine-CSLD2 proteins were also observed to be enriched in the apical plasma membranes of these root

hair cells. Therefore, the lack of redundancy observed in *csld2* and *csld3* mutants was not likely to be caused by distinct sub-cellular localizations. Finally, when expressed under the control of the *CSLD3* promoter, Cerulean-CSLD2 was able to fully rescue the root hair defects in *csld3* mutants. Therefore, it is likely that CSLD2 and CSLD3 proteins have interchangeable functions and whether they play roles in root hair initiation or later stages during root hair tip growth were determined primarily by differences in the timing of their expression during root hair development.

Interestingly, the fact that Cerulean-CSLD2 under the control of the *CSLD3* promoter quantitatively restored root hair growth in *csld3* mutants indicated that these fluorescently-tagged or endogenously-expressed CSLD2 proteins were the only CSLD proteins present at any significant level in the *csld3* root hairs. In other words, as long as expressed at the right time and place, CSLD2 alone was sufficient to provide cell wall synthase activities normally provided by both CSLD2 and CSLD3 during root hair development. This is distinct to the closely-related CESA proteins since cellulose synthase complexes involved in primary cell wall synthesis requires the participation of at least three distinct CESA isoforms, CESA1 proteins, CESA3 proteins, and either CESA6 or CESA6-like proteins (Persson et al., 2007; Desprez et al., 2007). Therefore, unlike CESA cell wall synthase complexes, functional CSLD cell wall synthases, either act as monomers or can assemble into homomeric complexes, at least during root hair development. If true, the polysaccharides synthesized by CSLD proteins in root hairs

might be structurally different to the arrayed crystalline cellulose microfibrils synthesized by the CESA cellulose synthase complexes. Taking into account previous observations that CSLD3 may provide a cellulose, or cellulose-like β-1,4-glucan synthase activity, an intriguing possibility is that CSLD2 and CSLD3 might synthesize the randomly oriented fibrillar elements, described in the initial cell walls at the apical region of growing root hairs (Newcomb and Bonnett, 1965).

While there is some evidence supporting a role for CSLD proteins in synthesis cellulose or cellulose-like β-1,4-glucan polysaccharides, this family of cell wall synthases have also been linked to synthesis of other classes of cell wall polysaccharides. Synthesis and deposition of the hemicellulose, xyloglucan, has been demonstrated to be necessary for proper root hair expansion and development (Cavalier et al., 2008; Park et al., 2011). It was also recently shown that plants lacking acidic xyloglucan displayed shorter root hairs, highlighting the importance of this class of polysaccharide in root hair development (Peña et al., 2012). In *Arabidopsis, CSLC4* encodes an enzyme with xyloglucan β-1,4-glycan backbone synthase activity (Cocuron et al., 2007). *CSLC4* is broadly expressed in vegetative tissues, but it did not appear to be specifically expressed to any significant degree in root hair cells (data obtained from online expression pattern database, data not shown)., Therefore it is tempting to speculate that CSLD proteins produce the xyloglucan β-1,4-glycan backbone. However, the plasma membrane localization of CSLD3 protein was shown to be essential for the ability of CSLD3 to rescue *csld3* mutants (Park et al.,

2011). If the β-1,4-glycan backbone of xyloglucan is synthesized by CSLD3 at the plasma membrane, how it could then be further modified by Golgi-localized xylosyltransferase, galactosyltransferase, fucosyltransferase, and galacturonosyltransferase enzymes is hard to envision (Perrin et al., 1999; Faik et al., 2002; Madson et al., 2003; Vanzin et al., 2002; Cavalier and Keegstra, 2006; Cavalier et al., 2008; Zabotina et al., 2008; Peña et al., 2012; Chou et al., 2012, 2014). As a result, it seems unlikely that if β-1,4-glucan polysaccharides are synthesized by CSLD proteins, that these serve solely as a substrate for xyloglucan biosynthesis. However, we cannot exclude the possibility that CSLD2 and CSLD3 synthesize other classes or polysaccharides in growing root hairs, and the exact function of these CSLD proteins can only be determined by further biochemical activity analyses.

Unlike *CSLD2* and *CSLD3*, loss of *CSLD5* did not cause root hair defects. We propose that the lack of root hair defects in *csld5* mutants is due to the lack of any appreciable transcription of the *CSLD5* gene in root hairs. However, unlike *CSLD2*, when *CSLD5* was expressed under the control of the *CSLD3* promoter, this was only able to partially rescue the root hair defects in *csld3* mutants. This might also due to the dosage effects since the fluorescence of Cerulean-CSLD5 in these root hairs was much lower compared to what observed for Cerulean-CSLD2 and eYFP-CSLD3 despite these transgenic constructs all displaying similar levels of mRNA accumulation based on RT-PCR (not shown). This is potentially due to a post-translationally regulation of CSLD5

protein stability in root hairs, which might be supported by at least two pieces of evidence. First, Cerulean-CSLD5 was shown to be degraded rapidly upon completion of cytokinesis (Figure 2.14, Figure 2.15, and Figure 2.17). Therefore, Cerulean-CSLD5 proteins might be degraded in a similar mechanism in root hair cells since these epidermal cells do not undergo additional rounds of cell division, and therefore should be uniformly in interphase stages of the cell cycle. Second, Citrine-CSLD5 constructs expressed under the control of the strong, constitutive *35S* promoter were shown to localize at punctate vesicle-like structures in growing root hairs and the fluorescence, as observed for Citrine-CSLD2 and eYFP-CSLD3 constructs, also accumulated at the apical regions. However, the relative levels of fluorescence detected for these Citrine-CSLD5 fusion proteins was dramatically lower than for the other 35S-driven fluorescent-CSLD constructs. In conclusion, the instability of CSLD5 proteins due to potential post-translationally regulations in root hair cells is likely to be the reason of the partial rescue of *csld3* mutants.

## Materials and Methods

### Plant material and growth conditions

*Arabidopsis* seeds were surface-sterilized for fifteen minutes in 30% sodium hypochlorite / 0.02% Triton X-100 solution. The seeds were washed with sterilized

double distilled water and stored at 4°C overnight before being transferred to ¼ MS growth medium. Seedlings were germinated and grown in growth chambers. After seven to fourteen days the seedlings were transferred from plates to soil and grown in growth rooms. Unless specified, the seedlings/plants were grown at 21°C in long-day condition (sixteen hours of light/eight hours of dark).

**Root hair and root phenotype analysis**

The root hair morphology was examined using five-day old seedlings. To measure the root hair length, the regions with mature root hairs were recorded using 4X lens (Fluorescent, NA=0.13) from a Nikon Eclipse 6600 microscope. The length of each non-bending mature root hairs in these images was measured using ImageJ (NIH). To record the root hair growth defects, the images of root hairs of interest were collected using 10X lens (Apochromatic, NA=0.45). seven-day-old seedlings were used for root length comparison. The seedlings were grown vertically to allow the fully elongation of the roots. The plates were scanned and the length of the roots was measured using ImageJ (NIH).

**Confocal microscopy**

The fluorescent imaging was performed with an Olympus spinning disk confocal using a 60x oil lens (Apochromatic, NA=1.42). Metamorph Advanced software (Molecular Devices, Inc) was used for image capture. For multi-channel imaging, the channels were switched sequentially from long wavelength to short wavelength. The signal from FM4-64 was excited at 561nm and collected at 607nm. The signal from YFP/Citrine was excited at 515nm and collected at 562nm. The Cerulean signal was excited at 445nm and collected at 483nm.

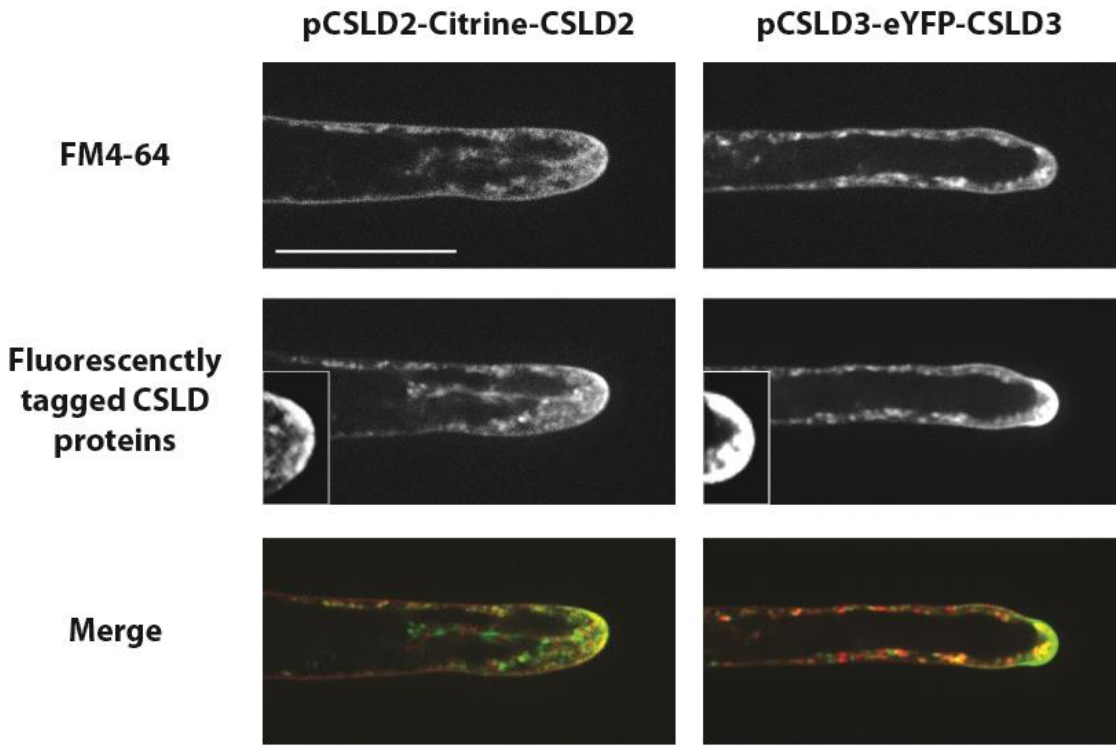


**Figure 3.1. Sub-cellular localization of CSLD2 and CSLD3 proteins in root hairs**

The fluorescence of CSLD proteins in actively growing root hairs from five-day old seedlings was examined by confocal microscopy. Citrine-CSLD2 and eYFP-CSLD3, expressed under control of their endogenous promoters, could be detected enriched at the apical plasma membrane regions (enlarged box). Scale bar represents 50 µm.

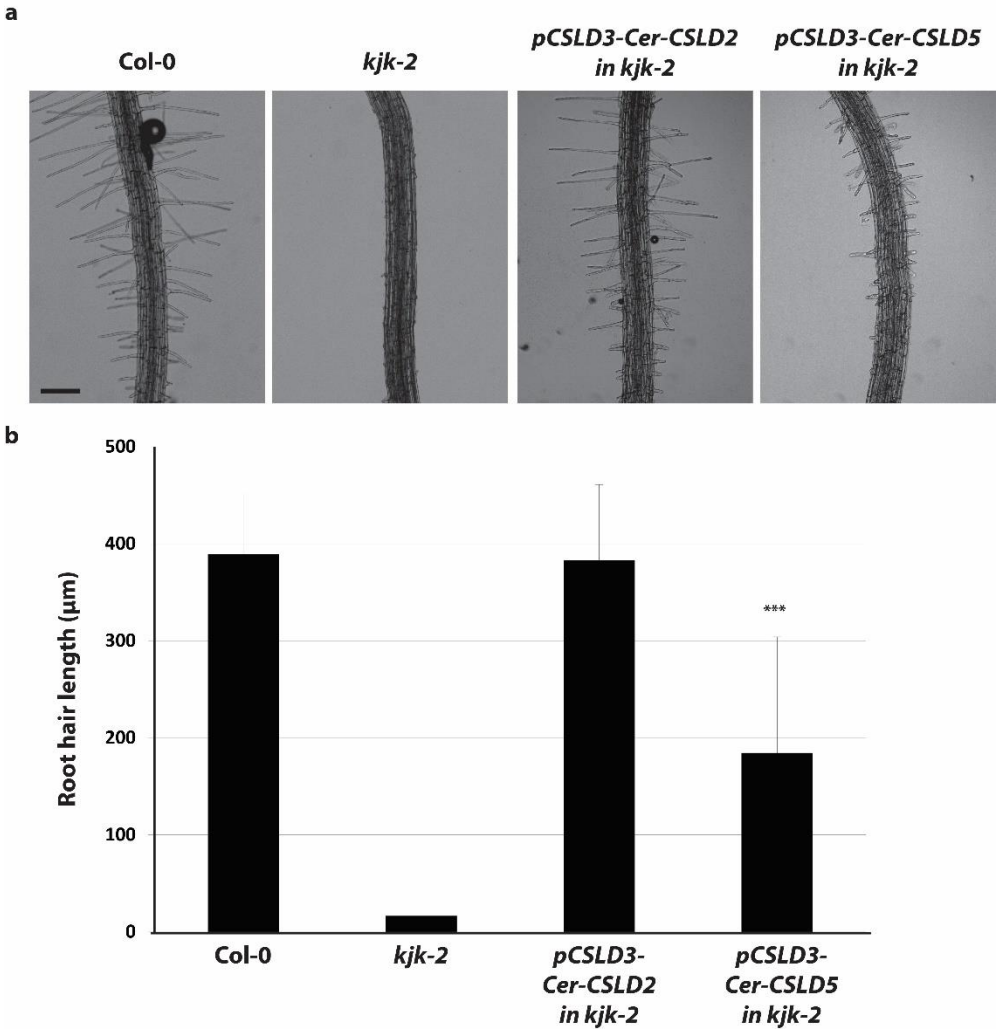


**Figure 3.2. *CSLD2* and *CSLD5* rescues the *csld3* (*kjk-2)* phenotype to different extents**

(**a**) The root hair morphology of five-day old wild type Col-0, *kjk-2* mutants, and *kjk-2* mutants expressing fluorescently tagged CSLD2 and CSLD5 proteins were examined. When expressed under the control of the *CSLD3* promoter, CSLD2 fully restored wild type root hair morphology in the *csld3(kjk-2)* mutant background. However, CSLD5 expressed under control of the *CSLD3* promoter failed to fully restore root hair growth and shorter root hairs were observed. (**b**) Quantitative analysis of the root hair length in different lines. Scale bar represents 200 µm. Error bars represent standard deviation. Asterisks represent p-value (*** = less than 0.005).

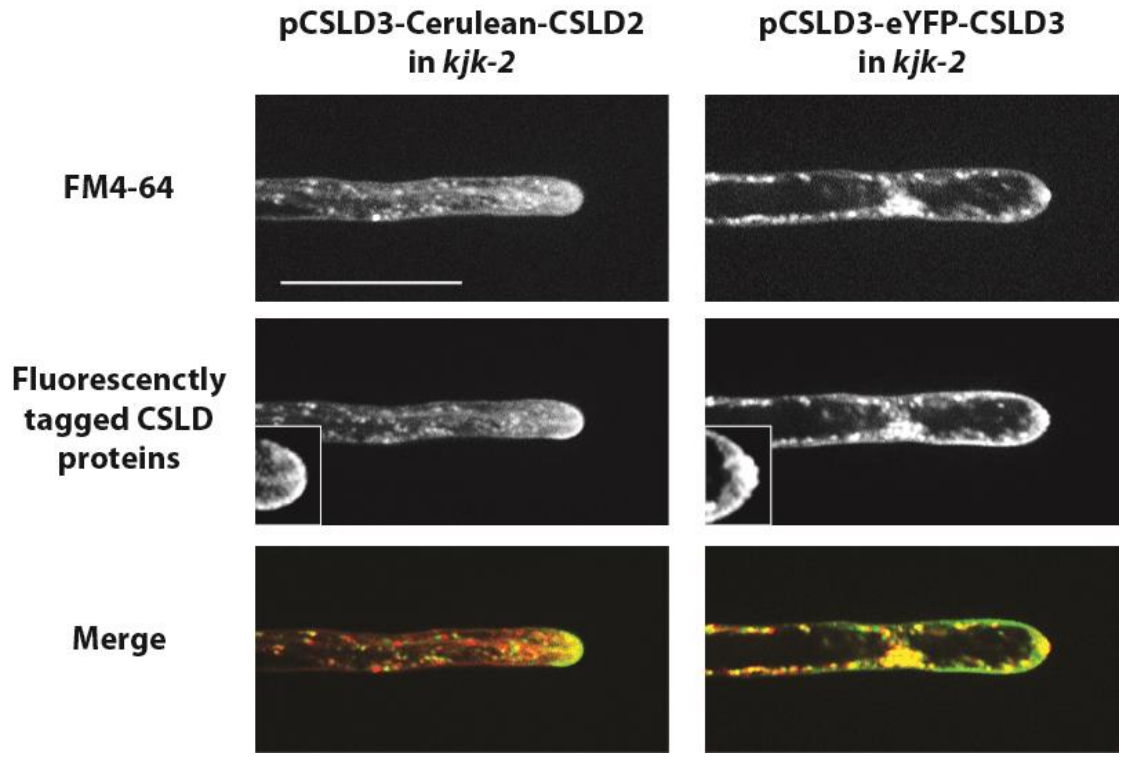


**Figure 3.3. Sub-cellular localization of fluorescently tagged CSLD2 and CSLD3 proteins when expressed under the control of the *CSLD3* promoter**

Both Cerulean-CSLD2 and eYFP-CSLD3 were expressed under the control of the *CSLD3* promoter. The fluorescence of these CSLD proteins in the growing root hairs from five-day-old seedlings was examined by confocal microscopy. For both Cerulean-CSLD2 and eYFP-CSLD3fusion proteins, fluorescence was highly enriched at the apical plasma membrane regions of growing root hairs (enlarged boxes). Scale bar represents 50 µm.

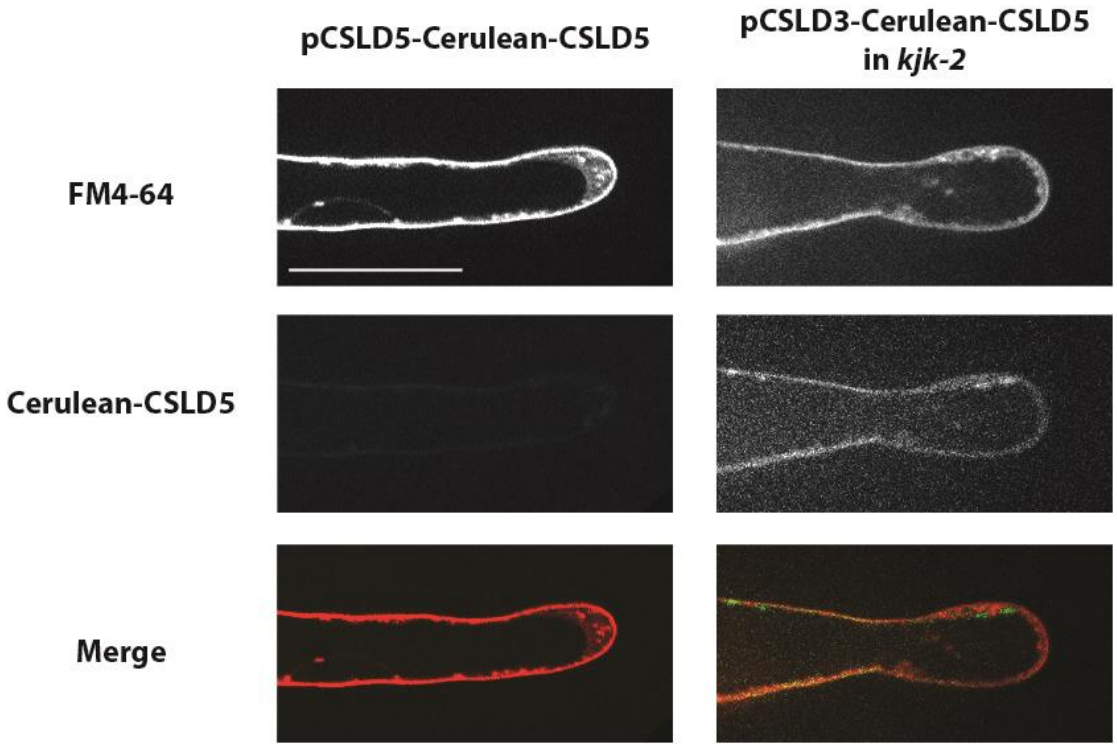


**Figure 3.4. Sub-cellular localization of fluorescently tagged CSLD5 proteins when expressed under the control of *CSLD3* or *CSLD5* promoters**

The fluorescence of Cerulean-CSLD5 fusion proteins in growing root hairs from five-day-old seedlings was examined by confocal microscopy. The fluorescence of Cerulean-CSLD5 was undetectable in root hairs when its expression was controlled by endogenous promoter sequences. However, when the Cerulean-CSLD5 protein was fused behind *CSLD3* promoter sequences, the weak Cerulean-CSLD5 fluorescence could be detected in growing root hairs. Scale bar represents 50 µm.

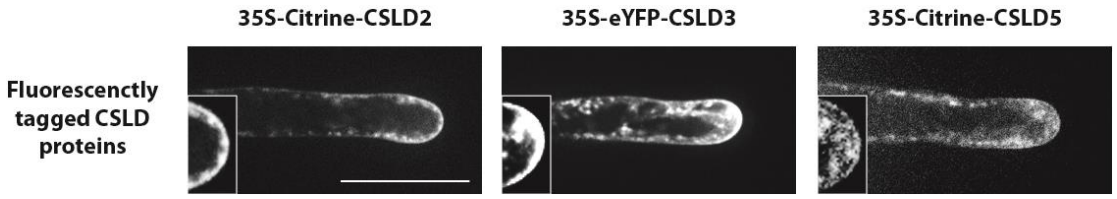


**Figure 3.5. Sub-cellular localization of fluorescently tagged CSLD proteins under the control of the *35S* promoter**

The fluorescence of CSLD fusion proteins in growing root hairs from five-day old seedlings was examined by confocal microscopy. The fluorescence of Citrine-CSLD2 and eYFP-CSLD3, expressed under control of *35S* promoter, was highly enriched at the apical plasma membrane regions of growing root hairs (enlarged box). The fluorescence of Citrine-CSLD5 was also detected at the same region of growing root hairs (enlarged box). However, the fluorescence intensity was less than observed for Citrine-CSLD2 and eYFP-CSLD3. Scale bar represents 50 µm.

# CHAPTER 4

# CONCLUSIONS AND FUTURE DIRECTIONS

## Conclusions

The work in this study has focused on investigating the roles of CSLD proteins in *Arabidopsis* development. The CSLD family belongs to the Cellulose Synthase Like superfamily, which includes the CESA family of higher plant cellulose synthases, as well as other predicted β-1,4-glycan synthases. Interestingly, CSLD proteins share a high sequence similarity, and their predicted protein structure is more closely related to CESA sequences than either of these two protein families share with other CSL subgroups (Richmond and Somerville, 2000). Initial studies of CSLD functions in *Arabidopsis* mutants have revealed important roles in polarized expansion associated with tip growth in both root hair cells and in pollen tubes (Wang et al., 2001; Favery et al., 2001; Bernal et al., 2007, 2008; Zhu et al., 2010; Wang et al., 2011). Previous studies have raised the possibility that CSLD proteins might be involved in the biosynthesis of xylan, homogalacturonan, or mannose (Bernal et al., 2007; Yin et al., 2011). However, recent reports have provided evidence that at least one member of the CSLD family may

synthesize β-1,4-glucan polymers and provide cellulose/cellulose-like polysaccharides during *Arabidopsis* root hair tip growth (Park et al., 2011; Galway et al., 2011). In this study, a novel role for CSLD family members during cytokinesis has been described. While CSLD5 provides essential activity, both other vegetatively expressed *CSLD* genes, *CSLD2* and *CSLD3*, were also demonstrated to function cooperatively during cytokinesis. In addition, CSLD5 protein accumulation and degradation was demonstrated to be tightly regulated by regulatory elements of the cell cycle. These results highlight important roles for CSLD cell wall synthases in addition to previously characterized roles in polarized secretion of cell wall components in tip-growing cells. They also highlight an interesting new connection between the cell cycle associated regulation of cytokinesis and how these regulatory mechanisms may be harnessed to provide appropriate cell wall synthase activities to newly forming cell plates during these terminal steps of cell division.

In a separate set of experiments, the degree of functional redundancy of the three vegetatively-expressed *CSLD* family members was assessed in the context of root hair growth. These studies relied primarily on promoter-swap studies, and demonstrated that CSLD2 can quantitatively replace CSLD3 function when expressed under control of endogenous *CSLD3* promoter sequences. These results support a model in which CSLD activity in root hairs only requires one CSLD protein, as *CSLD5* was shown to be transcriptionally inactive in these cells. However, while CSLD2 and CSLD3 proteins were shown to be functionally interchangeable, *CSLD5* was unable to completely replace

*CSLD3* function, and in the current model we interpret this to be due to the rapid degradation of this protein in non-mitotic cells. Collectively, these results provide important new understanding of the functional roles of CSLD cell wall synthases in plant growth and development. They have revealed novel plant-specific aspects of cell cycle regulation of cytokinesis. In addition, in demonstrating that normal root hair development can be restored in cellular contexts where only *CSLD2* gene product is present, these results further highlight important differences between the *CSLD* family and their closely related *CESA* cellulose synthase counterparts.

## Future Directions

Incomplete cell walls were found in *csld5* single mutants, and the cytokinesis defects were more severe in *csld2/csld5* and *csld3/csld5* double mutants. We showed that fluorescently tagged CSLD proteins localized on cell plates in dividing cells. These observations supported a model in which *CSLD2*, *CSLD3*, and *CSLD5* are all involved in nascent cell wall synthesis on cell plates during cytokinesis. Additionally, although these three proteins display some level of functional redundancy, *CSLD5* plays a particularly critical role during cell plate formation. By comparing the dynamics of CSLD5 to other cell plate localized proteins, we found that the accumulation and degradation of CSLD5 protein was tightly regulated by the cell cycle. CSLD5 protein was shown to selectively accumulate in dividing cells. In telophase, CSLD5 was almost exclusively localized on

membranes surrounding the elongating cell plate. When cytokinesis was complete, the level of CSLD5 was reduced rapidly. We showed that CSLD5 proteins were stabilized when the activity of the 26S proteasome was blocked. Additionally, we also showed that when CCS52A2, an anaphase promoting complex activator, was disrupted, the rapid Cerulean-CSLD5 protein turnover kinetics were lost. These observations support the possibility that CSLD5 proteins were degraded via the $APC^{CCS52A2}$ – 26S proteasome mediated proteolysis pathways.

Although these results support the current model in which the accumulation and degradation of CSLD5 is regulated by the cell cycle, the detailed mechanism for these processes remains unclear. The first question is how does CSLD5 proteins selectively accumulate in early telophase? One hint comes from the promoter region of *CSLD5*. We found a mitosis specific activator (MSA) element close to the start codon of *CSLD5* (Figure 2.22). MSA elements are cis-elements that are bound by transcription factors which regulate the expression of G2/M phase specific genes (Ito et al., 2001; Haga et al., 2011). Therefore, it is possible that G2/M phase specific transcription factors, such as MYB3R1 and MYB3R4 (Haga et al., 2011), might bind the promoter of *CSLD5* and trigger its expression during the G2 to M phase transition. However, we detected *Cerulean-CSLD5* mRNAs from seedlings whose cell cycle was arrested in early S phase by two days of aphidicolin treatment (Figure 4.1). Therefore we know the *Cerulean-CSLD5* mRNAs are stable and the effect of a potentially reduced expression of *Cerulean-*

*CSLD5* during G2/M transition therefore might not reflect only transcription during the G2/M transition. To better characterize the role of this MSA element for *CSLD5* transcription, we may need to utilize an aphidicolin-based cell cycle synchronization method (Ito et al., 2001; Menges and Murray, 2002). In this method, plant cells were first synchronized in early S phase by aphidicolin addition, and upon removal of aphidicolin the peak of G2/M phase was reached after nine to thirteen hours (Menges and Murray, 2002). Therefore, we can perform real-time PCR to compare the change of *CSLD5* transcript levels in MSA mutated lines and controls on an hourly basis during the G2/M transition. If the transcription of *CSLD5* is inhibited when the MSA site is mutated, then we can further test whether MYB3R1/MYB3R4 binds this MSA site, or identify other binding transcription factors that regulate *CSLD5* expression.

We also need to examine the detailed role CSLD5 plays during cell plate formation. To determine whether the enzymatic activity of CSLD5 is required for cytokinesis, we could test whether the *csld5* mutant phenotypes could be rescued by catalytically inactive CSLD5. To generate the inactive form of CSLD5, the D, D, D, QxxRW catalytic motif, which is conserved in the CSL protein superfamily (Richmond and Somerville, 2000), of CSLD5 protein would be mutated. When the amino acid sequence of multiple CESA and CSLD proteins were aligned, the D(443), D(664), D(884), QVLRW(922 – 926) catalytic motif in the CSLD5 amino acid sequence was identified (data not shown). It was shown that when these conserved Asp residues in CESA proteins were mutated, the amount of

cellulose in the mutants was reduced, indicating that the enzymatic activities of these CESA proteins were disrupted (Taylor et al., 2000; Beeckman et al., 2002). Based on the high sequence similarity/identity between CESA proteins and CSLD proteins, it is very likely that mutations of these Asp residues in CSLD5 protein might also disrupt its enzymatic activity. We would convert these three Asp residues into Ala residues by PCR based mutagenesis and examine whether the short root phenotypes of *csld5* mutants could be rescued by the potential catalytically inactive CSLD5 (expressed under the *CSLD5* promoter). If the phenotype cannot be rescued, then we would propose that the enzymatic activity of CSLD5 is disrupted. The failure to rescue *csld5* short root phenotype would therefore indicate that the enzymatic activity is essential for the function of CSLD5.

It is also possible that mutation of all these three conserved Asp residues is not sufficient to disrupt the enzymatic activity of CSLD5. If so, the short root phenotype of *csld5* could be rescued even if these Asp residues are mutated. If this is the case, we would further mutate the QVLRW (922 – 926) residues of the CSLD5 catalytic motif and examine whether the phenotypes of *csld5* mutants could still be rescued. Alternatively, we could replace the catalytic domain of CSLD5 with that of the catalytically inactive CESA1 or CESA3 proteins (Taylor et al., 2000; Beeckman et al., 2002). If the *csld5* mutant phenotypes could still be rescued by these mutated CSLD5 proteins, then we would propose that the D, D, D, QxxRW catalytic motif is not required for the function of CSLD5. If this is the case, then it might potentially mean that the presence of CSLD5,

rather than its enzymatic activity, is essential for the CSLD5 function. Based on the accumulation pattern of CSLD5 during cytokinesis, one way to explain this is that cell plate localized CSLD5 might use its N terminus or C terminus to recruit binding partners that are essential for cell division. To test this idea, we could replace the catalytic domain of CSLD3 with that of CSLD5, and express the chimeric protein under the control of the *CSLD5* promoter. If this chimeric protein also displayed cell plate localization, but failed to rescue the *csld5* mutant phenotypes, then we would propose that the N terminus or the C terminus of CSLD5 is required for its function.

Additionally, the regulated protein turnover mechanism of CSLD5 needs further investigation. Based on the changes in Cerulean-CSLD5 stability observed in *ccs52a2* mutants, the turnover of CSLD5 proteins has been proposed to occur via an $APC^{CCS52A2}$ – 26S proteasome mediated proteolysis pathway. However, we do not know whether this regulation is direct or indirect. One possibility is that $APC^{CCS52A2}$ directly ubiquitinates CSLD5. This could be directly tested by examining whether CSLD5 is ubiquitinated in wild type and in *ccs52a2* mutants. Anti-ubiquitin antibodies could be used to determine if ubiquitinated Cerulean-CSLD5 could be immunoprecipitated. Anti-GFP or anti-CSLD5 antibodies could be used to detect the existence of Cerulean-CSLD5 in the immunoprecipitated fractions. If CSLD5 is shown to be ubiquitinated in wild type plants, but fails to be ubiquitinated in *ccs52a2* mutants, then the role for $APC^{CCS52A2}$ to directly ubiquitinate CSLD5 would be supported.

Another possibility is that $APC^{CCS52A2}$ ubiquitinates other targets, which in turn regulate the stability of the CSLD5 protein. To identify these potential CCS52A2 targets, a forward genetics approach could be utilized to screen for mutations which result in stabilized CSLD5. This screen could be facilitated by the reagents generated in the promoter swap experiments discussed in Chapter Three. Based on the results in those studies, the incomplete rescue of *csld3* root hair defects by CSLD3p::Cerulean-CSLD5 appeared to be caused by the low levels of CSLD5 protein accumulation in root hair cells. Several strategies could be used to investigate this hypothesis. First, we might attempt to increase the amount of CSLD5 protein accumulation by MG132 treatment and examine whether *csld3* root hair phenotypes are rescued to a greater extent or not. Second, we might attempt to rescue *csld3* mutant root hair defects with a chimeric CSLD2 protein, in which we have integrated corresponding CSLD5 sequences. If the chimeric protein is more stable than CSLD5, then the root hair defects are expected to be rescued to a greater extent. Third, we might also further reduce the amount of overall CSLD protein accumulation in root hairs. The rationale is that if any root hair growth restored in *csld3* mutants expressing CSLD3p::Cerulean-CSLD5 is due to the remaining *CSLD2* gene activity, then the root hair phenotypes in *csld2/csld3* double mutants, in which the total levels of CSLD proteins are further reduced, might be rescued by CSLD3p::Cerulean-CSLD5 to a poorer extent. If the inability CSLD3p::Cerulean-CSLD5 to rescue *csld3* root hair phenotypes is confirmed as a result of rapid turnover of these proteins interfering with the ability to accumulate sufficient CSLD5 proteins in these root hairs, then the

*csld3* root hair defects would be expected to be rescued to a greater extent (root hairs with similar length to the wild type root hairs, etc) when the amount of CSLD5 proteins in these cells is increased. Therefore, we could use *csld3* mutants expressing *CSLD3p::Cerulean-CSLD5* as the background for mutagenesis, Mutants that resulted in the rescue of the *csld3* root hair phenotype would be identified, and then assessed to determine if this rescue was associated with stabilized Cerulean-CSLD5 stabilization. If this is the case, then the mutated gene locus (loci) would be further identified.

The functional redundancy in the CSLD family was also examined in these studies. We found that *csld2*, *csld3*, and *csld5* mutants displayed distinct types of root hair defects. Only *CSLD2* and *CSLD3*, but not *CSLD5*, were shown to be expressed in root hair cells. We also found that the transcription of *CSLD3* or *CSLD2* was observed in the epidermal cells undergoing root hair initiation or the root hair cells during active tip growth, respectively. We also examined the sub-cellular localization of CSLD2 in growing root hairs when the expression of this protein was controlled by the *CSLD2* endogenous promoter. The similar distribution of CSLD2 and CSLD3 in these cells suggested that the different root hair defects in *csld2* and *csld3* mutants were not caused by the distinct sub-cellular localizations of CSLD2 and CSLD3. Finally, we showed that CSLD3p::Cerulean-CSLD2 quantitatively rescued root hair defects in *csld3* mutants, indicating that CSLD2 and CSLD3 proteins were functionally interchangeable.

To further confirm CSLD2 and CSLD3 proteins are functionally interchangeable, we would generate and transform *CSLD2p::Cerulean-CSLD3* into *csld2* mutants. If the root hair growth defects in *csld2* mutants are rescued by Cerulean-CSLD3, then the interchangeable functions for CSLD2 and CSLD3 would be more strongly supported. However, we cannot exclude the possibility that Cerulean-CSLD3 fails to rescue the root hair growth defects in *csld2* mutants. This might be caused by several reasons. First, the polysaccharide CSLD2 provides has a more broad impact on root hair growth than the one synthesized by CSLD3. To test this, we need to perform *in vitro* enzymatic activity analysis to determine the polysaccharides these CSLD proteins make. A second possibility is that other than its biochemical activity, CSLD2 might have additional roles for root hair growth. One direction to test this is to find potential binding partners for CSLD2 proteins by yeast two-hybrid assays.

In *csld3* mutants expressing CSLD3p::Cerulean-CSLD2, CSLD activity in root hairs appears to be provided solely by CSLD2 proteins. However, whether the CSLD2 protein functions as a monomer or in homotypic multimers remain unclear. There are several strategies to investigate this further. First, we might examine whether CSLD2 interacts with itself in yeast two-hybrid assays. Second, we could attempt to examine the CSLD2 homodimerization *in planta* by Bimolecular Fluorescence Complementation (BiFC) assays. YFP fragments, either YFP/N or YFP/C, would be linked to the N-terminal part of CSLD2 proteins and transiently expressed in *Nicotiana benthamiana* or stably

expressed in *Arabidopsis*. If these experiments give us positive results, then formation of CSLD2-CSLD2 homotypic multimers would be supported. Therefore, we could further identify the region for CSLD2-CSLD2 interaction and examine whether mutations in this region might affect the function of CSLD2.

The root hair defects of different *csld* mutants may also provide information on their specific roles during root hair growth. In *csld2* mutants, the initiation of root hairs did not appear to be affected. However, after initiation, root hairs are prone to rupture or bulge formation (Bernal et al., 2008; Yoo et al., 2012). The root hair defects are more severe in *csld3* mutants, in which cells rupture during the initiation of root hair tip growth (Wang et al., 2001; Favery et al., 2001). These results would be consistent with a model in which *CSLD3* functions predominantly in root hair initiation, and *CSLD2* functions mainly in root hair elongation. To investigate whether *CSLD2* might also have a role during root hair initiation, the root hair frequency in *csld2* mutants could be measured and compared with that in Col-0 controls. If *CSLD2* also functions during root hair initiation, then we expect to see a decrease of root hair frequency in *csld2* mutants.

## Materials and Methods

### Plant material and growth conditions

*Arabidopsis* seeds were surface-sterilized for fifteen minutes in 30% sodium hypochlorite / 0.02% Triton X-100 solution. The seeds were washed with sterilized double distilled water and stored at 4°C overnight before transferred to ¼ MS growth medium. Seedlings were germinated and grown in growth chambers. After seven to fourteen days the seedlings were transferred from plates to soil and grown in growth rooms. Unless specified, the seedlings/plants were grown at 21°C in long-day condition (sixteen hour of light).

**Cell cycle inhibition**

Five-day old seedlings were transferred to liquid ¼ MS medium containing 75 μM aphidicolin for 48 hours before the seedlings were used for RNA extraction. The plant RNA was extracted using RNeasy® Plant Mini Kit (QIAGEN).

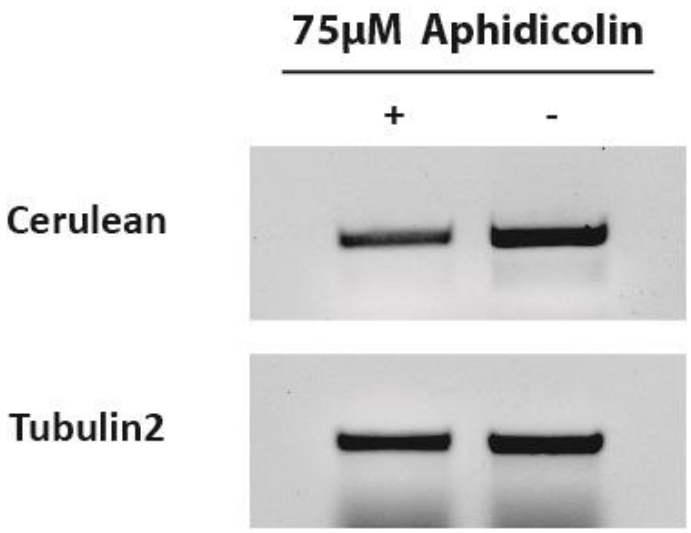


**Figure 4.1. The mRNA of *Cerulean-CSLD5* is stable**

The effect of 75µM aphidicolin on RNA level from five-day old seedlings expressing *Cerulean-CSLD5* was examined. The mRNA level of *TUBULIN2* was used as a control. The level of *Cerulean-CSLD5* mRNA was determined using reverse transcript PCR based methods. The mRNA level of *Cerulean-CSLD5* remained stable when the cell cycle was locked in early S phase for two days by addition of 75µM aphidicolin.

# APPENDIX

# IDENTIFICATION OF A NEW *FERONIA* TEMPERATURE-SENSITIVE MUTANT ALLELE THAT ALTERS ROOT HAIR GROWTH

One of my rotation projects was to use map-based cloning method to identify the locus responsible for a previously isolated temperature-sensitive root hair developmental mutant in *Arabidopsis*. During this time I was able to localize the site of the mutation to a ~2 Mb region of the lower arm of chromosome 3. I then utilized a high-throughput sequencing methodology to obtain ~25X sequencing coverage of this region of the *Arabidopsis* genome. Based on this, we were able to identify several putative mutations, of which one was located within the open-reading frame of *FERONIA (FER)*, a receptor-like kinase (RLK) which had previously been linked to root hair development (Duan et al., 2010). While this project was eventually taken over by a fellow colleague, Dr. Daewon Kim, I continued to participate in experiments associated with confirmation that the mutated *FER* locus was indeed responsible for the temperature-sensitive root hair defects, and in the experiments associated with the characterization of this novel, temperature-sensitive root hair mutant. The following appendix is based in part on the

eventual manuscript describing this study. I have clearly indicated which experiments were performed by myself, and which were performed by Dr. Daewon Kim or others.

## Introduction

In higher plants, root hairs are cellular protuberances resulting from the polarized outgrowth of specialized root epidermal cells, known as trichoblasts, and these root hairs effectively increase the surface area of the root region available for water absorption and nutrient uptake from the soil (Gilroy and Jones, 2000). Development of the root hair can be divided into three phases as follows: cell specification, initiation of the root hair bulge, and polarized tip growth (Cho and Cosgrove, 2002).

Recently, a number of *Catharanthus roseus* receptor-like kinases (CrRLK1Ls) have been identified that are involved in cellular elongation such as hypocotyl elongation, tip growth in pollen and root hairs (Hématy et al., 2007; Guo et al., 2009; Miyazaki et al., 2009; Duan et al., 2010). The CrRLK1L subfamily is named after the first member functionally characterized in *Catharanthus roseus* cell cultures (Schulze-muth et al., 1996). There are seventeen CrRLK1L subfamily members found in *Arabidopsis* (Hématy and Höfte, 2008). The majority of *Arabidopsis* CrRLK1L receptor-like kinase proteins are predicted serine/threonine kinases with a single transmembrane between an N-terminal extracellular domain and a C-terminal cytoplasmic kinase domain (Cheung and

Wu, 2011). The CrRLK1L proteins have an extracellular domain with two malectin-like domains showing limited homology to the carbohydrate-binding domain of the animal malectin protein, which binds $Glc_2$-N-glycan with a high selectivity (Schallus et al., 2008; Lindner et al., 2012).

In the CrRLK1L subfamily, THESEUS1 (THE1) was identified in a screen for suppressors that partially restored the dark-grown hypocotyl growth defects of *procuste1-1 (prc1-1),* in which cellulose synthase catalytic subunit CESA6 was mutated (Hématy et al., 2007). THE1 is localized to the plasma membrane of elongating cells and in vascular tissue. In addition, THE1 has an autophosphorylation activity and is highly phosphorylated in the kinase domain *in planta* (Hématy et al., 2007). The THE1 loss- and gain-of-function do not appear to display significant growth defects in wild-type backgrounds, but these mutants reduced and enhanced the growth and ectopic lignification in a number of plants with defects in cell wall integrity (Cheung and Wu, 2011). Another member of CrRLK1L subfamily, HERCULES1 (HERK1), was identified as functionally redundant with THE1 in regulating cell elongation (Guo et al., 2009). While mutant *herk1* plants displayed normal growth, *the1*/*herk1* double mutants were severely stunted (Guo et al., 2009). Two additional CrRLK1L subfamily members, ANXUR1 (ANX1) and ANXUR2 (ANX2), are exclusively expressed in the male gametophyte (Boisson-Dernier et al., 2009; Miyazaki et al., 2009). ANX1 and ANX2 proteins are responsible for maintaining pollen tube wall integrity during migration

through floral tissues, and their deactivation is thought to allow the pollen to burst during fertilization (Boisson-Dernier et al., 2009; Miyazaki et al., 2009). These proteins are localized to peripheral membranes in the growing pollen tube tips, and appeared to be associated with vesicles involved in polarized membrane trafficking during tip growth (Boisson-Dernier et al., 2009; Miyazaki et al., 2009).

Similar to ANX1 and ANX2, FER, which is allelic to SIRÈNE (SRN), was first identified in the regulation of female control of fertility (Huck, 2003; Rotman et al., 2003). Interestingly, *FER* is highly expressed in the synergid cells of the female gametophyte and in a variety of vegetative tissues, but not in the male gametophyte (Huck, 2003; Escobar-Restrepo et al., 2007). In the female gametophyte, the FER protein is involved in sensing pollen tube arrival and promoting its rupture, (Huck, 2003; Rotman et al., 2003). Intriguingly, FER has also been shown to play important roles in the regulation of root hair elongation (Duan et al., 2010). FER was identified as a ROP guanidine exchange factor 1 (ROPGEF1) interacting partner by yeast two-hybrid screening for root hair tip-growth in *Arabidopsis* (Duan et al., 2010). The kinase domain of FER recruits ROPGEF1, resulting in its phosphorylation and subsequent activation of ROP GTPases by GDP-GTP exchange (Duan et al., 2010). Finally, a secreted peptide, RALF (rapid alkalinization factor), was identified as ligand of the FER extracellular domain, and RALF signaling through the FER RLK was shown to regulate cell elongation of the primary root (Haruta et al., 2014).

Although several mutants of *FER* have been previously described, we identify here a novel temperature-sensitive mutation (G41S) in a highly conserved glycine residue found in the first malectin-like domain in the extracellular domain of FER. This temperature-sensitive mutant exhibited rapid and dramatically decreased root hair tip-growth upon transfer from permissive temperature (21˚C) to non-permissive growth temperature (30˚C). Cessation of root hair tip growth occurred within five minutes of transfer to non-permissive temperatures, suggesting that this mutant fails to properly transmit extracellular signals at non-permissive temperatures. Additionally, the accumulation of the fluorescently-tagged fer(G41S), the temperature-sensitive version, was increased in the internal membrane system when grown in 30˚C for 24 hours. This observation also indicated that the G41S mutation might also have a long-term effect on protein folding.

## Results

### Isolation of temperature-sensitive mutants defective in root hair tip growth

In plants, root hairs are highly polarized tubular structures that emerge from the root epidermal cell surface, and play important roles in absorption of water and inorganic nutrients, interactions with the rhizosphere, and in root anchorage in the soil substrate (Grierson et al., 2014). In order to understand molecular mechanisms that control and regulate root hair tip growth, EMS-mutagenized seeds in eYFP-RabA4b transgenic plant

were screened for seedlings that with wild-type root hairs at permissive temperatures (21˚C), but which displayed impaired root hair growth when grown at non-permissive temperatures (30˚C). The progeny of approximately 6,000 EMS-mutagenized seeds were screened. From the screening, four temperature-sensitive root hair growth defect mutants were isolated and named *ltl* (*loss of tip localization*) based on the rapid loss of polarized membrane trafficking compartments labeled by the regulatory Rab GTPase, eYFP-RabA4b. Among these *ltl* mutants, *ltl2* mutant was selected for further investigation of root hair tip growth dynamics under permissive (21˚C) and non-permissive temperatures (30˚C) conditions (Figure 5.1).

To locate the *ltl2* mutant locus, map-based cloning and full-genome sequencing was performed. F2 mapping populations were obtained by reciprocal crosses of back-crossed *ltl2* mutant plants (Col-0) with Ler wild-type plants, another *Arabidopsis* ecotype. Segregating F2 populations were used for the subsequent map-based cloning process. I found that the *ltl2* mutant lesion was initially located on chromosome 3 between the SSLP (Simple Sequence Length Polymorphism) markers *CIW4* and *35bp*, a region of approximately 261 kilo-base (Figure 5.2). To further locate the mutation site, I performed whole-genome sequencing, and determined that *ltl2* contained the G41S substitution mutation within the extracellular domain of the previously characterized FER receptor-like kinase protein (Figure 5.2). This Glycine residue is conserved in this superfamily (Figure 5.2) and a mutation in the same Glycine residue disrupts the function of

THESEUS, another member from the CrRLK1L superfamily (Hématy and Höfte, 2008). These observations indicated that the temperature dependent root hair growth defect in *ltl2* is likely to be the result of the G41S mutation in FER.

To confirm that the *ltl2* temperature sensitive phenotype was caused by the G41S mutation in the FER protein sequence, *ltl2* mutants were reciprocally crossed with wild type and two previously characterized FER mutants, *fer-4* and *fer-5* (Duan et al., 2010), by Dr. Daewon Kim. The F1 generation of *ltl2* crossed to wild-type plants displayed normal root hair growth in both permissive and non-permissive temperature conditions (manuscript in revision). However, The F1 generation of *ltl2* crossed with *fer-4* or *fer-5* mutant progenies displayed root hair growth defects at non-permissive temperatures (manuscript in revision). In addition, a mutant version of FER containing the G41S mutation, fer(G41S), driven by endogenous *FER* promoter sequences was introduced in *fer-4* mutant background. As expected, I found that the transformants exhibited the temperature sensitive phenotype of *ltl2* mutants. Although these plants displayed normal root hair growth at 20° C, no root hairs were formed when the temperature was switched to 30°C (Figure 5.3). Based on the results generated by Dr. Daewon Kim and myself, we confirmed that the G41S mutation in FER is the cause of *ltl2* mutant temperature sensitive phenotypes.

**The G41S mutation impaired ligand binding activity and folding of FER**

To explain the root hair growth defects of *ltl2* mutants at non-permissive temperature, we proposed two hypotheses. The fer(G41S) proteins might either lose the ability to properly bind ligand, or to appropriately transduce this information to downstream elements of the signaling pathway. Alternatively, the mutation might cause a folding defect which might result in either retention of newly synthesized fer(G41S) in the ER, or lead to rapid protein turnover, therefore reducing the amount of FER protein on the plasma membrane. To test the first possibility, we utilized a recent discovery that RALF, a short peptide hormone, is bound by FER (Haruta et al., 2014). This peptide, which was shown to suppress cell elongation of the *Arabidopsis* primary root, is thought to be bind directly with the FER extracellular domain (Haruta et al., 2014). To examine whether RALF suppression of primary root elongation might be affected in *ltl2* mutants, Dr. Daewon Kim examined the sensitivity of RALF in wild type and *ltl2* mutants. He found that the sensitivity of *ltl2* mutant seedlings to RALF peptide treatment was dramatically reduced in non-permissive temperature (manuscript in revision). These results would be consistent with a model in which the G41S mutation results in temperature sensitive inactivation of the extracellular ligand-binding domain of the FER protein. The result might explain the rapid root hair growth cessation within five minutes of transferal to non-permissive temperatures observed by Dr. Daewon Kim (manuscript in revision).

To test the second possibility, we fused eYFP to the carboxyl-terminus of FER(WT) and fer(G41S) and examined whether the sub-cellular localization of fer(G41S) might be

changed when grown in non-permissive temperatures. I found that both FER(WT)-eYFP and fer(G41S)-eYFP were predominantly localized on plasma membranes of different tissues including root cortical cells and root hair cells (Figure 5.4). The plasma membrane localization of FER(WT)-eYFP was not changed when the plants were grown in 30°C for 24 hours. However, a significant re-localization was observed for fer(G41S)-eYFP proteins and they displayed a strong internal membrane localization. These results support a model that due to the G41S mutation, the newly synthesized fer(G41S) might not fold properly in non-permissive temperature and the mis-folded fer(G41S) proteins are retained in ER. Based on these results generated by Dr. Daewon Kim and myself, we propose that the G41S mutation causes both short term and long term effects on FER proteins, resulting in the temperature sensitive root hair growth defects in *ltl2* mutants.

## Discussion

In eukaryotes, receptor like kinases (RLKs) have been implicated to play important roles in many crucial eukaryotic cellular processes, such as cell cycle progression, cell signaling, embryogenesis, abiotic and biotic stress responses (Shiu and Bleecker, 2001). In this study, we isolated and identified the genetic locus of a novel temperature-sensitive root hair elongation mutant, which we have called *ltl2* (loss of tip localization 2). The *ltl2* mutant displays normal overall growth characteristics at permissive temperature (21˚C), but root hair initiation and elongation are specifically and rapidly inhibited within

approximately five minutes upon transfer of these plants to non-permissive temperature (30˚C). We have shown that *ltl2* mutant contain a substitution mutation in which a highly conserved glycine residue in FER extracellular domain is changed to serine (G41S). FER is a member of the CrRLK1L subfamily of receptor-like kinases (RLKs) in *Arabidopsis* and the mutated glycine residue (G41S) is highly conserved in multiple members of the CrRLK1L family of receptor proteins.

Based on sequence comparison, the extracellular domains of members of the CrRLK1L subfamily of plant RLK proteins are predicted to be structurally similar to the mammalian malectin protein (Schallus et al., 2008). Malectin was first identified and characterized in *X. laevis* as a carbohydrate binding protein of the endoplasmic reticulum where it plays an important role in the early steps of protein N-glycosylation for biogenesis of glycoproteins (Schallus et al., 2008). Based on NMR structure analysis, there are five key residues in the malectin domain (Y67, Y89, Y116, F117, D186) that are located in pocket-shape structure and these aromatic residues and the aspartate mediate interactions with the glucose residues of maltose and nigerose disaccharide ligands (Schallus et al., 2008). In plants, malectin-like domains are mainly found in CrRLK1L subfamily with a low overall sequence homology with animal malectins (Lindner et al., 2012). In FER, two malectin-like domains, ML1 and ML2, are found as tandem-repeat in the extracellular domain. Interestingly, several key residues found in the ligand-binding pocket of the animal malectin structure are conserved in the malectin-like

domains of FER and other plant CrRLK1L family members (Schallus et al., 2008). Analysis of the animal and plant malectin domains reveals an additional invariant glycine residue, that is present in all animal and plant malectin sequences, and this invariant glycine is replaced with a serine (G41S) in the temperature-sensitive version of FER that we have determined is responsible for the *ltl2* mutation described in this thesis. The highly conserved nature of this glycine, and its close proximity to the potential ligand-binding cleft of the malectin domain suggests a critical role for this residue in ligand binding and/or transduction of the ligand-binding signal in members of the CrRLK1L family of receptor-like kinases. Indeed, mutation of a similar glycine residue to aspartic acid (G37D) in the extracellular domain of THESEUS in the *the1* mutant also results in a loss of function mutation in this RLK (Hématy et al., 2007). The presence of malectin-like domains in FER and the fact that key residues are conserved in the putative ligand binding sites of these proteins might provide some hint as to potential ligands for these proteins. Given the conserved nature of these structural elements it might be expected that domains would have carbohydrate binding activity. However, FER function was recently shown to be important for the perception and downstream signaling of the secreted peptide hormone, RALF (rapid alkalinization factor), which inhibits cell expansion of the primary root in *Arabidopsis*. In addition, it has been suggested that physical interaction between RALF and FER by specific binding assays both *in vitro* and *in vivo* is responsible for the signaling events associated with inhibition of root elongation (Haruta et al., 2014). Therefore, it appears, that at least in the case of FER, that the small,

extracellular peptide, RALF, is a physiologically relevant ligand. Accordingly, the responses of *ltl2* mutant to treatment with active, synthetic RALF peptide were dramatically reduced under non-permissive temperature conditions. These results support the identification of FER, either as the direct receptor for the RALF peptide, or as an essential component of the receptor protein complex. Because the G41S mutation of the *ltl2* mutant is predicted to reside in close proximity to a putative ligand-binding cleft in the FER protein, this could support the explanation that the temperature-sensitive phenotype is due to either inability of this extracellular domain to interact with the RALF peptide, or alternatively effectively transduce this ligand binding, at non-permissive temperatures. How precisely the RALF peptide interacts with FER extracellular domains, and whether RALF is the only ligand that interacts with FER remain interesting questions in the functioning and signal transduction functions of this receptor protein family.

According to the previous reports, FER has also been implicated to play an important role in root hair tip growth as well as various crucial plant processes, such as pollen tube reception, hypocotyl elongation, regulation of ABA signaling and controlling seed size (Escobar-Restrepo et al., 2007; Deslauriers and Larsen, 2010; Duan et al., 2010; Yu et al., 2012, 2014). However, many questions remain unanswered why and how FER could regulate these diverse cellular functions in plants?

In recent years, it has become apparent that ROS plays an important signaling role in plants controlling processes such as growth, development, response to biotic and abiotic

environmental stimuli and programmed cell death (Bailey-Serres and Mittler, 2006). Many genes involved in the response to ROS are elevated in the *the1* mutant and these are thought to participate in the ectopic lignin production observed in this mutant. ROS production is thought to be regulated downstream of THE1 signaling pathway (Hématy et al., 2007; Hématy and Höfte, 2008). Furthermore, *fer* loss of function mutants exhibit decreased levels of ROS, and the elevated ROS levels in cells overexpressing FER, indicating that at least one important downstream effect of FER signal transduction is regulation of ROS production. This was recently elegantly explained by the discovery that FER recruits ROPGEFs, which in turn activate ROP GTPases, leading to the stimulation of RHD2 NADPH oxidase dependent ROS production (Duan et al., 2010). Therefore, FER mediated regulation of ROS production is likely important and tightly controlled for many cellular functions.

ROPGEF1 was initially identified as a FER interacting partner by yeast two-hybrid screening for root hair tip growth in *Arabidopsis* (Duan et al., 2010). More recently, ROPGEF4 and ROPGEF10 have also been shown to be FERIONIA interacting proteins important specifically during root hair development. Loss and gain of function analyses demonstrated distinct roles of ROPGEF4 and ROPGEF10 such that ROPGEF4 is important for root hair tip growth, while ROPGEF10 is mainly involved in root hair initiation (Yu et al., 2012; Huang et al., 2013). Furthermore, RLK family proteins may interact with other receptor like kinase or signaling proteins for fully activation in plasma

membrane (Li et al., 2002). From this, it is presumed that FER receptor proteins may have either multiple ligands or distinct downstream interacting partners that might explain its diverse roles in various cellular functions.

## Materials and Methods

### Plant material and growth conditions

*Arabidopsis* seeds were surface-sterilized for fifteen minutes in 30% sodium hypochlorite / 0.02% Triton X-100 solution. The seeds were washed with sterilized double distilled water and stored at 4°C overnight before being transferred to ¼ MS growth medium. Seedlings were germinated and grown in growth chambers. After seven to fourteen days the seedlings were transferred from plates to soil and grown in growth rooms. The seedlings/plants were grown at 21°C (permissive temperature) or 30°C (non-permissive temperature) in long-day condition (sixteen hours of light/eight hours of dark).

### Root hair and root phenotypes analysis

The root hair morphology was examined using five-day old seedlings. To measure the root hair length, the regions with mature root hairs were recorded using 4X lens (Fluorescent, NA=0.13) from a Nikon Eclipse 6600 microscope. The length of each non-

bending mature root hairs in these images was measured using ImageJ (NIH). To record the root hair growth defects, the images of root hairs of interest were collected using 10X lens (Apochromatic, NA=0.45). Seven-day old seedlings were used for root length comparison. The seedlings were grown vertically to allow the fully elongation of the roots. The plates were scanned and the length of the roots was measured using ImageJ (NIH).

**DNA extraction from plant tissues**

DNA was extracted from leaves of three-four week old plants. For regular genotyping purpose, the tissue was placed in a 1.5ml centrifuge tube containing DNA extraction buffer (200mM Tris-HCl pH 7.5, 250 mM NaCl, 20mM EDTA, 0.5% SDS) before it is thoroughly grinded with a pestle. After two minutes of sedimentation at the highest speed in an Eppendorf centrifuge, the supernatant was removed to a new tube and an equal volume of isopropanol was added into the tube to precipitate the DNA. The mixture was spun at the highest speed for 10 minutes and the precipitation was resuspended in water.

For whole genome sequencing, the genomic DNA was extracted using QIAGEN's DNeasy® Plant Mini Kit. The DNA (10µg in total) was concentrated to 50ng/µl before being sent for whole genome sequencing. The DNA was sheared and the library was

constructed in the University of Michigan DNA Sequencing Core (http://seqcore.brcf.med.umich.edu/). The high-throughput sequencing was conducted using Illumina Genome Analyzer IIx service. The reads were aligned to the genome of *Arabidopsis* (TAIR10) by BOWTIE aligner (University of Maryland) and an average coverage of 25X was achieved.

**Map-based Cloning of the *LTL2* gene**

To locate the mutation site, the original *ltl2* mutants (in Col-0 ecotype) were crossed with plants from Ler ecotype. The F1 plants were self-fertilized to generate the F2 plants. The F2 plants showing *ltl2* mutant phenotypes were selected and their genomic DNA was extracted. Several SSLP (Simple Sequence Length Polymorphism) markers were used to examine the recombination rate in order to calculate the distance from the mutation site to different markers.

**Confocal microscopy**

The fluorescent imaging was performed with an Olympus spinning disk confocal using a 60x oil lens (Apochromatic, NA=1.42). Metamorph Advanced software (Molecular Devices, Inc) was used for image capture. For multi-channel imaging, the channels were switched sequentially from long wavelength to short wavelength. The

signal from FM4-64 was excited at 561nm and collected at 607nm. The signal from eYFP was excited at 515nm and collected at 562nm.

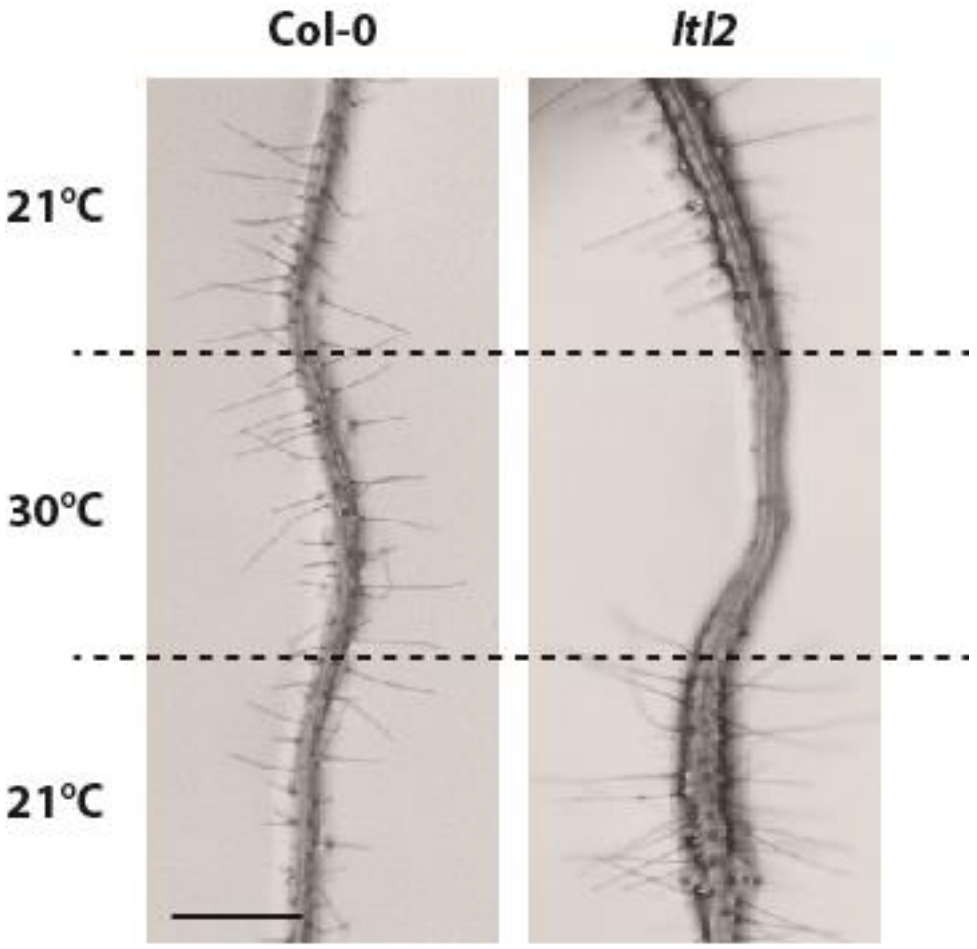


**Figure 5.1. Phenotype of five-day-old *ltl2* mutants**

The roots from five-day old wild type Col-0 and *ltl2* mutants were compared. Root hair growth was completely abolished when *ltl2* mutants were grown in non-permissive temperature (30°C). Root hair growth was restored after the *ltl2* mutants being transferred back to permissive temperature (21°C). Scale bar represents 1mm.

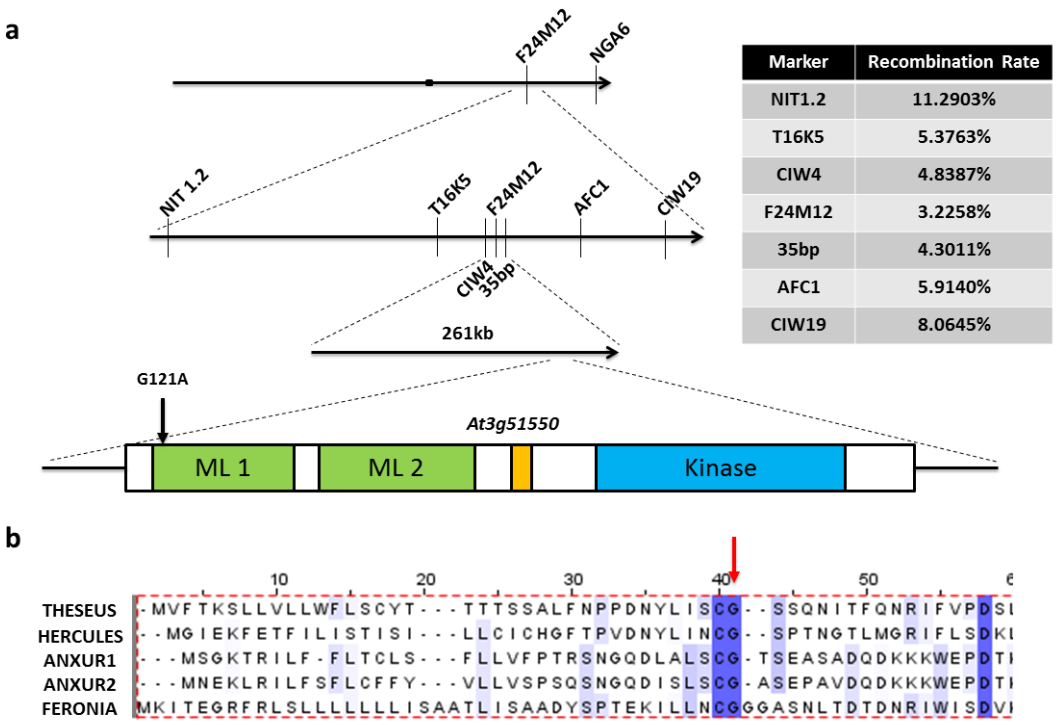


| Marker | Recombination Rate |
|---|---|
| NIT1.2 | 11.2903% |
| T16K5 | 5.3763% |
| CIW4 | 4.8387% |
| F24M12 | 3.2258% |
| 35bp | 4.3011% |
| AFC1 | 5.9140% |
| CIW19 | 8.0645% |

**Figure 5.2. G121A mutation in *At3g51550* causes a change of a conserved amino acid in the superfamily**

(**a**) The mutation locus was identified in a region of 261kb on the third chromosome using map-based cloning methods. A Guanine to Adenine mutation in the 121$^{th}$ nucleotide of At3g51550, a receptor like kinase FERONIA, was identified through a high-throughput whole genome sequencing method. The G121A mutation caused a Glycine to Serine amino acid change in the first malectin like (ML) domain of FERONIA protein. (**b**) The Glycine residue mutated (red arrow) was conserved in the members from CrRLK1L superfamily. The protein sequences were aligned using Clustal Omega (http://www.ebi.ac.uk/Tools/msa/clustalo/).

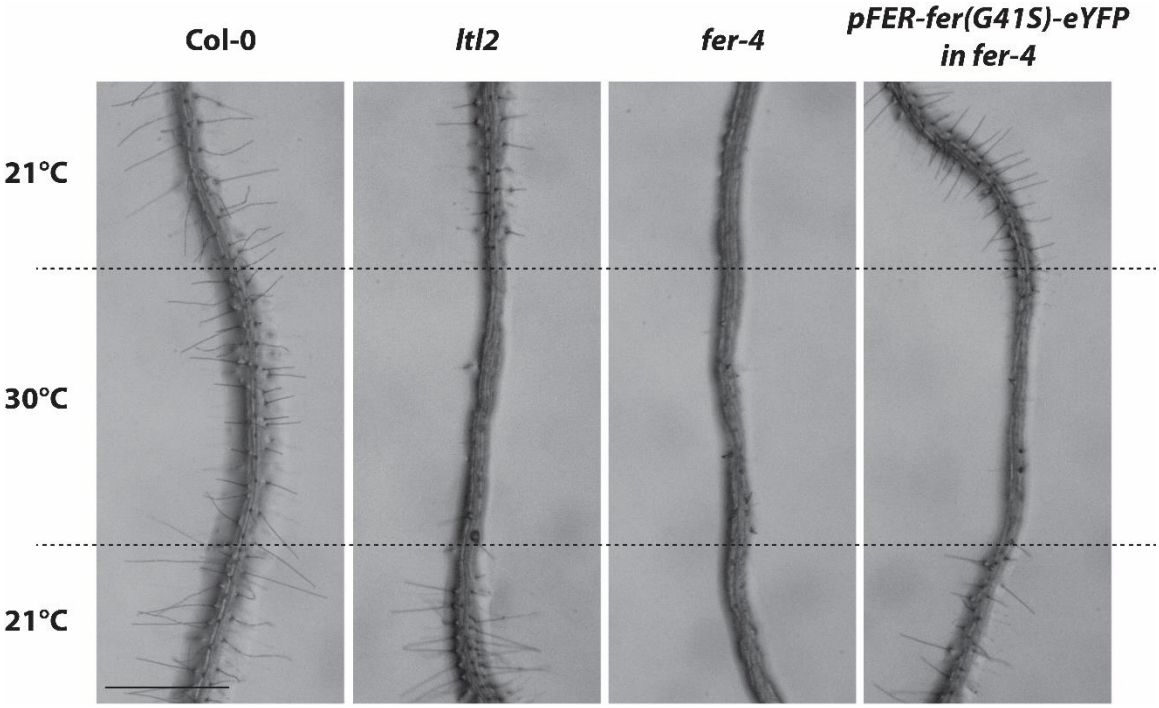


**Figure 5.3. fer(G41S)-eYFP restores the *ltl2* phenotype in *fer-4* mutant background**

The roots from five-day old wild type Col-0, *ltl2* mutants, *fer-4* mutants, and *fer-4* mutants expressing fer(G41S)-eYFP was examined. In permissive temperature (21°C), root hair growth was completely abolished in *fer-4* mutants when grown, while *fer-4* mutants expressing fer(G41S)-eYFP displayed normal root hair growth. In non-permissive temperature (30°C), *fer-4* mutants expressing fer(G41S)-eYFP displayed root hair growth defects as observed for *ltl2* mutants. Like the *ltl2* mutants, root hair growth in *fer-4* mutants expressing fer(G41S)-eYFP was restored after the seedlings being transferred back to permissive temperature (21°C). Scale bar represents 1mm.

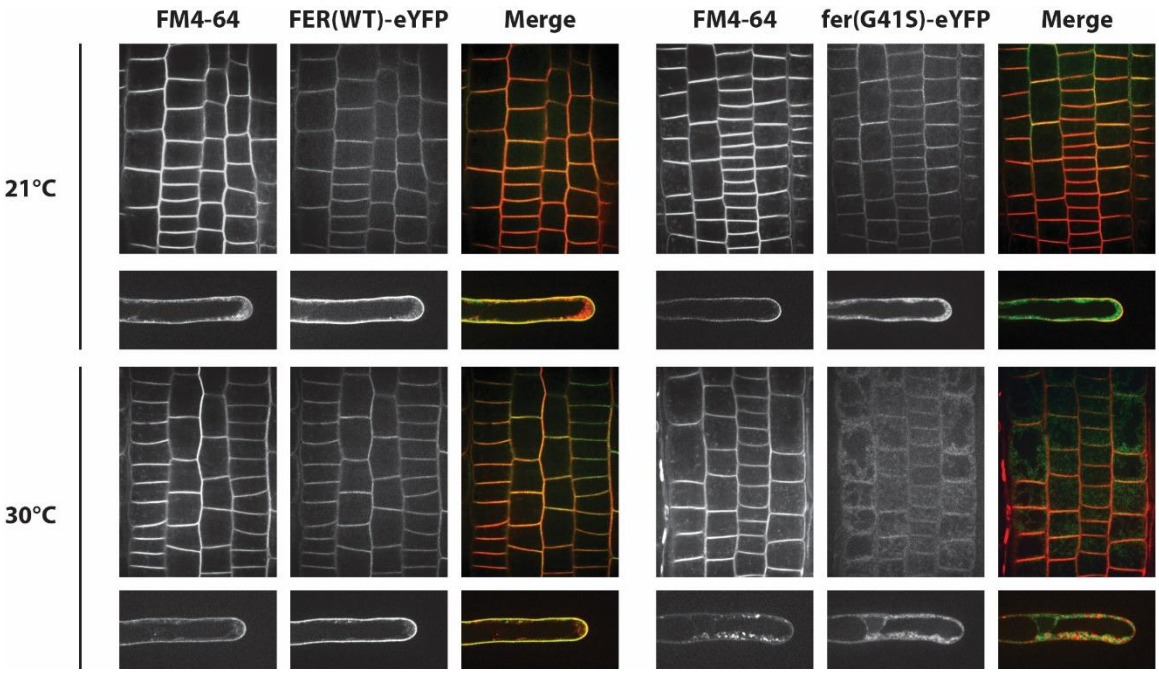


**Figure 5.4. fer(G41S)-eYFP shows internal membrane localization in 30°C**

The fluorescence of FER fusion proteins in root tissues and in growing root hairs from five-day old seedlings was examined by confocal microscopy. The fluorescence of FER(WT)-eYFP was detected on plasma membranes in root tissues and growing root hairs. The distribution of the FER(WT)-eYFP fluorescence was unchanged after the seedlings being transferred to non-permissive temperature (30°C). fer(G41S)-eYFP displayed a similar plasma membrane localization in root tissues and growing root hairs as observed for FER(WT)-eYFP in permissive temperature (21°C). However, in non-permissive temperature (30°C), a significant level of the fluorescence of fer(G41S)-eYFP re-localized to the internal membrane system.

# REFERENCES

**Arioli, T., Peng, L., Betzner, A., Burn, J., Wittke, W., Herth, W., Camilleri, C., Hofte, H., Plazinski, J., Rosemary, B., Ann, C., Glover, J., Redmond, J., and Williamson, R.E.** (1998). Molecular Analysis of Cellulose Biosynthesis in Arabidopsis. Science **279**: 717–720.

**Atmodjo, M.A., Hao, Z., and Mohnen, D.** (2013). Evolving Views of Pectin Biosynthesis. Annual Review of Plant Biology **64**: 747–779.

**Atmodjo, M.A., Sakuragi, Y., Zhu, X., Burrell, A.J., Mohanty, S.S., Atwood, J.A., Orlando, R., Scheller, H. V., and Mohnen, D.** (2011). Galacturonosyltransferase (GAUT)1 and GAUT7 are the core of a plant cell wall pectin biosynthetic homogalacturonan:galacturonosyltransferase complex. Proceedings of the National Academy of Sciences of the United States of America **108**: 20225–20230.

**Bailey-Serres, J. and Mittler, R.** (2006). The Roles of Reactive Oxygen Species in Plant Cells. Plant Physiology **141**: 311.

**Basu, D., Liang, Y., Liu, X., Himmeldirk, K., Faik, A., Kieliszewski, M., Held, M., and Showalter, A.M.** (2013). Functional identification of a hydroxyproline-o-galactosyltransferase specific for arabinogalactan protein biosynthesis in Arabidopsis. The Journal of Biological Chemistry **288**: 10132–43.

**Beeckman, T., Przemeck, G.K.H., Stamatiou, G., Lau, R., Terryn, N., Rycke, R. De, Inze, D., and Berleth, T.** (2002). Genetic Complexity of Cellulose Synthase A Gene Function in Arabidopsis Embryogenesis. Plant Physiology **130**: 1883–1893.

**Bernal, A.J., Jensen, J.K., Harholt, J., Sørensen, S., Moller, I., Blaukopf, C., Johansen, B., De Lotto, R., Pauly, M., Scheller, H.V., and Willats, W.G.T.** (2007). Disruption of ATCSLD5 results in reduced growth, reduced xylan and homogalacturonan synthase activity and altered xylan occurrence in Arabidopsis. The Plant Journal **52**: 791–802.

**Bernal, A.J., Yoo, C.-M., Mutwil, M., Jensen, J.K., Hou, G., Blaukopf, C., Sørensen, I., Blancaflor, E.B., Scheller, H.V., and Willats, W.G.T.** (2008). Functional analysis of the cellulose synthase-like genes CSLD1, CSLD2, and CSLD4 in tip-growing Arabidopsis cells. Plant Physiology **148**: 1238–53.

**Bernhardt, C. and Tierney, M.L.** (2000). Expression of AtPRP3, a proline-rich structural cell wall protein from Arabidopsis, is regulated by cell-type-specific developmental pathways involved in root hair formation. Plant Physiology **122**: 705–714.

**Biswal, A.K., Hao, Z., Pattathil, S., Yang, X., Winkeler, K., Collins, C., Mohanty, S.S., Richardson, E. a, Gelineo-Albersheim, I., Hunt, K., Ryno, D., Sykes, R.W., Turner, G.B., Ziebell, A., Gjersing, E., Lukowitz, W., Davis, M.F., Decker, S.R., Hahn, M.G., and Mohnen, D.** (2015). Downregulation of GAUT12 in Populus deltoides by RNA silencing results in reduced recalcitrance, increased growth and reduced xylan and pectin in a woody biofuel feedstock. Biotechnology for Biofuels **8**: 1–25.

**Boisson-Dernier, A., Kessler, S. a, and Grossniklaus, U.** (2011). The walls have ears: the role of plant CrRLK1Ls in sensing and transducing extracellular signals. Journal of experimental botany **62**: 1581–91.

**Boisson-Dernier, A., Roy, S., Kritsas, K., Grobei, M.A., Jaciubek, M., Schroeder, J.I., and Grossniklaus, U.** (2009). Disruption of the pollen-expressed FERONIA homologs ANXUR1 and ANXUR2 triggers pollen tube discharge. Development **136**: 3279–3288.

**Boron, A.K., Van Loock, B., Suslov, D., Markakis, M.N., Verbelen, J.-P., and Vissenberg, K.** (2015). Over-expression of AtEXLA2 alters etiolated arabidopsis hypocotyl growth. Annals of Botany **115**: 67–80.

**Boron, A.K., Van Orden, J., Markakis, M.N., Mouille, G., Adriaensen, D., Verbelen, J.-P., Hofte, H., and Vissenberg, K.** (2014). Proline-rich protein-like PRPL1 controls elongation of root hairs in Arabidopsis thaliana. Journal of Experimental Botany **65**: 5485–5495.

**Bouché, N. and Bouchez, D.** (2001). Arabidopsis gene knockout : phenotypes wanted. Current Opinion in Plant Biology **4**: 111–117.

**Bouton, S., Leboeuf, E., Mouille, G., Leydecker, M.-T., Talbotec, J., Granier, F., Lahaye, M., Höfte, H., and Truong, H.-N.** (2002). QUASIMODO1 encodes a

putative membrane-bound glycosyltransferase required for normal pectin synthesis and cell adhesion in Arabidopsis. The Plant Cell **14**: 2577–2590.

**Brady, S.M., Orlando, D.A., Lee, J.-Y., Wang, J.Y., Koch, J., Dinneny, J.R., Mace, D., Ohler, U., and Benfey, P.N.** (2007). A high-resolution root spatiotemporal map reveals dominant expression patterns. Science **318**: 801–6.

**Brady, S.M., Zhang, L., Megraw, M., Martinez, N.J., Jiang, E., Yi, C.S., Liu, W., Zeng, A., Taylor-Teeples, M., Kim, D., Ahnert, S., Ohler, U., Ware, D., Walhout, A.J.M., and Benfey, P.N.** (2011). A stele-enriched gene regulatory network in the Arabidopsis root. Molecular Systems Biology **7**: 459.

**Cannon, M.C., Terneus, K., Hall, Q., Tan, L., Wang, Y., Wegenhart, B.L., Chen, L., Lamport, D.T. a, Chen, Y., and Kieliszewski, M.J.** (2008). Self-assembly of the plant cell wall requires an extensin scaffold. Proceedings of the National Academy of Sciences of the United States of America **105**: 2226–2231.

**Cavalier, D.M. and Keegstra, K.** (2006). Two xyloglucan xylosyltransferases catalyze the addition of multiple xylosyl residues to cellohexaose. The Journal of Biological Chemistry **281**: 34197–34207.

**Cavalier, D.M., Lerouxel, O., Neumetzler, L., Yamauchi, K., Reinecke, A., Freshour, G., Zabotina, O.A., Hahn, M.G., Burgert, I., Pauly, M., Raikhel, N. V, and Keegstra, K.** (2008). Disrupting two Arabidopsis thaliana xylosyltransferase genes results in plants deficient in xyloglucan, a major primary cell wall component. The Plant Cell **20**: 1519–37.

**Chen, X.-Y. and Kim, J.-Y.** (2009). Callose synthesis in higher plants. Plant Signaling & Behavior **4**: 489–492.

**Chen, X.-Y., Liu, L., Lee, E., Han, X., Rim, Y., Chu, H., Kim, S.-W., Sack, F., and Kim, J.-Y.** (2009). The Arabidopsis callose synthase gene GSL8 is required for cytokinesis and cell patterning. Plant Physiology **150**: 105–113.

**Cheung, A.Y. and Wu, H.-M.** (2011). THESEUS 1, FERONIA and relatives: a family of cell wall-sensing receptor kinases? Current Opinion in Plant Biology **14**: 632–41.

**Cho, H.T. and Cosgrove, D.J.** (2000). Altered expression of expansin modulates leaf growth and pedicel abscission in Arabidopsis thaliana. Proceedings of the National Academy of Sciences of the United States of America **97**: 9783–8.

**Cho, H.-T. and Cosgrove, D.J.** (2002). Regulation of root hair initiation and expansin gene expression in Arabidopsis. The Plant Cell **14**: 3237–3253.

**Choi, D., Lee, Y., Cho, H., and Kende, H.** (2003). Regulation of Expansin Gene Expression Affects Growth and Development in Transgenic Rice Plants. The Plant Cell **15**: 1386–1398.

**Chou, Y.-H., Pogorelko, G., Young, Z.T., and Zabotina, O.A.** (2014). Protein-Protein Interactions Among Xyloglucan-Synthesizing Enzymes and Formation of Golgi-Localized Multiprotein Complexes. Plant and Cell Physiology **56**: 255–267.

**Chou, Y.-H., Pogorelko, G., and Zabotina, O. a** (2012). Xyloglucan xylosyltransferases XXT1, XXT2, and XXT5 and the glucan synthase CSLC4 form golgi-localized multiprotein complexes. Plant physiology **159**: 1355–66.

**Chow, C.-M., Neto, H., Foucart, C., and Moore, I.** (2008). Rab-A2 and Rab-A3 GTPases define a trans-golgi endosomal membrane domain in Arabidopsis that contributes substantially to the cell plate. The Plant Cell **20**: 101–123.

**Cocuron, J.-C., Lerouxel, O., Drakakaki, G., Alonso, A.P., Liepman, A.H., Keegstra, K., Raikhel, N., and Wilkerson, C.G.** (2007). A gene from the cellulose synthase-like C family encodes a beta-1,4 glucan synthase. Proceedings of the National Academy of Sciences of the United States of America **104**: 8550–5.

**Colon-Carmona, A., You, R., Haimovitch-Gal, T., and Doerner, P.** (1999). Spatio-temporal analysis of mitotic activity with a labile cyclin-GUS fusion protein. The Plant Journal **20**: 503–508.

**Cosgrove, D.J.** (2005). Growth of the plant cell wall. Nature Reviews. Molecular Cell Biology **6**: 850–61.

**Cosgrove, D.J., Li, L.C., Cho, H.-T., Hoffmann-Benning, S., Moore, R.C., and Blecker, D.** (2002). The growing world of expansins. Plant & Cell Physiology **43**: 1436–44.

**Deslauriers, S.D. and Larsen, P.B.** (2010). FERONIA is a key modulator of brassinosteroid and ethylene responsiveness in Arabidopsis hypocotyls. Molecular Pant **3**: 626–40.

**Desprez, T., Juraniec, M., Crowell, E.F., Jouy, H., Pochylova, Z., Parcy, F., Höfte, H., Gonneau, M., and Vernhettes, S.** (2007). Organization of cellulose synthase complexes involved in primary cell wall synthesis in Arabidopsis thaliana.

Proceedings of the National Academy of Sciences of the United States of America **104**: 15572–7.

**Dong, J., MacAlister, C.A., and Bergmann, D.C.** (2009). BASL Controls Asymmetric Cell Division in Arabidopsis. Cell **137**: 1320–1330.

**Duan, Q., Kita, D., Li, C., Cheung, A.Y., and Wu, H.-M.** (2010). FERONIA receptor-like kinase regulates RHO GTPase signaling of root hair development. Proceedings of the National Academy of Sciences of the United States of America **107**: 17821–6.

**Egelund, J., Petersen, B.L., Motawia, M.S., Damager, I., Faik, A., Olsen, C.E., Ishii, T., Clausen, H., Ulvskov, P., and Geshi, N.** (2006). Arabidopsis thaliana RGXT1 and RGXT2 encode Golgi-localized (1,3)-alpha-D-xylosyltransferases involved in the synthesis of pectic rhamnogalacturonan-II. The Plant Cell **18**: 2593–607.

**Emons, A.M.C.** (1985). Plasma-membrane rosettes in root hairs of Equisetum hyemale. Planta **163**: 350–359.

**Emons, A.M.C.** (1994). Winding threads around plant cells: a geometrical model for microfibril deposition. Plant, Cell & Environment **17**: 3–14.

**Emons, A.M.C. and Mulder, B.M.** (2000). How the deposition of cellulose microfibrils builds. Trends in Plant Science **5**: 35–40.

**Emons, A.M.C. and Wolters-Arts, A.M..** (1983). Cortical microtubules and microfibril deposition in the cell wall of root hairs ofEquisetum hyemale. Protoplasma **117**: 68–81.

**Endler, A. and Persson, S.** (2011). Cellulose synthases and synthesis in Arabidopsis. Molecular Plant **4**: 199–211.

**Escobar-Restrepo, J.-M., Huck, N., Kessler, S., Gagliardini, V., Gheyselinck, J., Yang, W.-C., and Grossniklaus, U.** (2007). The FERONIA receptor-like kinase mediates male-female interactions during pollen tube reception. Science **317**: 656–60.

**Fagard, M., Desnos, T., Desprez, T., Goubet, F., Refregier, G., Mouille, G., McCann, M., Rayon, C., Vernhettes, S., and Höfte, H.** (2000). PROCUSTE1 encodes a cellulose synthase required for normal cell elongation specifically in roots and dark-grown hypocotyls of Arabidopsis. The Plant Cell **12**: 2409–2424.

**Faik, A., Price, N.J., Raikhel, N. V, and Keegstra, K.** (2002). An Arabidopsis gene encoding an alpha-xylosyltransferase involved in xyloglucan biosynthesis. Proceedings of the National Academy of Sciences of the United States of America **99**: 7797–7802.

**Favery, B., Ryan, E., Foreman, J., Linstead, P., Boudonck, K., Steer, M., Shaw, P., and Dolan, L.** (2001). KOJAK encodes a cellulose synthase-like protein required for root hair cell morphogenesis in Arabidopsis. Genes & Development **15**: 79–89.

**Fowler, T.J., Bernhardt, C., and Tierney, M.L.** (1999). Characterization and expression of four proline-rich cell wall protein genes in Arabidopsis encoding two distinct subsets of multiple domain proteins. Plant Physiology **121**: 1081–1092.

**Fülöp, K., Tarayre, S., Kelemen, Z., Horváth, G., Kevei, Z., Nikovics, K., Bakó, L., Brown, S., Kondorosi, A., and Kondorosi, E.** (2005). Arabidopsis Anaphase-Promoting Complexes: Multiple Activators and Wide Range of Substrates Might Keep APC Perpetually Busy. Cell Cycle **4**: 4084–4092.

**Funakawa, H. and Miwa, K.** (2015). Synthesis of borate cross-linked rhamnogalacturonan II. Frontiers in Plant Science **6**: 1–8.

**Galway, M.E., Eng, R.C., Schiefelbein, J.W., and Wasteneys, G.O.** (2011). Root hair-specific disruption of cellulose and xyloglucan in AtCSLD3 mutants, and factors affecting the post-rupture resumption of mutant root hair growth. Planta **233**: 985–99.

**Galway, M.E., Heckman, J.W., and Schiefelbein, J.W.** (1997). Growth and ultrastructure of Arabidopsis root hairs: the rhd3 mutation alters vacuole enlargement and tip growth. Planta **201**: 209–18.

**Gaspar, Y., Johnson, K.L., McKenna, J.A., Bacic, A., and Schultz, C.J.** (2001). The complex structures of arabinogalactan-proteins and the journey towards understanding function. Plant Molecular Biology **47**: 161 – 176.

**Gilroy, S. and Jones, D.L.** (2000). Through form to function : root hair development and nutrient uptake. Trends in Plant Science **5**: 56–60.

**Goodman, C.** (2014). Cell walls: Cellulose snakes along. Nature Chemical Biology **10**: 984–984.

**Grierson, C., Nielsen, E., Ketelaarc, T., and Schiefelbein, J.** (2014). Root hairs. The Arabidopsis book / American Society of Plant Biologists **12**: e0172.

**Gu, F. and Nielsen, E.** (2013). Targeting and regulation of cell wall synthesis during tip growth in plants. Journal of Integrative Plant Biology **55**: 835–46.

**Gu, Y., Kaplinsky, N., Bringmann, M., Cobb, A., Carroll, A., Sampathkumar, A., Baskin, T.I., Persson, S., and Somerville, C.R.** (2010). Identification of a cellulose synthase-associated protein required for cellulose biosynthesis. Proceedings of the National Academy of Sciences of the United States of America **107**: 12866–71.

**Guertin, D.A., Trautmann, S., and McCollum, D.** (2002). Cytokinesis in Eukaryotes. Microbiology and Molecular Biology Reviews **66**: 155–178.

**Guo, H., Li, L., Ye, H., Yu, X., Algreen, A., and Yin, Y.** (2009). Three related receptor-like kinases are required for optimal cell elongation in Arabidopsis thaliana. Proceedings of the National Academy of Sciences of the United States of America **106**: 7648–53.

**Haga, N., Kobayashi, K., Suzuki, T., Maeo, K., Kubo, M., Ohtani, M., Mitsuda, N., Demura, T., Nakamura, K., Jurgens, G., and Ito, M.** (2011). Mutations in MYB3R1 and MYB3R4 Cause Pleiotropic Developmental Defects and Preferential Down-Regulation of Multiple G2/M-Specific Genes in Arabidopsis. Plant Physiology **157**: 706–717.

**Hall, Q. and Cannon, M.C.** (2002). The cell wall hydroxyproline-rich glycoprotein RSH is essential for normal embryo development in Arabidopsis. The Plant Cell **14**: 1161–1172.

**Harholt, J., Jensen, J.K., Sørensen, S.O., Orfila, C., Pauly, M., and Scheller, H.V.** (2006). ARABINAN DEFICIENT 1 is a putative arabinosyltransferase involved in biosynthesis of pectic arabinan in Arabidopsis. Plant Physiology **140**: 49–58.

**Harholt, J., Jensen, J.K., Verhertbruggen, Y., Søgaard, C., Bernard, S., Nafisi, M., Poulsen, C.P., Geshi, N., Sakuragi, Y., Driouich, A., Knox, J.P., and Scheller, H.V.** (2012). ARAD proteins associated with pectic Arabinan biosynthesis form complexes when transiently overexpressed in planta. Planta **236**: 115–128.

**Haruta, M., Sabat, G., Stecker, K., Minkoff, B.B., and Sussman, M.R.** (2014). A Peptide Hormone and Its Receptor Protein Kinase Regulate Plant Cell Expansion. Science **343**: 408–411.

**Heidstra, R. and Sabatini, S.** (2014). Plant and animal stem cells: similar yet different. Nature reviews. Molecular cell biology **15**: 301–12.

**Hématy, K. and Höfte, H.** (2008). Novel receptor kinases involved in growth regulation. Current Opinion in Plant Biology **11**: 321–8.

**Hématy, K., Sado, P.-E., Van Tuinen, A., Rochange, S., Desnos, T., Balzergue, S., Pelletier, S., Renou, J.-P., and Höfte, H.** (2007). A receptor-like kinase mediates the response of Arabidopsis cells to the inhibition of cellulose synthesis. Current Biology **17**: 922–31.

**Van Hengel, A.J. and Roberts, K.** (2002). Fucosylated arabinogalactan-proteins are required for full root cell elongation in arabidopsis. The Plant Journal **32**: 105–113.

**Herth, W.** (1983). Arrays of plasma-membrane "rosettes" involved in cellulose microfibril formation of Spirogyra. Planta **159**: 347–356.

**Hong, Z., Delauney, A.J., and Verma, D.P.S.** (2001). A Cell Plate Specific Callose Synthase and Its Interaction with Phragmoplastin. The Plant Cell **13**: 755–768.

**Hong, Z., Jin, H., Fitchette, A.-C., Xia, Y., Monk, A.M., Faye, L., and Li, J.** (2009). Mutations of an alpha1,6 mannosyltransferase inhibit endoplasmic reticulum-associated degradation of defective brassinosteroid receptors in Arabidopsis. The Plant Cell **21**: 3792–802.

**Huang, G.-Q., Li, E., Ge, F.-R., Li, S., Wang, Q., Zhang, C.-Q., and Zhang, Y.** (2013). Arabidopsis RopGEF4 and RopGEF10 are important for FERONIA-mediated developmental but not environmental regulation of root hair growth. The New Phytologist **200**: 1089–101.

**Huck, N.** (2003). The Arabidopsis mutant feronia disrupts the female gametophytic control of pollen tube reception. Development **130**: 2149–2159.

**Inagaki, S. and Umeda, M.** (2011). Cell-cycle control and plant development. 1st ed. (Elsevier Inc.).

**Ito, M., Araki, S., Matsunaga, S., Itoh, T., Nishihama, R., Machida, Y., Doonan, J.H., and Watanabe, A.** (2001). G2/M-phase-specific transcription during the plant cell cycle is mediated by c-Myb-like transcription factors. The Plant Cell **13**: 1891–1905.

**Jürgens, G.** (2005). Cytokinesis in higher plants. Annual Review of Plant Biology **56**: 281–99.

**Kakimoto, T. and Shibaoka, H.** (1992). Synthesis of Polysaccharides in Phragmoplasts Isolated from Tobacco by-2 Cells. Plant and Cell Physiology **33**: 353–361.

**Kessler, S.A., Shimosato-Asano, H., Keinath, N.F., Wuest, S.E., Ingram, G., Panstruga, R., and Grossniklaus, U.** (2010). Conserved molecular components for pollen tube reception and fungal invasion. Science **330**: 968–71.

**Kieliszewski, M.J. and Lamport, D.T.A.** (1994). Extensin: Repetitive motifs, functional sites, post-translational codes, and phylogeny. Plant Journal **5**: 157–172.

**Kiermayer, O. and Sleytr, U.B.** (1979). Hexagonally ordered "Rosettes" of particles in the plasma membrane of Micrasterias denticulata Breb. and their significant for microfibril formation and orientation. Protoplasma **101**: 133–138.

**Kimura, S., Laosinchai, W., Itoh, T., Cui, X., Linder, C., and Brown, R.** (1999). Immunogold labeling of rosette terminal cellulose-synthesizing complexes in the vascular plant vigna angularis. The Plant Cell **11**: 2075–86.

**Knoch, E., Dilokpimol, A., Tryfona, T., Poulsen, C.P., Xiong, G., Harholt, J., Petersen, B.L., Ulvskov, P., Hadi, M.Z., Kotake, T., Tsumuraya, Y., Pauly, M., Dupree, P., and Geshi, N.** (2013). A β-glucuronosyltransferase from Arabidopsis thaliana involved in biosynthesis of type II arabinogalactan has a role in cell elongation during seedling growth. The Plant Journal **76**: 1016–29.

**Kong, Y., Zhou, G., Abdeen, A.A., Schafhauser, J., Richardson, B., Atmodjo, M.A., Jung, J., Wicker, L., Mohnen, D., Western, T., and Hahn, M.G.** (2013). GALACTURONOSYLTRANSFERASE-LIKE5 is involved in the production of Arabidopsis seed coat mucilage. Plant Physiology **163**: 1203–17.

**Kumar, M. and Turner, S.** (2014). Plant cellulose synthesis: CESA proteins crossing kingdoms. Phytochemistry **112**: 91–99.

**Lamport, D.T. a, Kieliszewski, M.J., Chen, Y., and Cannon, M.C.** (2011). Role of the extensin superfamily in primary cell wall architecture. Plant Physiology **156**: 11–19.

**Larson, E.R., Tierney, M.L., Tinaz, B., and Domozych, D.S.** (2014). Using monoclonal antibodies to label living root hairs: a novel tool for studying cell wall microarchitecture and dynamics in Arabidopsis. Plant Methods **10**: 30.

**Lauber, M.H., Waizenegger, I., Steinmann, T., Schwarz, H., Mayer, U., Hwang, I., Lukowitz, W., and Jürgens, G.** (1997). KNOLLE protein is a cytokinesis-specific syntaxin. The Journal of Biological Chemistry **139**: 1485–1493.

**Lei, L., Li, S., Du, J., Bashline, L., and Gu, Y.** (2013). CELLULOSE SYNTHASE INTERACTIVE3 Regulates Cellulose Biosynthesis in Both a Microtubule-

Dependent and Microtubule-Independent Manner in Arabidopsis. The Plant Cell **25**: 4912–23.

**Lei, L., Li, S., and Gu, Y.** (2012). Cellulose synthase interactive protein 1 (CSI1) mediates the intimate relationship between cellulose microfibrils and cortical microtubules. Plant Signaling & Behavior **7**: 714–718.

**Lei, L., Zhang, T., Strasser, R., Lee, C.M., Gonneau, M., Mach, L., Vernhettes, S., Kim, S.H., Cosgrove, D., Li, S., and Gu, Y.** (2014). The jiaoyao1 Mutant Is an Allele of korrigan1 That Abolishes Endoglucanase Activity and Affects the Organization of Both Cellulose Microfibrils and Microtubules in Arabidopsis. The Plant Cell **26**: 2601–2616.

**Li, C., Yeh, F.-L., Cheung, A.Y., Duan, Q., Kita, D., Liu, M.-C., Maman, J., Luu, E.J., Wu, B.W., Gates, L., Jalal, M., Kwong, A., Carpenter, H., and Wu, H.-M.** (2015). Glycosylphosphatidylinositol-anchored proteins as chaperones and co-receptors for FERONIA receptor kinase signaling in Arabidopsis. eLife **4**: 1–21.

**Li, J., Wen, J., Lease, K.A., Doke, J.T., Tax, F.E., and Walker, J.C.** (2002). BAK1 , an Arabidopsis LRR Receptor-like Protein Kinase , Interacts with BRI1 and Modulates Brassinosteroid Signaling. Cell **110**: 213–222.

**Li, L.-C., Bedinger, P. a, Volk, C., Jones, a D., and Cosgrove, D.J.** (2003). Purification and characterization of four beta-expansins (Zea m 1 isoforms) from maize pollen. Plant Physiology **132**: 2073–2085.

**Li, S., Lei, L., Somerville, C.R., and Gu, Y.** (2012). Cellulose synthase interactive protein 1 (CSI1) links microtubules and cellulose synthase complexes. Proceedings of the National Academy of Sciences **109**: 185–190.

**Liang, Y., Basu, D., Pattathil, S., Xu, W.-L., Venetos, A., Martin, S.L., Faik, A., Hahn, M.G., and Showalter, A.M.** (2013). Biochemical and physiological characterization of fut4 and fut6 mutants defective in arabinogalactan-protein fucosylation in Arabidopsis. Journal of Experimental Botany **64**: 5537–51.

**Liang, Y., Faik, A., Kieliszewski, M., Tan, L., Xu, W.-L., and Showalter, A.M.** (2010). Identification and characterization of in vitro galactosyltransferase activities involved in arabinogalactan-protein glycosylation in tobacco and Arabidopsis. Plant Physiology **154**: 632–42.

**Liepman, A.H. and Cavalier, D.M.** (2012). The CELLULOSE SYNTHASE-LIKE A and CELLULOSE SYNTHASE-LIKE C families: recent advances and future perspectives. Frontiers in Plant Science **3**: 1–7.

**Liepman, A.H., Wightman, R., Geshi, N., Turner, S.R., and Scheller, H.V.** (2010). Arabidopsis - a powerful model system for plant cell wall research. The Plant Journal **61**: 1107–21.

**Liepman, A.H., Wilkerson, C.G., and Keegstra, K.** (2005). Expression of cellulose synthase-like (Csl) genes in insect cells reveals that CslA family members encode mannan synthases. Proceedings of the National Academy of Sciences of the United States of America **102**: 2221–6.

**Lin, C., Choi, H.-S., and Cho, H.-T.** (2011). Root hair-specific EXPANSIN A7 is required for root hair elongation in Arabidopsis. Molecules and Cells **31**: 393–7.

**Lindner, H., Müller, L.M., Boisson-Dernier, A., and Grossniklaus, U.** (2012). CrRLK1L receptor-like kinases: not just another brick in the wall. Current Opinion in Plant Biology **15**: 659–69.

**Liwanag, A.J.M., Ebert, B., Verhertbruggen, Y., Rennie, E. a, Rautengarten, C., Oikawa, A., Andersen, M.C.F., Clausen, M.H., and Scheller, H.V.** (2012). Pectin Biosynthesis: GALS1 in Arabidopsis thaliana Is a β-1,4-Galactan β-1,4-Galactosyltransferase. The Plant Cell **24**: 5024–5036.

**Madson, M., Dunand, C., Li, X., Verma, R., Vanzin, G.F., Caplan, J., Shoue, D.A., Carpita, N.C., and Reiter, W.-D.** (2003). The MUR3 gene of Arabidopsis encodes a xyloglucan galactosyltransferase that is evolutionarily related to animal exostosins. The Plant Cell **15**: 1662–1670.

**Marrocco, K., Bergdoll, M., Achard, P., Criqui, M.-C., and Genschik, P.** (2010). Selective proteolysis sets the tempo of the cell cycle. Current Opinion in Plant Biology **13**: 631–9.

**McCann, M.C. and Carpita, N.C.** (2008). Designing the deconstruction of plant cell walls. Current Opinion in Plant Biology **11**: 314–320.

**Menges, M. and Murray, J.A.H.** (2002). Synchronous Arabidopsis suspension cultures for analysis of cell-cycle gene activity. The Plant Journal **30**: 203–212.

**Miart, F., Desprez, T., Biot, E., Morin, H., Belcram, K., Höfte, H., Gonneau, M., and Vernhettes, S.** (2014). Spatio-temporal analysis of cellulose synthesis during cell plate formation in Arabidopsis. The Plant Journal **77**: 71–84.

**Miyazaki, S., Murata, T., Sakurai-Ozato, N., Kubo, M., Demura, T., Fukuda, H., and Hasebe, M.** (2009). ANXUR1 and 2, sister genes to FERONIA/SIRENE, are male factors for coordinated fertilization. Current Biology **19**: 1327–1331.

**Mohnen, D.** (2008). Pectin structure and biosynthesis. Current Opinion in Plant Biology **11**: 266–77.

**Mølhøj, M., Jørgensen, B., Ulvskov, P., and Borkhardt, B.** (2001). Two Arabidopsis thaliana genes, KOR2 and KOR3, which encode membrane-anchored endo-1,4-beta-D-glucanases, are differentially expressed in developing leaf trichomes and their support cells. Plant Molecular Biology **46**: 263–75.

**Mølhøj, M., Pagant, S., and Höfte, H.** (2002). Towards understanding the role of membrane-bound endo-beta-1,4-glucanases in cellulose biosynthesis. Plant & cell physiology **43**: 1399–406.

**Moore, P.J. and Staehelin, L.A.** (1988). Planta of the cell-wall-matrix polysaccharides rhamnogalacturonan I and xyloglucan during cell expansion and cytokinesis in Trifolium pratense L .; implication for secretory pathways. 433–445.

**Mueller, S.C. and Brown, R.M.** (1980). Evidence for an intramembrane component associated with a cellulose microfibril-synthesizing complex in higher plants. The Journal of Cell Biology **84**: 315–26.

**Newcomb, E.H. and Bonnett, H.T.** (1965). Cytoplasmic microtubule and wall microfibril orientation in root hairs of radish. The Journal of Cell Biology.

**Nguema-Ona, E., Vicré-Gibouin, M., Gotté, M., Plancot, B., Lerouge, P., Bardor, M., and Driouich, A.** (2014). Cell wall O-glycoproteins and N-glycoproteins: aspects of biosynthesis and function. Frontiers in Plant Science **5**: 499.

**Nicol, F., His, I., Jauneau, A., Vernhettes, S., Canut, H., and Höfte, H.** (1998). A plasma membrane-bound putative endo-1,4-beta-D-glucanase is required for normal wall assembly and cell elongation in Arabidopsis. The EMBO Journal **17**: 5563–76.

**Nielsen, E.** (2009). Plant cell wall biogenesis during tip growth in root hair cells. Root Hairs **12**: 85–102.

**Ogawa-Ohnishi, M., Matsushita, W., and Matsubayashi, Y.** (2013). Identification of three hydroxyproline O-arabinosyltransferases in Arabidopsis thaliana. Nature chemical biology **9**: 726–30.

**Orfila, C., Sørensen, S.O., Harholt, J., Geshi, N., Crombie, H., Truong, H.N., Reid, J.S.G., Knox, J.P., and Scheller, H.V.** (2005). QUASIMODO1 is expressed in vascular tissue of Arabidopsis thaliana inflorescence stems, and affects homogalacturonan and xylan biosynthesis. Planta **222**: 613–622.

**Paredez, A.R., Somerville, C.R., and Ehrhardt, D.W.** (2006). Visualization of cellulose synthase demonstrates functional association with microtubules. Science **312**: 1491–5.

**Park, E., Díaz-Moreno, S.M., Davis, D.J., Wilkop, T.E., Bulone, V., and Drakakaki, G.** (2014). Endosidin 7 Specifically Arrests Late Cytokinesis and Inhibits Callose Biosynthesis, Revealing Distinct Trafficking Events during Cell Plate Maturation. Plant Physiology **165**: 1019–1034.

**Park, S., Szumlanski, A.L., Gu, F., Guo, F., and Nielsen, E.** (2011). A role for CSLD3 during cell-wall synthesis in apical plasma membranes of tip-growing root-hair cells. Nature Cell Biology **13**: 973–80.

**Peña, M.J., Kong, Y., York, W.S., and O'Neill, M. a** (2012). A Galacturonic Acid-Containing Xyloglucan Is Involved in Arabidopsis Root Hair Tip Growth. The Plant Cell **24**: 4511–4524.

**Perrin, R.M., DeRocher, a E., Bar-Peled, M., Zeng, W., Norambuena, L., Orellana, A., Raikhel, N. V, and Keegstra, K.** (1999). Xyloglucan fucosyltransferase, an enzyme involved in plant cell wall biosynthesis. Science **284**: 1976–1979.

**Persson, S., Paredez, A., Carroll, A., Palsdottir, H., Doblin, M., Poindexter, P., Khitrov, N., Auer, M., and Somerville, C.R.** (2007). Genetic evidence for three unique components in primary cell-wall cellulose synthase complexes in Arabidopsis. Proceedings of the National Academy of Sciences of the United States of America **104**: 15566–71.

**Persson, S., Wei, H., Milne, J., Page, G.P., and Somerville, C.R.** (2005). Identification of genes required for cellulose synthesis by regression analysis of public microarray data sets. Proceedings of the National Academy of Sciences of the United States of America **102**: 8633–8.

**Qi, X. and Zheng, H.** (2013). Rab-A1c GTPase defines a population of the trans-golgi network that is sensitive to endosidin1 during cytokinesis in Arabidopsis. Molecular Plant **6**: 847–859.

**Qu, Y., Egelund, J., Gilson, P.R., Houghton, F., Gleeson, P. a, Schultz, C.J., and Bacic, A.** (2008). Identification of a novel group of putative Arabidopsis thaliana beta-(1,3)-galactosyltransferases. Plant Molecular Biology **68**: 43–59.

**Richmond, T. a and Somerville, C.R.** (2000). The cellulose synthase superfamily. Plant Physiology **124**: 495–8.

**Rotman, N., Boavida, L., Dumas, C., Faure, J., Bernard, C., Lyon, I., Lyon, D., and Cedex, L.F.-** (2003). Female Control of Male Gamete Delivery during Fertilization in Arabidopsis thaliana. Current Biology **13**: 432–436.

**Sampedro, J. and Cosgrove, D.J.** (2005). The expansin superfamily. Genome Biology **6**: 242.

**Samuels, L., Giddings, T., and Staehelin, A.** (1995). Cytokinesis in Tobacco BY-2 and Root Tip Cells : The Journal of Cell Biology **130**: 1345–1357.

**Saxena, I.M., Brown, R.M., Fevre, M., Geremia, R.A., and Henrissat, B.** (1995). Multidomain Architecture of β-Glycosyl Transferases : Implications for Mechanism of Action. Journal of Bacteriology **177**: 1419–1424.

**Schallus, T., Jaeckh, C., Fehér, K., Palma, A.S., Liu, Y., Simpson, J.C., Mackeen, M., Stier, G., Gibson, T.J., Feizi, T., Pieler, T., and Muhle-goll, C.** (2008). Malectin : A Novel Carbohydrate-binding Protein of the Endoplasmic Reticulum and a Candidate Player in the Early Steps of Protein N-Glycosylation. Molecular Biology of the Cell **19**: 3404–3414.

**Scheller, H.V. and Ulvskov, P.** (2010). Hemicelluloses. Annual Review of Plant Biology **61**: 263–289.

**Schiefelbein, J., Kwak, S.-H., Wieckowski, Y., Barron, C., and Bruex, A.** (2009). The gene regulatory network for root epidermal cell-type pattern formation in Arabidopsis. Journal of Experimental Botany **60**: 1515–21.

**Schindelman, G., Morikami, A., Jung, J., Baskin, T.I., Carpita, N.C., Derbyshire, P., McCann, M.C., and Benfey, P.N.** (2001). COBRA encodes a putative GPI-anchored protein, which is polarly localized and necessary for oriented cell expansion in Arabidopsis. Genes & Development **15**: 1115–27.

**Schulze-muth, P., Irmler, S., Schro, G., and Schro, J.** (1996). Novel Type of Receptor-like Protein Kinase from a Higher Plant ( Catharanthus roseus ). The Journal of Biological Chemistry **271**: 26684–26689.

**Seguí-Simarro, J.M., Austin Ii, J.R., White, E.A., and Staehelin, L.A.** (2004). Electron Tomographic Analysis of Somatic Cell Plate Formation in Meristematic Cells of Arabidopsis Preserved by High-Pressure Freezing. The Plant Cell **16**: 836–856.

**Shiu, S. and Bleecker, A.B.** (2001). Receptor-like kinases from Arabidopsis form a monophyletic gene family related to animal receptor kinases. Proceedings of the National Academy of Sciences of the United States of America **98**: 10763–10768.

**Showalter, a M.** (1993). Structure and function of plant cell wall proteins. The Plant cell **5**: 9–23.

**Showalter, A.M., Keppler, B., Lichtenberg, J., Gu, D., and Welch, L.R.** (2010). A bioinformatics approach to the identification, classification, and analysis of hydroxyproline-rich glycoproteins. Plant Physiology **153**: 485–513.

**Somerville, C.** (2006). Cellulose synthesis in higher plants. Annual Review of Cell and Developmental Biology **22**: 53–78.

**Somerville, C., Bauer, S., Brininstool, G., Facette, M., Hamann, T., Milne, J., Osborne, E., Paredez, A., Persson, S., Raab, T., Vorwerk, S., and Youngs, H.** (2004). Toward a systems approach to understanding plant cell walls. Science **306**: 2206–11.

**Sorek, N., Sorek, H., Kijac, A., Szemenyei, H.J., Bauer, S., Wemmer, D.E., and Chris, R.** (2014). The Arabidopsis COBRA Protein Facilitates Cellulose Crystallization at the Plasma Membrane. The Journal of Biological Chemistry **289**: 34911–34920.

**Sterling, J.D., Atmodjo, M. a, Inwood, S.E., Kumar Kolli, V.S., Quigley, H.F., Hahn, M.G., and Mohnen, D.** (2006). Functional identification of an Arabidopsis pectin biosynthetic homogalacturonan galacturonosyltransferase. Proceedings of the National Academy of Sciences of the United States of America **103**: 5236–41.

**Tan, L., Eberhard, S., Pattathil, S., Warder, C., Glushka, J., Yuan, C., Hao, Z., Zhu, X., Avci, U., Miller, J.S., Baldwin, D., Pham, C., Orlando, R., Darvill, A., Hahn, M.G., Kieliszewski, M.J., and Mohnen, D.** (2013). An Arabidopsis cell wall

proteoglycan consists of pectin and arabinoxylan covalently linked to an arabinogalactan protein. The Plant Cell **25**: 270–87.

**Taylor, N.G., Laurie, S., and Turner, S.R.** (2000). Multiple Cellulose Synthase Catalytic Subunits Are Required for Cellulose Synthesis in Arabidopsis. **12**: 2529–2539.

**The Arabidopsis Genome Initiative** (2000). Analysis of the genome sequence of the flowering plant Arabidopsis thaliana. Nature **408**: 796–815.

**Thiele, K., Wanner, G., Kindzierski, V., Jürgens, G., Mayer, U., Pachl, F., and Assaad, F.F.** (2009). The timely deposition of callose is essential for cytokinesis in Arabidopsis. Plant Journal **58**: 13–26.

**Touihri, S., Knöll, C., Stierhof, Y.-D., Müller, I., Mayer, U., and Jürgens, G.** (2011). Functional anatomy of the Arabidopsis cytokinesis-specific syntaxin KNOLLE. The Plant Journal **68**: 755–64.

**Tryfona, T., Theys, T.E., Wagner, T., Stott, K., Keegstra, K., and Dupree, P.** (2014). Characterisation of FUT4 and FUT6 α-(1 → 2)-fucosyltransferases reveals that absence of root arabinogalactan fucosylation increases Arabidopsis root growth salt sensitivity. PloS ONE **9**: e93291.

**Ueda, T.** (2014). Cellulase in Cellulose Synthase: A Cat among the Pigeons? Plant Physiology **165**: 1397–1398.

**Vain, T., Crowell, E.F., Timpano, H., Biot, E., Desprez, T., Mansoori, N., Trindade, L.M., Pagant, S., Robert, S., Höfte, H., Gonneau, M., and Vernhettes, S.** (2014). The cellulase KORRIGAN is part of the Cellulose Synthase Complex. Plant Physiology **165**: 1521–1532.

**Vanzin, G.F., Madson, M., Carpita, N.C., Raikhel, N. V, Keegstra, K., and Reiter, W.-D.** (2002). The mur2 mutant of Arabidopsis thaliana lacks fucosylated xyloglucan because of a lesion in fucosyltransferase AtFUT1. Proceedings of the National Academy of Sciences of the United States of America **99**: 3340–5.

**Velasquez, S.M., Ricardi, M.M., Dorosz, J.G., Fernandez, P. V, Nadra, A.D., Pol-Fachin, L., Egelund, J., Gille, S., Harholt, J., Ciancia, M., Verli, H., Pauly, M., Bacic, A., Olsen, C.E., Ulvskov, P., Petersen, B.L., Somerville, C., Iusem, N.D., and Estevez, J.M.** (2011). O-glycosylated cell wall proteins are essential in root hair growth. Science (New York, N.Y.) **332**: 1401–3.

**Wang, W., Wang, L., Chen, C., Xiong, G., Tan, X.-Y., Yang, K.-Z., Wang, Z.-C., Zhou, Y., Ye, D., and Chen, L.-Q.** (2011). Arabidopsis CSLD1 and CSLD4 are required for cellulose deposition and normal growth of pollen tubes. Journal of Experimental Botany **62**: 5161–77.

**Wang, X., Cnops, G., Vanderhaeghen, R., De Block, S., Van Montagu, M., and Van Lijsebettens, M.** (2001). AtCSLD3, a cellulose synthase-like gene important for root hair growth in arabidopsis. Plant Physiology **126**: 575–86.

**Wu, Y., Williams, M., Bernard, S., Driouich, A., Showalter, A.M., and Faik, A.** (2010). Functional identification of two nonredundant Arabidopsis alpha(1,2)fucosyltransferases specific to arabinogalactan proteins. The Journal of Biological Chemistry **285**: 13638–45.

**Yin, L., Verhertbruggen, Y., Oikawa, A., Manisseri, C., Knierim, B., Prak, L., Jensen, J.K., Knox, J.P., Auer, M., Willats, W.G.T., and Scheller, H.V.** (2011). The cooperative activities of CSLD2, CSLD3, and CSLD5 are required for normal Arabidopsis development. Molecular Plant **4**: 1024–37.

**Yoo, C.-M., Quan, L., and Blancaflor, E.B.** (2012). Divergence and Redundancy in CSLD2 and CSLD3 Function During Arabidopsis Thaliana Root Hair and Female Gametophyte Development. Frontiers in Plant Science **3**: 111.

**Yu, F., Li, J., Huang, Y., Liu, L., Li, D., Chen, L., and Luan, S.** (2014). FERONIA receptor kinase controls seed size in Arabidopsis thaliana. Molecular Plant **7**: 920–2.

**Yu, F., Qian, L., Nibau, C., Duan, Q., Kita, D., Levasseur, K., Li, X., Lu, C., Li, H., Hou, C., Li, L., Buchanan, B.B., Chen, L., Cheung, A.Y., Li, D., and Luan, S.** (2012). FERONIA receptor kinase pathway suppresses abscisic acid signaling in Arabidopsis by activating ABI2 phosphatase. Proceedings of the National Academy of Sciences of the United States of America **109**: 14693–8.

**Zabotina, O.A., Van de Ven, W.T.G., Freshour, G., Drakakaki, G., Cavalier, D., Mouille, G., Hahn, M.G., Keegstra, K., and Raikhel, N. V** (2008). Arabidopsis XXT5 gene encodes a putative alpha-1,6-xylosyltransferase that is involved in xyloglucan biosynthesis. The Plant Journal **56**: 101–15.

**Zheng, B., Chen, X., and McCormick, S.** (2011). The anaphase-promoting complex is a dual integrator that regulates both MicroRNA-mediated transcriptional regulation of cyclin B1 and degradation of Cyclin B1 during Arabidopsis male gametophyte development. The Plant Cell **23**: 1033–46.

**Zhu, J., Lee, B.-H., Dellinger, M., Cui, X., Zhang, C., Wu, S., Nothnagel, E. a, and Zhu, J.-K.** (2010). A cellulose synthase-like protein is required for osmotic stress tolerance in Arabidopsis. The Plant Journal **63**: 128–40.

**Zuo, J., Niu, Q., Nishizawa, N., Wu, Y., Kost, B., and Chua, N.** (2000). KORRIGAN, an Arabidopsis Endo-1,4- b -Glucanase, Localizes to the Cell Plate by Polarized Targeting and Is Essential for Cytokinesis. The Plant Cell **12**: 1137–1152.